DEPARTMENT OF TRANSPORTATION

Mitigation of Tenting of Transverse Cracks and Joints in Asphalt Pavement

Manik Barman, Principal Investigator

Department of Civil and Environmental Engineering
University of Minnesota Duluth

April 2026

Research Report
Final Report 2026-16

LOCAL ROAD RESEARCH BOARD

To get this document in an alternative format or language, please call 651-366-4720 (711 or 1-800-627-3529 for MN Relay). You can also email your request to ADArequest.dot@state.mn.us. Please make your request at least two weeks before you need the document.

Technical Report Documentation Page

1. Report No. MN 2026-16	2.	3. Recipients Accession No.	
4. Title and Subtitle Mitigation of Tenting of Transverse Cracks and Joints in Asphalt Pavement		5. Report Date April 2026 6.	
7. Author(s) Manik Barman, Manik Chakraborty, Chrysogonus Asante, Mihai Marasteanu, Mugurel Turos		8. Performing Organization Report No.	
9. Performing Organization Name and Address Department of Civil and Environmental Engineering University of Minnesota Duluth 1405 Univ. Drive, Duluth, MN 55812		10. Project/Task/Work Unit No. # 2023003 11. Contract (C) or Grant (G) No. (c) 1036342 (wo) 51	
12. Sponsoring Organization Name and Address Minnesota Department of Transportation Office of Research & Innovation 395 John Ireland Boulevard, MS 330 St. Paul, Minnesota 55155-1899		13. Type of Report and Period Covered Final Report 14. Sponsoring Agency Code	
15. Supplementary Notes http://mdl.mndot.gov/			
16. Abstract (Limit: 250 words) Transverse cracking, a primary distress in cold-climate asphalt pavements, can lead to tenting, an upward distortion caused by ice formation in the base layer and at the interface of the surface and base layers. This research investigated pavement treatment efficacy and core tenting mechanisms through field measurements in six selected roads in Minnesota and through laboratory testing of base layer materials. A critical outcome was the development of the Coarse Void/Fine Void (CV/FV) index to predict frost susceptibility. Results indicated that the distribution of voids was a more significant predictor than fine content alone. A CV/FV index below 0.88 was found to lower tenting potential. Furthermore, the study identified micro-surfacing as an effective treatment for mitigating roughness on Bituminous over Aggregate Base (BAB) and Bituminous over Bituminous (BOB) pavements. The project concluded with the creation of three decision trees, offering engineers a practical framework for selecting base materials and maintenance strategies to enhance pavement longevity in frost-prone regions.			
17. Document Analysis/Descriptors Asphalt pavements, Transverse cracking, Frost heaving, Preventive maintenance, Pavement base course, Aggregate gradation		18. Availability Statement No restrictions. Document available from: National Technical Information Services, Alexandria, Virginia 22312	
19. Security Class (this report) Unclassified	20. Security Class (this page) Unclassified	21. No. of Pages 109	22. Price

Mitigation of Tenting of Transverse Cracks and Joints in Asphalt Pavement

Final Report

Prepared by:

Manik Barman, Ph. D.
Manik Chakraborty
Chrysogonus Asante
Department of Civil and Environmental Engineering
University of Minnesota Duluth

Mihai Marasteanu, Ph. D.
Mugurel Turos
Department of Civil, Environmental, and Geo- Engineering
University of Minnesota

April 2026

Published by:

Minnesota Department of Transportation
Office of Research & Innovation
395 John Ireland Boulevard, MS 330
St. Paul, Minnesota 55155-1899

Acknowledgments

The authors sincerely acknowledge the financial support provided by the Minnesota Local Road Research Board (LRRB), which made this important research possible. The financial assistance from the University of Minnesota Duluth, particularly through graduate teaching assistantships, is also greatly appreciated.

The authors extend their heartfelt gratitude to the project's technical liaison, Mr. Matt Hemmila, P.E., Deputy Public Works Director for Engineering and Program Delivery at St. Louis County, whose involvement—from identifying the research need through the completion of the project—was invaluable. The research team is also grateful to all members of the Technical Advisory Panel (TAP) for their valuable suggestions during meetings and for their thoughtful reviews of the task reports. Special thanks are due to Project Coordinators Mr. Chad Kooistra and Mr. David Glyer, as well as colleagues at CTS, for their time and administrative support.

St. Louis County provided exceptional support throughout this project, particularly during field work by assisting with site selection and providing necessary traffic control. The contributions of Duluth's Northland Constructors and Ulland Brothers, who supplied base material samples from their plants, are also deeply appreciated.

The research team sincerely acknowledges the contributions of numerous graduate and undergraduate students, laboratory staff, especially Oscar Toftegaard, and the Sponsored Projects Administration (SPA) staff at the University of Minnesota Duluth (UMD), all of whom supported various phases of this project.

TAP Members

1. Amy Thorson, MnDOT
2. Bruce Hasbargen, Beltrami County
3. Eddie Johnson, MnDOT
4. Matt Hemmila, St Louis County (TL)
5. Thomas Calhoon, MnDOT

Table of Contents

Chapter 1: Introduction **1**

1.1 Objectives 2

Chapter 2: Literature Review **4**

2.1 Causes and Development of Tenting 4

2.2 Assessment of Tenting 7

2.3 Effect of Pavement Treatment Methods 10

2.4 Online Survey 13

2.5 Summary 13

Chapter 3: Research Methodology **15**

3.1 Field Work 16

3.1.1 Tenting Measurement in Field 16

3.2 Pavement Performance Data Analysis 19

3.3 Laboratory Investigation 19

3.3.1 Materials Collection 19

3.3.2 Gradation / Sieve Analysis 22

3.3.3 Proctor Test 22

3.3.4 Salinity Test 23

3.3.5 Frost Heave Test 24

3.3.6 Permeability/ Hydraulic Conductivity Test 27

3.3.7 Specific Gravity Test 30

3.3.8 Test for Studying Moisture Affinity of Salt-mixed Aggregate Samples 33

Chapter 4: Results and Discussions **34**

4.1 Quantitative Assessment of Tenting in Field Conditions 34

4.1.1 Tenting Measurement in this Study 34
4.1.2 Tenting Measurement in Zegeye-Teshale et al. (2021) Study 36
4.1.3 MnDOT District 1 Roads with Tenting Distress 40
4.2 Effectiveness of Pavement Treatments 42
4.2.1 Correlation between ET and different variables through Machine Learning Models 46
4.2.2 Results of the Machine Learning Models 47
4.2.3 Ranking of Treatments 49
4.3 Laboratory Test Results 51
4.3.1 Aggregate Gradation 51
4.3.2 Moisture- Density Relationships 56
4.3.3 Frost Heave Test Results 58
4.3.4 Permeability / Hydraulic Conductivity Test Result 63
4.4 Comparison of Field and Plant Samples 66
4.5 Road Condition vs. Tenting vs. CV/FV index 75
Chapter 5: Development of Decision Trees 77
Chapter 6: Conclusions and Recommendations 82
REFERENCES 85
APPENDIX A: BonfrroPost-Tests results for Ranking Pavement Treatments

List of Figures

Figure 1.1 (a) The anatomy of the tenting, (b) a photograph of tenting showing the slope of the pavement at either side of the cracks, and (c) distorted pavement profile because of tenting. 2

Figure 2.1: Survey results of tenting distress severity across road networks (Johnson and Olson, 2008) ... 4

Figure 2.2 Frost susceptibility chart of different types of soil as per grain size (Kestler et al., 2000) 6

Figure 2.3 Freezing process in pavement base material due to salt intrusion (Doré et al., 1997) 7

Figure 2.4: PHV and SBP, tenting parameters developed in Zegeye-Teshale et al. (2021) study. 7

Figure 2.5: Graphs illustrating the relationship between the International Roughness Index (IRI) and the tenting parameters: (a) IRI versus peak height value (PHV); and (b) IRI versus spacing between peaks (SBP) (Zegeye-Teshale et al., 2021) 8

Figure 2.6: Aggregate base materials conductivity test results (Johnson & Olson, 2008) 9

Figure 2.7: Salinity level at different vertical and horizontal distances from the crack (Kestler et al., 2000) 10

Figure 2.8: Percentage of crack length reflected from the original HMA layer to the overlay (Bush and Brookes, 2007) 12

Figure 3.1 Flow chart showing different activities in the study 15

Figure 3.2 Locations of the tenting measurement project sites (Google Map). 17

Figure 3.3 Tenting measuring device and the location of the measurements in a transverse crack 18

Figure 3.4 Procedure for calculating the peak height of tenting 18

Figure 3.5 Aggregate base material collection from the Plants 21

Figure 3.6 MnDOT Class 5 Materials used in the lab for testing 21

Figure 3.7 Photographs showing Proctor test of the base material 23

Figure 3.8 Complete frost heave testing process and the setup 26

Figure 3.9 Diagram of the constant head permeability test setup 28

Figure 3.10 Aggregate mixed with water at OMC and Compacted sample in the permeability test mold. 29

Figure 3.11 Permeability test setup images..... 30

Figure 3.12 Coarse aggregate submerged in the water..... 31

Figure 3.13 Fine aggregate drying using heat gun (left) and checking for SSD condition (right) 32

Figure 3.14 Moisture affinity study..... 33

Figure 4.1: Average winter and summer tenting peak height of different roads..... 35

Figure 4.2: Average winter tenting peak height data of Wallace Avenue (CSAH 9). 35

Figure 4.3: Tenting comparison with the base thickness, HMA thickness, and traffic volume (AADT)..... 36

Figure 4.4: MN-37D Test Section. 37

Figure 4.5: US-169D Test Section (red line - 2021, and magenta line -2020). 38

Figure 4.6: US-169I Test Section (red line - 2021, and magenta line -2020). 38

Figure 4.7: Tenting Results for MN-37D. 39

Figure 4.8: Tenting Results for US-169. 39

Figure 4.9: Tenting Results for US-169I. 40

Figure 4.10: The Average IRI improvement and the distribution of the IRI improvement data of different treatment; (a) &(b): cheap seal, (c) &(d): crack fill, (e) &(f): crack repair, (g) &(h): crack seal, (i) &(j): micro surfacing, (k) &(l): patching..... 46

Figure 4.11: Actual vs. predicted IRI improvement comparison (training data) 48

Figure 4.12: Actual vs. predicted IRI improvement comparison (validation data) 48

Figure 4.13 Gradation curves of the four different aggregate samples 52

Figure 4.14: Comparison of the theoretical uncompacted void area of the four different aggregate samples 54

Figure 4.15: Fine void area and course void area. 55

Figure 4.16: Comparison of the CV/FV value of the four different blend 55

Figure 4.17: Moisture density relation of the four different aggregate blends 56

Figure 4.18: Relationship between MDD and percentage of fine 57

Figure 4.19: Relationship between maximum dry density and the CV/FV different aggregate blends 58

Figure 4.20: Frost heave test results of samples prepared from SO blend 59

Figure 4.21: Frost heave test results of samples prepared from SN blend 60

Figure 4.22: Frost heave test results of samples prepared with different deicers having the same salt dosage. 61

Figure 4.23: Frost heave test results of the aggregate blends using uniform temperature gradient 62

Figure 4.24: Correlation between frost heave and the CV/FV index 63

Figure 4.25: Permeability/ Hydraulic conductivity test results of the aggregate blends 64

Figure 4.26: Relation between hydraulic conductivity and CV/FV index 64

Figure 4.27: Permeability/ Hydraulic conductivity vs Frost heave relation 65

Figure 4.28: Aggregate blends performance parameters comparison with the percentage of fine content 66

Figure 4.29: Locations (yellow circled) of the project sites from where base material samples were collected 67

Figure 4.30: Base materials collection from the project site 68

Figure 4.31: Gradation curves of the plant samples and the field samples together 69

Figure 4.32: Quantitative comparison of the theoretical uncompacted void of the four different plant samples and the three different field samples 70

Figure 4.33: Comparison of CV/FV value of the plant samples and the field samples 71

Figure 4.34: Moisture density relation of the four plant samples and the three field samples 72

Figure 4.35: Frost heave test results of the aggregate blends using uniform temperature gradient 73

Figure 4.36: Comparison of measured tenting values between laboratory tests and field observations . 74

Figure 4.37: Updated frost heave vs. CV/FV index. 74

Figure 4.38: Correlation between field-measured tenting values and laboratory-measured frost values. 75

Figure 4.39: Road condition vs tenting peak height value (PHV) in Zegeye-Teshale et al. (2021) study. .. 76

Figure 5.1: Decision tree for selecting pavement treatment to decrease tenting on the existing pavement. 78

Figure 5.2: Decision tree for selecting localized and pavement surface treatment to decrease tenting on the existing pavement. 80

Figure 5.3: Decision tree for selecting CV/FV ratio based on the road condition. 81

List of Tables

Table 2.1: Federal pavement roughness thresholds for interstate roads 9

Table 2.2: Comparison of the tenting data between the mill and overlay section and a control section (Johnson and Olson, 2008)..... 11

Table 2.3: Comparison of the tenting and roughness improvement data (Johnson and Olson, 2008)..... 11

Table 2.4: Relative ranking of pavement preventive maintenance strategies (Khattak and Alrashidi., 2013) 13

Table 3.1 Details of road sections where tenting was measured. 16

Table 3.2 An example of performance data of a road section in the HPMA tool..... 20

Table 4.1: Details of the three highways where tenting was measured in Zegeye-Teshale et al. (2021) study..... 37

Table 4.2: List of some Roads in MnDOT District 1 that experienced tenting distress..... 40

Table 4.3: Assumed traffic categories. 46

Table 4.4: Summary of the Decision Tree model statistics 47

Table 4.5: Summary of the Random Forest model statistics 47

Table 4.6: Summary of the Boosted Tress (gradient boosting) model statistics 47

Table 4.7:Hypotheses of the ANOVA test 49

Table 4.8: ANOVA test results 50

Table 4.9: Ranking of the different treatments on different pavement types based on the composite score..... 50

Table 4.10 : Composition of Aggregate Blends 53

Table 4.11: Maximum dry density and optimum moisture content of four blends 57

Table 4.12: Sample weight increments due to salt concentration of different blends 61

Table 4.13: Composition of plant blends and field samples 69

Table 4.14: Comparison of plant and field sample with respect to their MDD and OMC 72

Table 4.15: Road Condition vs. Tenting height and CV/FV index. 76

Executive Summary

Transverse cracking is a dominant distress in asphalt pavements, particularly in cold climates like Minnesota, where the asphalt layer contracts in frigid winter conditions. This contraction induces tensile stresses that crack the pavement perpendicular to the direction of traffic, allowing moisture infiltration that leads to a secondary and often more severe distress known as tenting or heaving. Tenting is characterized by the upward movement of asphalt at the edges of a crack, driven by ice formation in the base materials and at the interface between the base and surface layers. This distortion creates a significant peak resembling a small tent, which reduces ride quality, poses safety risks to motorists, and accelerates pavement deterioration, often leading to potholes. While the general mechanism of frost heave is well understood, transportation agencies have historically lacked data regarding the effectiveness of current pavement treatments in mitigating tenting or pavement roughness related to tenting, as well as specific guidance on how base layer aggregate structures influence the tenting formation process.

To address this gap, this research project aimed to investigate the efficacy of available pavement treatments in mitigating the tenting and road roughness and to isolate the core mechanisms of tenting, specifically the influence of base layer material properties. The primary goal was developing guidance for new roads to be constructed and for the existing roads that experience tenting. The study's objectives were comprehensive: conduct a literature review and field measurements on selected Minnesota roads to characterize the physical extent of tenting; analyze how existing treatments influence pavement roughness; and study base layer material gradations through laboratory testing to determine their frost-heaving potential. A central aim was to develop a method to classify base materials by frost susceptibility, specifically by implementing the coarse void/fine void ratio (CV/FV index) as a selection parameter, and create decision trees for both designing new pavements and selecting optimal pavement treatments for distressed roads.

The research methodology combined pavement performance data analysis, extensive fieldwork, and comprehensive laboratory testing. Fieldwork involved measuring tenting profiles on six roads in St. Louis County, Minnesota, while pavement roughness data from eight MnDOT districts was reviewed to evaluate the impact of various treatment strategies on road roughness. In the laboratory, MnDOT Class 5 aggregate samples were collected from local plants and tented road sections to undergo testing for gradation, hydraulic conductivity, moisture-density relationships, and frost-heave potential. The test results facilitated the development of the CV/FV index, correlating aggregate void structure with frost susceptibility.

Field data confirmed that tenting is a localized distress caused by moisture infiltration into the base layer and the intrusion of fines at the interface between the surface and base layers. Its severity can increase with traffic volume, regardless of pavement layer thickness. Crucially, the study found that tenting does not completely disappear during summer; the intrusion of fines results in permanent tenting. In some

cases, a depression forms along the crack in summer—known as cupping—due to the loss of pavement materials. These findings indicate that tenting contributes to pavement roughness throughout the year.

A critical contribution of the study was the identification of the CV/FV index as a predictor of frost performance, revealing that the overall distribution of voids was more significant than the simple fraction of fine content. A high CV/FV index correlated with higher permeability and frost susceptibility. The pavement roughness study results revealed that improvement in road riding quality is a function of pavement type and maintenance method. It also showed that micro-surfacing is a good method for mitigating road roughness, particularly on Bituminous over Aggregate Base (BAB) and Bituminous over Bituminous layer (BOB) pavement types.

The study concluded with practical recommendations for implementation, specifically utilizing the CV/FV index and new decision trees. For new pavement construction, it is recommended that base materials be selected with a target CV/FV index of less than 0.88 to limit potential tenting to less than 2.5 mm. In addition, three decision trees were developed to assist engineers in selecting treatments based on roughness thresholds, differentiating between localized repairs and surface treatments, and guiding base material gradation.

Chapter 1: Introduction

Transverse cracking is a common distress in asphalt pavements, typically caused by contraction of the asphalt layer in frigid winter conditions. As the asphalt cools, it contracts and induces tensile stresses that eventually lead to cracking perpendicular to the direction of traffic. If left untreated or improperly sealed, these cracks allow water to infiltrate the pavement structure, increasing the risk of moisture-related damage.

In climates similar to Minnesota's, transverse cracks frequently develop a secondary winter distress known as tenting or heaving. Tenting refers to the upward movement of asphalt along the edges of the crack due to ice formation beneath the pavement surface. This upward movement increases pavement roughness and decreases ride quality. Figure 1.1 illustrates the anatomy of tenting and shows two photographs of tented transverse cracks. The first photograph demonstrates the significant slope of the pavement in the immediate vicinity of a tented crack. The second photograph, taken at night, highlights the distorted profile of a pavement section heavily impacted by multiple tented cracks. Tented cracks with peak heights exceeding 2.5 mm can affect ride quality (Johnson & Olson, 2008) and pose safety concerns for motorists, especially under low-visibility winter conditions. Additionally, tented cracks deteriorate more rapidly than non-tented cracks and often evolve into potholes before the pavement reaches its intended service life.

The prevailing theory behind the formation of tented cracks is the frost heaving of base materials in winter. This process is influenced by several factors, including moisture infiltration from the road surface, deicing salts, fine particles in the unstable base and subgrade layers, and moisture drawn by capillary action from the subbase. In addition, ice formation at the interface of the base and surface layers directly contributes to tenting.

While the fundamental causes of tenting are understood, further research is required to isolate the core issue, specifically within the base layer aggregate structure, and to identify effective mitigation and prevention techniques. The scope of this project involves an investigation of the tenting phenomenon through field measurements of asphalt roads in Minnesota, an analysis of how current pavement treatment activities affect road roughness, and a study of base layer material gradations to identify frost-heaving potential through laboratory testing.

The study further focused on developing a procedure to characterize base materials based on their frost-susceptibility and introduced a new parameter, the coarse void/fine void ratio (CV/FV index), to provide guidance for selecting base materials in asphalt pavements. The study concluded with the development of decision trees for mitigating frost-heaving in new base materials and for selecting the most suitable treatments to reduce tenting on existing, distressed pavements.

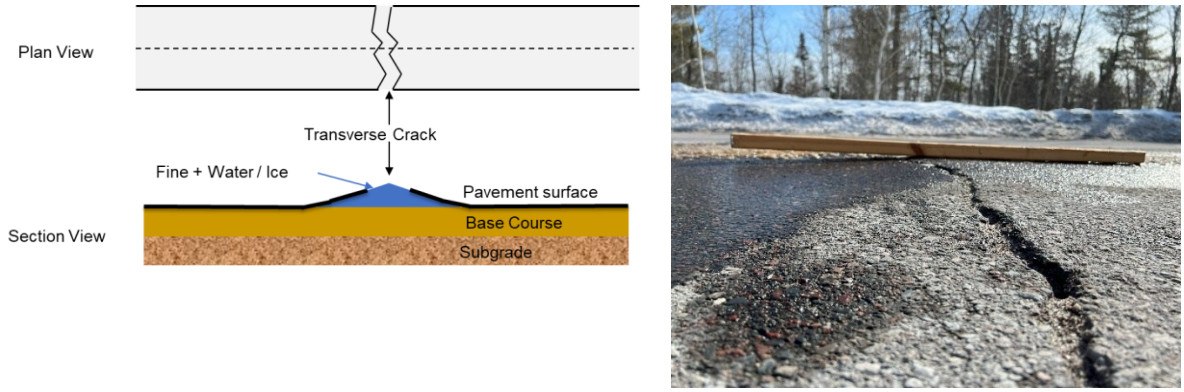

(a) (b)

(c)

Figure 1.1 (a) The anatomy of the tenting, (b) a photograph of tenting showing the slope of the pavement at either side of the cracks, and (c) distorted pavement profile because of tenting.

1.1 Objectives

The key objectives of the study are listed below:

- Conduct a literature review on the tenting process and its mitigation practices.
- Conduct field measurements on selected asphalt roads in Minnesota to characterize the physical extent of tenting.
- Analyze how existing road treatment activities influence pavement roughness in relation to tenting.

- Study base layer material gradations and determine their frost-heaving potential through laboratory testing.
- Develop a standardized method to classify base materials according to their susceptibility to frost.
- Create decision trees to assist in:
    - Mitigating frost-heaving in the design of new pavements.
    - Selecting optimal pavement treatments for existing and distressed pavements.

Chapter 2: Literature Review

The literature review thoroughly examines previous studies and research on winter tenting in asphalt pavements. This chapter discusses the underlying causes of tenting, the factors that affect its development, progression and severity, and the effectiveness of various pavement treatments. This chapter sets the foundation for identifying gaps in current research by studying the previous studies. It highlights the need for further investigation into effective solutions for preventing and addressing tenting in asphalt pavements. Additionally, this chapter also presents the results of a survey conducted in this study to collect the feedback from the practitioners in relation to the tenting distress observed in Minnesota.

2.1 Causes and Development of Tenting

Tenting in asphalt pavements is primarily driven by environmental and material factors that affect the overall integrity of road surfaces. A research work conducted by Kestler et al. (2000) characterized tenting as a near-surface phenomenon that is distinct from conventional frost heaving. In conventional frost, the entire pavement section or large areas experience heaving due to freezing and the expansion of water in the soil underneath the pavement. Conversely, tenting occurs when the water/ moisture specifically in the upper part of the pavement base layer becomes ice due to freezing. In other words, it occurs due to differential frost heaving in pavement base layers. Tenting affects the road network badly. According to a survey conducted in the Johnson and Olson (2008) study, as much as 38% of respondents stated that their local road network experienced winter pavement tenting (44% mild, 30% moderate, and 26% high severe). While high-severity cases are less frequent, low-to-moderate severity tenting is widespread across the network, as illustrated in Figure 2.1.

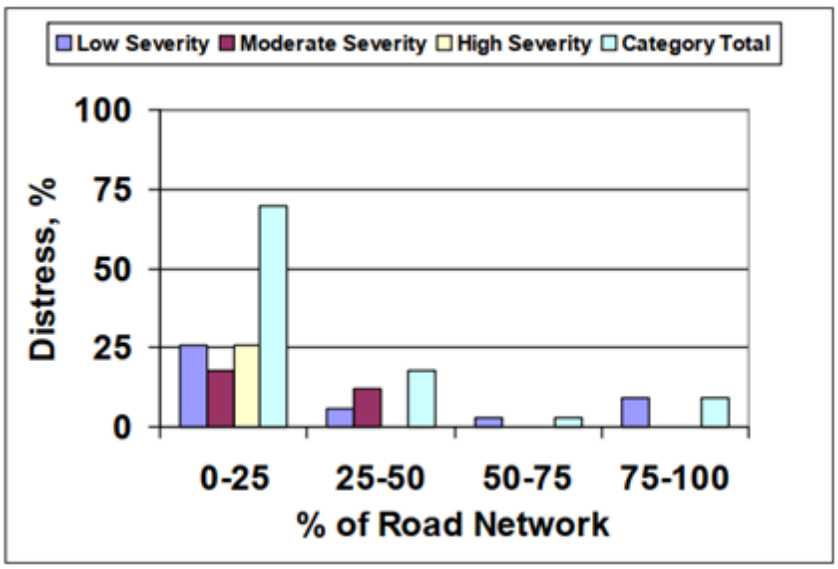

Figure 2.1: Survey results of tenting distress severity across road networks (Johnson and Olson, 2008)

Kestler et al. (2000) concluded that the intrusion of fines from sand-salt mix used in winter road maintenance, and smaller grain-size particles in the base material play a major role in the development of tenting. The excessive fine content accumulated underneath the crack keep the crack raised or tented even during the summer months, which was identified as summer tenting in this study.

According to Casagrande's (1938) study, soils that contain at least 3% of finer particles by weight (specifically those with a grain size smaller than 0.02 mm) are highly susceptible to frost action. The average rates of heave for gravels, sands, silts, and clays are shown in Figure 2.2. As the percentage of the fine particle increases, the average heave rate also increases. In contrast, gravels containing only 1.5% to 3% of particles finer than 0.02 mm may be prone to freezing, whereas uniform sandy soils can contain up to 10% fine particles by weight without becoming frost-susceptible. Consequently, fine content remains a primary metric for characterizing the frost sensitivity of both soils and aggregate blends.

As per the Unified Soil Classification System (USCS) Guide (2018), fines are defined as particles smaller than 0.075 mm, or material that passes through a No. 200 sieve. The frost susceptibility criterion based on the fine fraction differs from agency to agency. Many agencies classify soils and aggregates as frost-susceptible if they contain more than 10% fines (passing the No. 200 sieve) or more than 3% particles smaller than 0.02 mm (passing No. 635 sieve).

The Minnesota Department of Transportation (MnDOT) similarly identifies materials with more than 10% passing the No. 200 sieve as being highly prone to frost-related damage (MnDOT, 2019). MnDOT suggests the fine fraction in the MnDOT Class-5 aggregate base material shall be within 3-10%. Despite the increased risk of frost action, fine fraction is required for several critical reasons. Fines fill the voids between the larger particles which leads to denser mix and better compaction and stability. Moreover, fines increase the workability of the mix, which makes it easier to spread, compact, and finish. However, due to having a greater surface area, the fines retain higher amount of moisture than the larger sized particles. This high moisture retention makes the material highly susceptible to both frost heave and the phenomenon of tenting.

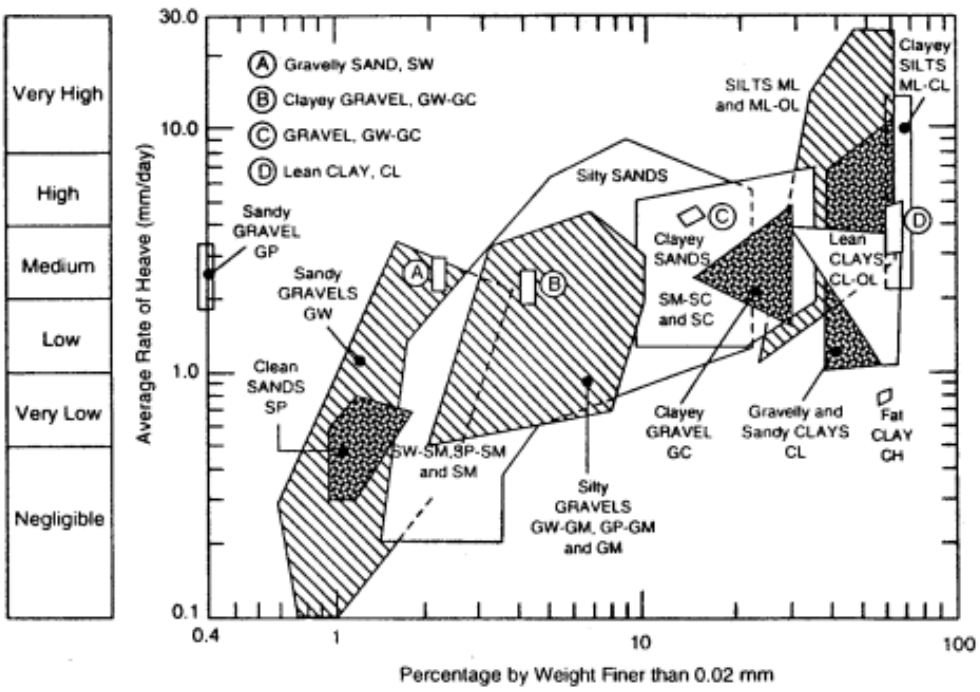

Figure 2.2 Frost susceptibility chart of different types of soil as per grain size (Kestler et al., 2000)

Another important factor is the salt concentration level in the aggregate base around the crack vicinity, which increases the severity of tenting (Kestler et al., 2000). The study conducted by Dore et al. (1997) on the influence of deicing salt on the pavement base frost heave identified that the salt affects the frost heave occurrence significantly even though it is not responsible for its development. During winter maintenance, salt granules or brines enter the pavement structure through transverse cracks, contaminating the base material and underlying layers. Figure 2.3 shows the freezing process of the base materials due to salt contamination. Since salt has a high moisture affinity, it attracts more water from the surroundings of the base material. When the salt concentration level gets diluted, the water freezes, and more heaving occurs. As shown in Figure 2.3, the frost front progresses toward these salt-enriched zones because the salt continues to draw in water, even though the salt-water solution has a lower freezing point than pure water. The study concluded that even materials classified as non-frost-susceptible can behave as frost-susceptible once contaminated by salt due to this enhanced moisture accumulation.

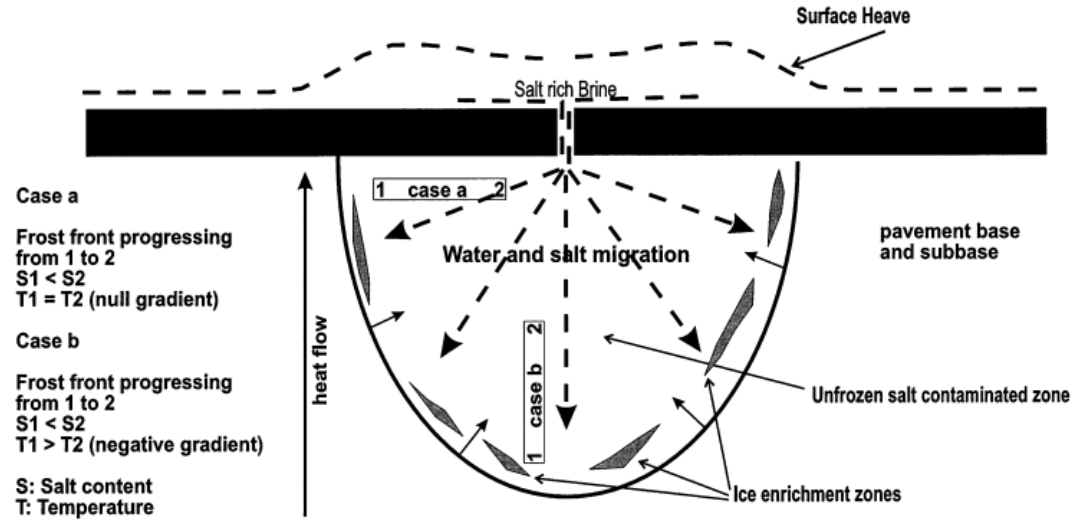

Figure 2.3 Freezing process in pavement base material due to salt intrusion (Doré et al., 1997)

2.2 Assessment of Tenting

The assessment of tenting is crucial for understanding its impact on pavement roughness and ride quality, as well as for studying the effectiveness of various mitigation strategies. The severity of tenting is defined by the peak height of the heaved crack. The research conducted by Teshale et al. (2021) made significant developments in this area by developing a non-destructive testing methodology for the tenting measurement. This research introduced two specific parameters, which are the peak height value (PHV) of the heaved crack and spacing between peaks (SBP) of the consecutive tented cracks, as shown in Figure 2.4.

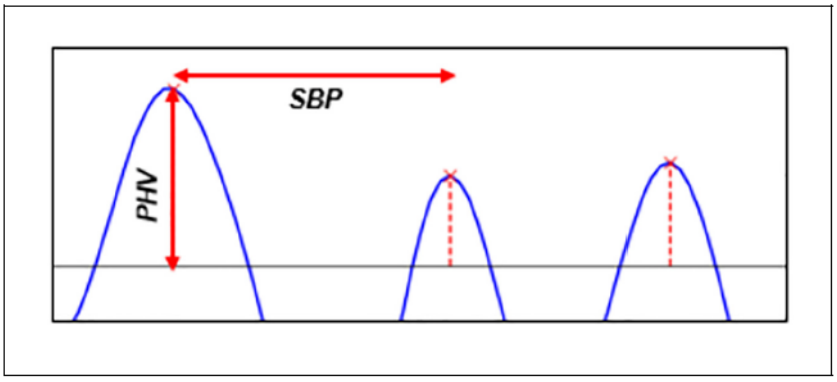

Figure 2.4: PHV and SBP, tenting parameters developed in Zegeye-Teshale et al. (2021) study.

These metrics were used to quantify tenting severity and was correlated with the International Roughness Index (IRI), which quantifies the smoothness of road surfaces. The research findings indicated that the tenting occurrence significantly affects the pavement IRI value. It was found that the higher PHV and lower SBP value leads to higher IRI values, suggesting a direct relationship between the extent of tenting and the overall ride quality of a pavement, as shown in Figure 2.5.

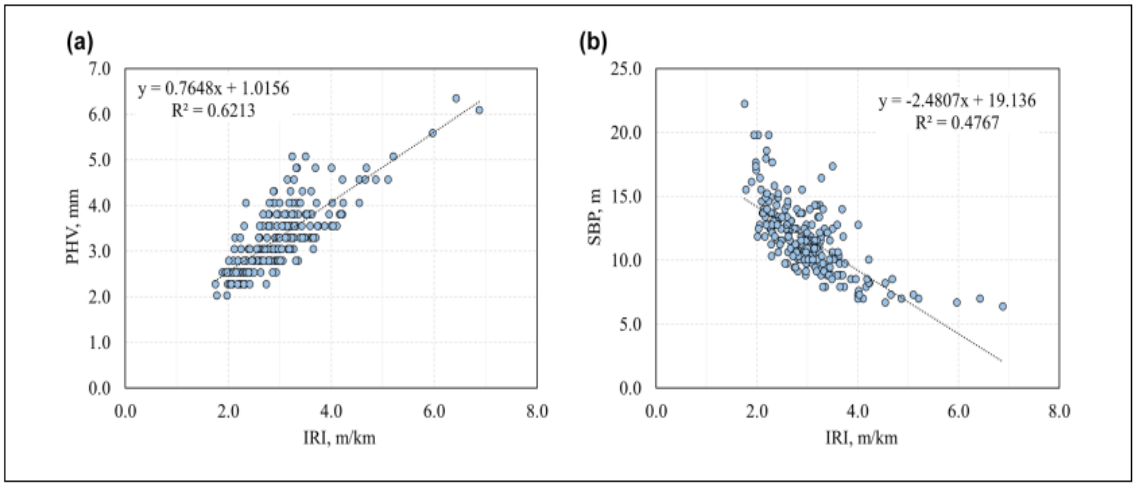

Figure 2.5: Graphs illustrating the relationship between the International Roughness Index (IRI) and the tenting parameters: (a) IRI versus peak height value (PHV); and (b) IRI versus spacing between peaks (SBP) (Zegeye-Teshale et al., 2021)

Research conducted by Johnson and Olson (2008) indicated that the threshold for a tented crack's peak height is 2.5 mm. Beyond this value, tenting significantly compromises ride quality and pavement serviceability. In this study, the vertical heaving of the transverse crack was measured manually by using a steel rule and a 2-ft straight edge placed near the crack. The horizontal movement of the crack over time was also measured by setting up PK nails on both sides of the crack, and the distance between the nails was taken manually at certain time intervals.

The tenting threshold value mentioned in the Johnson & Olson (2008) study can be easily converted to the pavement surface IRI value using the relationship from Figure 2.5(a), which is approximately 2 m/km or 127 in/mile. According to the Federal Highway Administration, an IRI value of 2 m/km or 127 in/mile indicates mediocre pavement roughness, as shown in Table 2.1. Therefore, even the least severe tenting occurrence can significantly reduce pavement surface smoothness.

Table 2.1: Federal pavement roughness thresholds for interstate roads

Condition Term	PSR Rating	IRI
Very Good	≥ 4.0	< 60 in/mi (< 0.95 m/km)
Good	3.5 - 3.9	60 - 94 in/mi (0.95 - 1.48 m/km)
Fair	3.1 - 3.4	95 - 119 in/mi (1.50 - 1.88 m/km)
Mediocre	2.6 - 3.0	120 - 170 in/mi (1.89 - 2.68 m/km)
Poor	≤ 2.5	> 170 in/mi (> 2.68 m/km)

Source: (1999 Status of the Nation's Highways, Bridges, and Transit: Conditions and Performance, Report to Congress, 2001)

Johnson & Olson (2008) determined the concentration of the deicing chemicals in base materials by testing the conductivity of the material and their potential contribution to tenting. The base material samples were collected directly from the tented crack. The conductivity values at different locations and depths showed significant variations, indicating that the salt contamination level is inconsistent but generally decreases with depth and distance from cracks, as shown in Figure 2.6. This suggests that the upper part of the base layer will have more water accumulation, leading to higher tenting susceptibility.

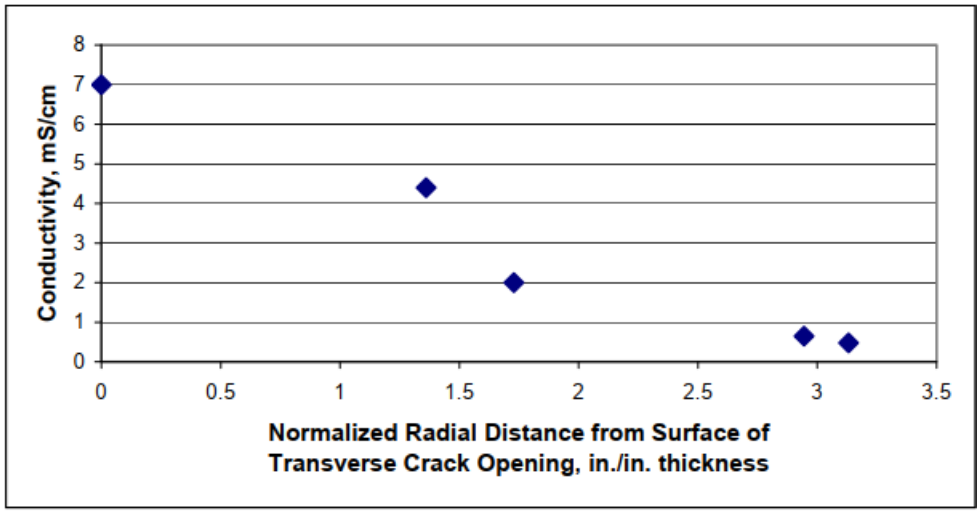

Figure 2.6: Aggregate base materials conductivity test results (Johnson & Olson, 2008)

Kestler et al., (2000) also determined the salt content in the base material by using a soil moisture sensor to understand the role of salinity in freezing point depression and tenting. Higher salinity levels were found closer to the cracks, which indicated that salt contamination from deicing chemicals was concentrated more in the upper part of the base layer around the crack vicinity. However, the salt contamination level varied significantly with depth and distance from the cracks, and the variation was not consistent throughout, as shown in Figure 2.7, which is opposite to the findings of the Johnson & Olson (2008) study. This indicates the complexity of the salt contamination patterns due to environmental and traffic factors.

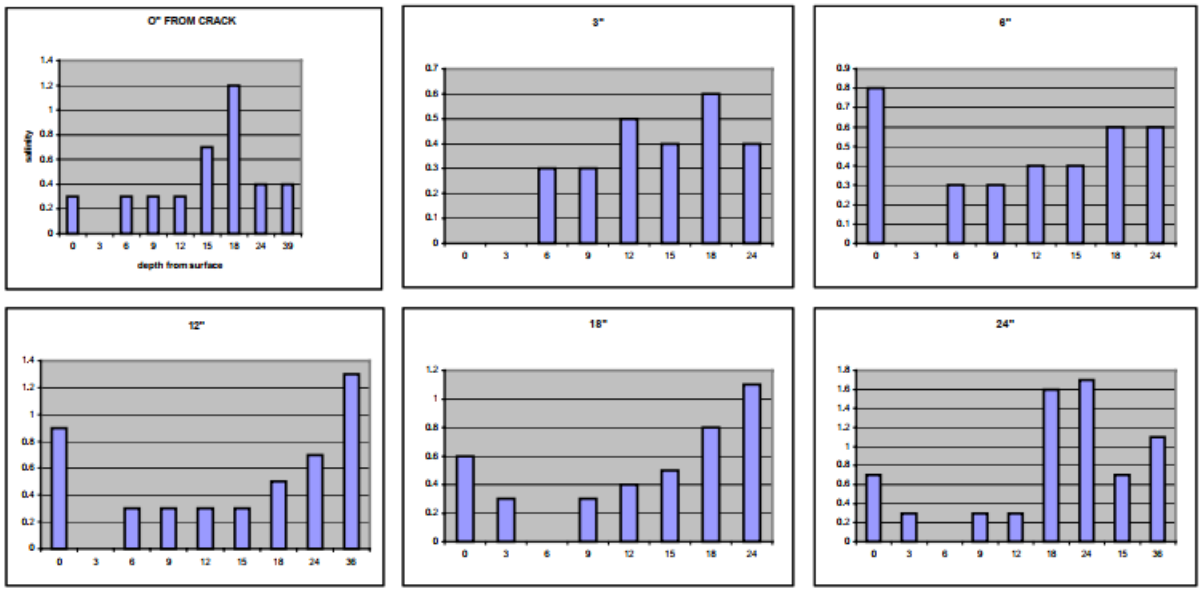

Figure 2.7: Salinity level at different vertical and horizontal distances from the crack (Kestler et al., 2000)

2.3 Effect of Pavement Treatment Methods

This section describes the different treatments that were suggested to mitigate tenting and their effects. Sharma & McIntyre (1991) constructed Retrofit Edge Drains, Retrofit Transverse Interchannel Flow Drains, and crack sealing to mitigate the tenting issue. Edge drain and slotted pipe were directly placed under the transverse crack as the transverse drain was used to remove the infiltrated water from the aggregate base so that less water remains in the crack vicinity to freeze and less heaving occurs. However, they were not found effective in tackling the tenting issue which indicates the poor drainage and permeability of the base layer. C Early attempts at sealing without prior cleaning yielded poor results; however, performance improved significantly when cracks were routed, cleaned, and dried before the sealant was applied. This underscores the necessity of proper surface preparation for sealant adhesion and longevity.

The study conducted by Johnson & Olson (2008) found crack sealing can potentially reduce the tenting height and roughness by up to 35% during the first year. However, crack sealing gets damaged by traffic passing and other environmental factors. The study suggested that using elastic and durable sealant materials that could enhance the longevity and effectiveness of crack sealing. They also discussed the use of mill and overlay treatments to reduce the tenting. It was found that initially, it showed some degree of success in reducing tenting, but it suffered from reflective cracking in subsequent winters and the tenting appears again. The mill and overlay in this study section experienced approximately 50% less tenting than the control section in the first year as shown in Table 2.2. However, the difference in the tenting profiles between the overlayed section and the control section was negligible starting the second winter.

Table 2.2: Comparison of the tenting data between the mill and overlay section and a control section (Johnson and Olson, 2008)

Roadway	Direction	Lane	2006 winter tenting profile, in.	2007 winter tenting profile, in.
Control Section Blackhawk-Kyllo	SB	-	0.221	0.210
Blackhawk-Cochrane	NB	-	0.112	0.210

This study also included a project that treated the pavement with the crack seal followed by a seal coat. It was observed that IRI for the treated project dropped by 18 % compared to the untreated project, as shown in Table 2.3. In this study, the average IRI of the study was 236.1 in./mile, which dropped to194 in./mile after the crack seal and the seal coat were implemented. The highest percentage of winter IRI improvement was observed for the saw and seal joint. The study recommended using highly elastic and durable sealant materials at the cracks prone to tenting.

Table 2.3: Comparison of the tenting and roughness improvement data (Johnson and Olson, 2008)

Roadway	Direction	Lane	2006 winter IRI, in./mile	2007 winter IRI, in./mile	2006 control ratio	2007 control ratio	2006 summer maintenance action	Winter IRI % improvement	Control ratio % improvement
All D1 sections	-	-	133.8	114.7	1.6	1.5	-	14%	3%
Control Section US53	Increasing	Right	84.6	74.6	1	1	None	12%	0%
MN37	Increasing	NA	236.1	194	2.8	2.6	Crack seal and seal coat	18%	7%
US169	Decreasing	Right	110	78	1.3	1	Seal all sawed joints	29%	20%
US169	Increasing	Right	-	72.1	-	1	None	NA	NA
US169	Increasing	Shoulder	151.1	143.8	1.8	1.9	None	5%	-8%
All US 169			130.6	98	1.8	1.9		25%	-8%

The mill and overlay treatment successfully eliminated tenting to some extent, but reflecting cracks were visible during the first winter. It was recommended that the base material's moisture sensitivity and salt contamination level should be taken into account before considering overlay to reduce the possibility of tenting recurrence.

Bush and Brookes (2007) investigated the application of geosynthetic materials to control reflective cracking and Marquis, B. (2004) evaluated the saw-and-seal method to prevent or retard the formation of thermal and reflective cracking on the bituminous overlay. It was found that the saw and seal method in closer spacing (30 ft.) showed some effectiveness in controlling the thermal and reflective cracking. It

was mentioned that the sealant of the two sawed joints was missing on the wheel path, which indicates the possibility of sealant damage because of the high traffic passing. However, deicing salt snow plowing has a detrimental effect on sealant stability, especially when the temperature drops below 15 degrees Fahrenheit.

It was found that the geosynthetic material helped decrease the percentage of cracking. In their study, the percentage of reflective cracking was studied as a function of different categories of geosynthetic material and crack-fill-only options. Figure 2.8 shows the comparison of the percentage of reflective crack length from the year 1999 to 2007. It was found that the GlasGrid 8502 geosynthetic material performed the best in reducing reflective cracking. Since the geosynthetic material can reduce tension transfer to the overlay, the possibility of reflective cracking is minimized.

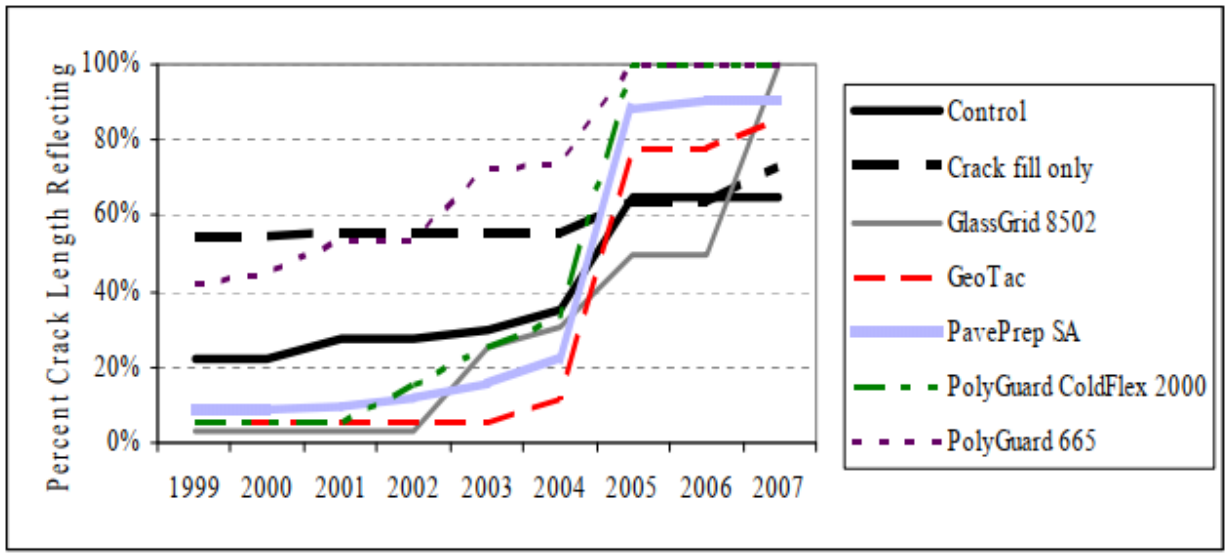

Figure 2.8: Percentage of crack length reflected from the original HMA layer to the overlay (Bush and Brookes, 2007)

Chip seal, slurry seal, patch seal, and crack seal are some of the common preventative maintenance types used in the pavement. Khattak et al. (2013) compared different preventive maintenance strategies for asphalt pavement using the Long-Term Pavement Performance (LTPP) distress data based on the actual pavement performance. This study did not explicitly investigate tenting mitigation but considered the pavement roughness level. Table 2.4 shows the relative ranking of pavement maintenance strategies. It was found that the chip seal exhibited the highest performance factors, and it was ranked the best in terms of overall performance which was calculated by aggregating the average rate of distress acceleration, average duration of fix, and average distress measure together, followed by the slurry seal, patch seal, and crack seal. Although there is no direct relationship between the Pavement Condition Index (PCI) and the overall performance factor, the ranking of the treatments was consistent using both indices.

Table 2.4: Relative ranking of pavement preventive maintenance strategies (Khattak and Alrashidi., 2013)

Maintenance Type	No. of Sections	Normalized Average Duration of Fix	Normalized Average Slope of Distress	Normalized Average Distress Measure	Overall Performance Factor	Average Pavement Condition Index (PCI)
Chip/Aggr Seal	10	3	2	2	1	80 [Very Good]
Slurry Seal	17	2	1	1	2	73 [Very Good]
Patch Seal	11	4	3	4	3	70 [Good]
Crack Seal	10	1	4	3	4	71 [Very Good]

2.4 Online Survey

This study included one online survey to collect the feedback of the practitioners in related to the tenting distress. The online survey questions for this study were prepared in consultation with the TAP members and Technical Liaison, and the survey was shared with stakeholders by the Project coordinator. It may be noted that only two responses were received. Both literature review and responses of the online survey indicated that tenting is a concern and can be caused because of the frosting of the base layer. Excessive fines, de-icing salt, drainage issues are some causes that are responsible for the tenting according to the survey responders. Crack sealing, resurfacing, thin mill, and overlay, etc. have been identified as the potential pavement treatments that can mitigate tenting.

2.5 Summary

- Tenting of the transverse crack is primarily caused by moisture and fine particle accumulation underneath the surface layer through the crack opening. The presence of deicing salt exacerbates the issue by attracting more water.
- Tenting severity is measured by the peak height of the heaved crack. The higher the peak height value, the more severe the tenting. Pavement surface smoothness is significantly affected by the occurrence of tenting, and the surface roughness index (IRI) directly correlates with the tenting peak height value and severity.
- Several pavement treatment methods, such as crack sealing, crack filling, and mill and overlay, have been evaluated to address this issue. Crack sealing was found to be a partially effective localized crack repair for the tenting issue, but the sealant often gets damaged due to traffic and other environmental factors, causing tenting to recur.
- Overlay can significantly reduce pavement roughness levels, but reflective cracking appears on the overlay, creating favorable conditions for tenting development.
- The use of geosynthetic materials and the saw-and-seal method has been evaluated to control reflective cracking and tenting. Geosynthetic materials minimize reflective cracking by reducing

tension transfer to the overlay. The saw-and-seal method showed some success in reducing tenting, but cracks appear parallel to the saw joints, which eventually damages the joints.

- Overall, tenting occurrence and severity depend on several factors, such as fine content, moisture content, and salt content. Different researchers identified each of these factors. It is a complex phenomenon, and there is a need to understand how these factors work together in its development. Different pavement treatment methods were used to mitigate this problem, but none of them were found to be significantly effective. Moreover, there is a lack of understanding of which treatment method is more effective on different types of pavements. Additionally, there is a knowledge gap regarding potential mitigation strategies and the understanding of base materials characteristics that affects the tenting susceptibility which indicates a need for further research to develop effective solutions.

Chapter 3: Research Methodology

This chapter discusses the research methodology. The research work was completed by conducting multiple tasks including a fieldwork, pavement distress data analysis, a laboratory investigation.

The pavement distress data review and analysis work focused on evaluating the effectiveness of various pavement treatment strategies on the road surface roughness. In the field work, tenting was measured at six roads in St. Louis County. For the laboratory investigation, MnDOT Class 5 aggregate samples were collected from two local plants and three road sections where tenting was measured. A total of four samples were collected that vary with respect to gradation. Several laboratory tests were carried out on the collected aggregate base material, including gradation, Proctor/moisture-density relationship, hydraulic conductivity, frost-heave, and salt content vs moisture-absorption relationship.

Figure 3.1 shows the sequence of the key tasks of the project in a flowchart and the sections below provide a comprehensive discussion of these tasks.

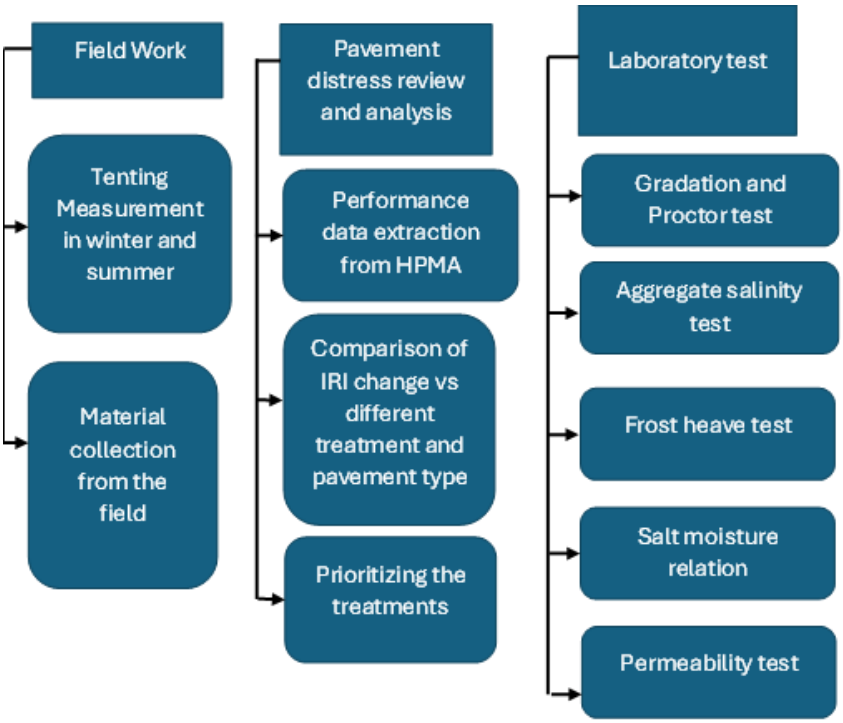

Note: HPMA (Highway Pavement Management Application)

Figure 3.1 Flow chart showing different activities in the study

3.1 Field Work

The comprehensive fieldwork program comprised multiple sub-tasks, primarily focusing on measuring the extent of tenting across selected roadways in St. Louis County, Minnesota. To capture seasonal effects, measurements were taken during both the winter and summer of the same year. Complementing this, loose base material samples were collected from local Duluth roads in late spring 2023 to establish typical salinity levels. Crucially, base samples were also retrieved directly from the three specific project locations where tenting was monitored, allowing for a direct correlation between material properties and field performance.

3.1.1 Tenting Measurement in Field

Six roads with varying designs and traffic levels were selected for measuring the tenting. The measurements were conducted in both winter and summer at identical locations on each road to ensure consistency. The road sections were selected after consulting with the St. Louis County of Minnesota, which also provided traffic control support during the field work. Table 3.1 and Figure 3.2 present the details of the locations, average annual daily traffic (AADT), surface and base layer thicknesses, and names of the roads where tenting was measured.

Table 3.1 Details of road sections where tenting was measured.

Road Name	Begin Ref. point	End Ref. point	AADT (Constr. year)	HMA thickness (in)	Base thickness (in)
CSAH 9 (Wallace Ave)	CSAH 9 (E 4th St)	East St. Marie Street	3,650 (2015)	5	7
CSAH 11 (Stark Rd)	CSAH 13 (Midway Rd)	Summit Ave in Proctor	945 (2021)	3.5	10.5
CSAH 19 (St. Louis River Rd)	CSAH 13 (Midway Rd)	CR 898 (Lindahl Rd)	531 (2021)	5	7.5
CSAH 34 (Howard Gnesen Rd)	CSAH 9 (Martin Rd)	CSAH 43 (Emerson Rd)	940 (2019)	3.5	12
CSAH 89 (Stebner/Getchell Rd)	Vinland St	Approx 0.25 mi N of St. Louis River Rd	5,100 (2019)	7	5

Road Name	Begin Ref. point	End Ref. point	AADT (Constr. year)	HMA thickness (in)	Base thickness (in)
CSAH 48 (Lavaque Rd)	CSAH 14 (5th Street)	CSAH 56 (Morris Thomas Rd)	3,000 (2015)	5.5	14.5

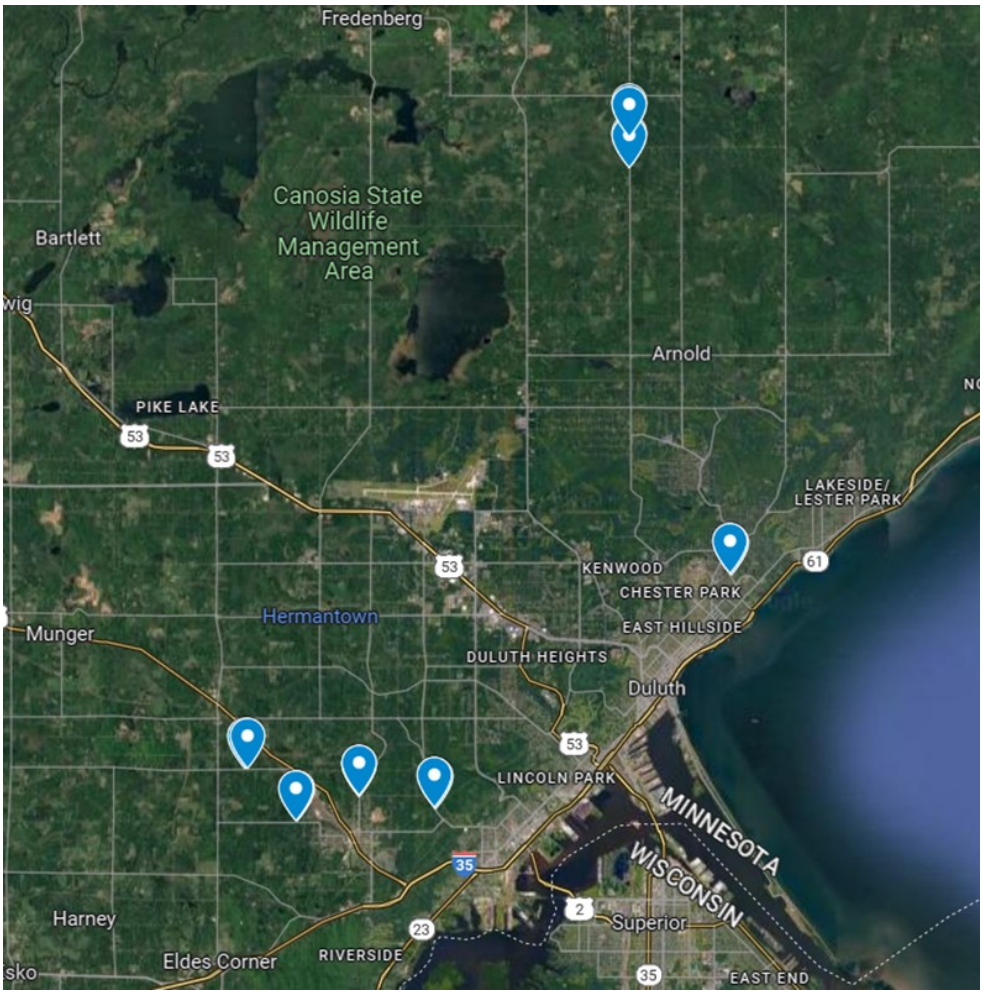

Figure 3.2 Locations of the tenting measurement project sites (Google Map).

Figure 3.3 shows the tenting measuring device fabricated at UMD and the measurement process in the field. The length and height of this device are 1,200 mm and 150 mm, respectively. A steel angle was used for fabricating this device. The peak height of the tented transverse crack was measured at three different locations along the length of the crack—the center and the two road edges. A vernier caliper

was used to measure the elevations of the crack from the datum line (horizontal member of the tenting measuring device).

Figure 3.4 shows the tenting peak height calculation procedure. For each tenting measurement, at first, the measuring device was placed on the road centering crack as shown in Figure 3.3. Three elevation readings, h_1, h_2, and h_3 were taken. The peak height was calculated using Equation 1.

Figure 3.3 Tenting measuring device and the location of the measurements in a transverse crack

$$\text{Peak height} = h_3 - \frac{h1+h2}{2} \qquad \text{Equation 1}$$

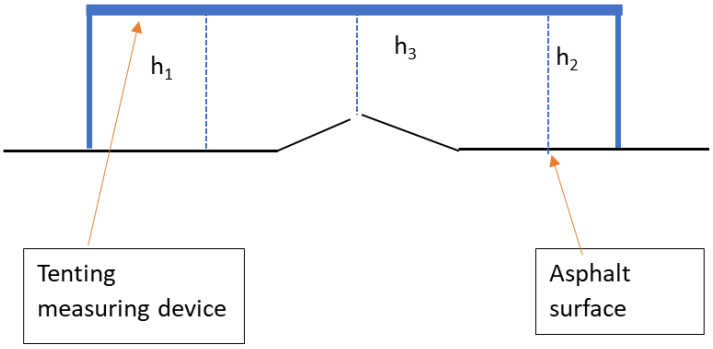

Figure 3.4 Procedure for calculating the peak height of tenting

3.2 Pavement Performance Data Analysis

To investigate the effect of pavement treatments on the transverse cracks, indirectly on tenting, the distress and roughness data from various roads across eight MnDOT districts were reviewed and analyzed. Only road sections where the primary distress was transverse cracking were included in this analysis, as tenting is specifically associated with transverse cracks.

Data was extracted from MnDOT's road performance database, the Highway Pavement Management Application (HPMA). A total of 8,087 data points (road sections) were considered in the statistical analysis. The IRI data utilized as the primary roughness indicator. IRI values were extracted for the periods immediately before and after each treatment. The change in IRI was then calculated and expressed as a percentage to quantify effectiveness of treatment, using the following equation.

$$\text{Effectiveness of treatment (ET) \%} = \frac{\text{IRI before applying the treatment} - \text{IRI after applying the treatment}}{\text{IRI before applying the treatment}} \times 100$$

Equation 2

The positive value of ET indicates an improvement in the riding quality or a decrease in the roughness and the negative value of ET indicates the opposite. Table 3.2 is an example of the historical performance/distress of a pavement section in the HPMA database. In 2010, the IRI was of this section was 253.11 inches/mile, which was treated with the "Reclaim and Overlay" in 2011. The IRI after the treatment was recorded as 44.35 inches/mile. The ET for this section is calculated as 82.48 %, indicating an increase in the riding quality.

For the pavement performance data analysis, three different pavement types were considered: bituminous over aggregate base (BAB), bituminous over bituminous (BOB), and bituminous over concrete (BOC). Six different types of treatments were considered. The ET values were categorized and compared based on the pavement types. The treatments were ranked based on the average ET value.

3.3 Laboratory Investigation

3.3.1 Materials Collection

Four different aggregate base materials were collected directly from two construction plants, each having a different gradation. These four samples were labeled as SO, SON, SN, and SNN. These base materials were used for laboratory testing. A small amount of base material was also collected from some potholes (locations were close to UMD) to determine the salinity level in the aggregate base layer in the early spring. Figure 3.5 and Figure 3.6 show a few photographs related to the aggregate base materials collection.

Table 3.2 An example of performance data of a road section in the HPMA tool

Year	PQI	RQI	SR	SAR	IRI	Rut	Friction	Activity	Pavement
2021	3.6	3.5	3.8	0	74.33	0.22	0		BAB
2020	3.6	3.6	3.6	0	69.05	0.21	0		BAB
2019	3.6	3.6	3.6	0	66.35	0.24	0		BAB
2018	3.8	3.7	3.9	0	60.94	0.21	0		BAB
2017	3.8	3.7	4	0	56.25	0.26	0		BAB
2016	3.8	3.8	3.9	0	52.55	0.13	0		BAB
2015	3.9	3.8	0	0	52.2	0.13	0		
2014	3.9	3.9	4	0	48.19	0.11	0		BAB
2013	3.9	3.9	4	0	46.79	0.11	0		BAB
2012	3.9	3.9	4	0	45.95	0.12	0		BAB
2011	4	4	4	0	44.35	0.11	0		BAB
2010	1.9	1.6	2.2	0	253.11	0.33	0	Reclaim & Overlay	BAB
2009	2	1.7	0	0	259.89	0.3	0		
2008	2.2	2.1	2.4	0	215.22	0.26	0		BAB
2007	2.1	1.9	0	0	239.8	0.31	0		
2006	2	1.8	2.3	0	248.83	0.33	0		BAB
2005	2.3	2.2	0	0	202.9	0.29	0		
2004	2.2	2.1	2.4	0	218.86	0.17	0		BAB
2003	2.6	2.2	0	0	208.7	0.24	0		
2002	2.8	2.5	3.1	0	170.5	0.21	0		BAB
2001	3	2.5	0	0	169.79	0.13	0		
2000	3.3	2.9	3.7	0	115.32	0	0		BAB
1998	3.4	3.1	3.7	0	99.32	0	0		BAB
1996	3.4	3.2	3.7	0	125.16	0	0	Spot overlay (Maint)	BAB
1994	3.2	3.2	3.2	0	120.73	0	0		BAB
1992	3.5	3.5	3.5	0	107.56	0	0		BAB
1991	3.7	3.7	3.7	0	96.54	0	0		BAB
1988	3.7	3.8	3.7	0	0	0	0		BAB
1985	3.7	3.6	3.8	0	0	0	0		BAB

Figure 3.5 Aggregate base material collection from the Plants.

Figure 3.6 MnDOT Class 5 Materials used in the lab for testing

The laboratory tests were carried out to evaluate the properties and performance of the collected aggregate base materials from plants and road sections. Various tests, including gradation, proctor, salinity, frost heave, and permeability tests, were conducted. These tests were conducted to understand

how different aggregate blends affect moisture retention, compaction, and resistance to frost action. By analyzing these properties, the study sought to identify the best approach to characterize the base layer materials that can minimize tenting and improve pavement durability. All these testing procedures are described below.

3.3.2 Gradation / Sieve Analysis

Sieve analysis was conducted on the base material sample to determine the particle size distribution. Previous research had indicated that tenting is caused by excessive fine content, so obtaining the actual fine content was very crucial for this investigation. The wash gradation method was adopted since it gives more accurate results than the dry method. The test was conducted in accordance with the AASHTO T 11 guidelines.

Approximately 3,000 g of aggregates were taken from each aggregate blend and subjected to washing over the No. 200 sieve to remove particles smaller than 0.075 mm from the mix. The aggregate blend was delicately mixed with water and rinsed, facilitating the dissociation of fine particles from the coarse aggregate. The mixed water was drained through the No.200 sieve very carefully so that only the fines were removed from the mix. The washing process continued until the mixed water exhibited a relatively clean color, which is an indication of the removal of a significant amount of fines. Subsequently, the washed aggregates were dried in an oven for 24 hours at a temperature of 110 °C. Once completely dried, aggregate sample was sieved. The retained weight of aggregates on each sieve was then measured.

3.3.3 Proctor Test

Proctor test was performed to determine the relationship between the moisture content and the dry density of the compacted aggregate base materials. It was performed in accordance with AASHTO T 99, method C (Mn/DOT Modified) standard.

The aggregates were dried at 60°C temperature in the oven since it is dampened after being collected from the field. Then, the lumps in the dried aggregate were broken gently so that the natural size of the individual aggregate did not change. The aggregates were sieved through a ¾" sieve, and the retained aggregates were discarded. The discarded weight was replaced by the aggregates, which passed through the ¾" sieve and retained on the #4 sieve. The aggregates were thoroughly mixed again and considered as a representative sample of the actual field mix. After making the sample mix, around 2,500 grams of dry aggregates were taken from the mix and dampened with a very low moisture content (2%). After mixing the aggregates thoroughly with the water, the aggregates were put in the steel mold and compacted with the rammer. It was compacted in three layers, with each layer tamped 25 times. After the compaction, the extension collar was removed, and the surface was leveled off with a straightedge and spatula. Then, the weight of the compacted sample was taken. After taking the weight, the sample was dismantled from the cylindrical mold, and approximately 500 grams of the representative sample were taken in the container for a moisture content test. The remaining material was thoroughly

pulverized and mixed with the required amount of water and aggregate. A subsequent mix was prepared with a 2% increase in moisture content, and the compaction procedure was repeated. This cycle continued in 2% increments until the compacted sample weight began to decrease, indicating the optimum moisture content had been exceeded. Figure 3.7 shows pictures of the proctor test of the aggregate base material.

Figure 3.7 Photographs showing Proctor test of the base material

3.3.4 Salinity Test

The aggregate salinity test was conducted using the electrical conductivity and total dissolved solids (TDS) method. The electrical conductivity test was performed by following ASTM D1125 method and the TDS was determined in accordance with the ASTM D5907 method. The TDS method was used to get more accurate or direct results. As stated before, the aggregate base samples for salinity test were collected from a few potholes. Electrical conductivity (EC) is a rapid method for determining the salt content by measuring the conductive current passing through the sample. The equation given below was used to determine the salt content from the conductivity reading.

$$TDS\ [ppm] = 0.54\text{-}0.96 * EC\ [uS/cm] \quad \text{……. Equation 3}$$

The aggregate base samples were submerged in water for 24 hours to dissolve the salt in the water. After 24 hours, the water was taken out for the submerged aggregate sample and used for testing. For

the electrical conductivity test, two different stock samples were prepared with a known conductivity of 4,000 uS/cm and 2,000 uS/cm, respectively. The stock solutions were used to calibrate the conductivity meter.

First, the conductivity meter was calibrated using the stock solution. Then, the meter probe was inserted into the liquid sample, and the conductivity value was determined. The salt concentration values were obtained from the conductivity and the total dissolved solids (TDS) concentration equation (Equation 3).

For the TDS test, 100 ml porcelain crucibles were dried and weighed first. Then, approximately 50-75 ml of properly mixed liquid samples were taken and poured into the vacuum flask through the filter paper. After pouring through the filter paper, the liquid samples were placed in the crucible again. The flask was cleaned with an extra 10 ml of distilled water to make sure that there was no sample remaining in the flask. The crucibles were then weighed and put in the oven for 24 hours. After the crucibles were completely dried, the dried crucibles' weight was recorded, and the TDS value was obtained by using the equation below (Equation 4).

$$\text{Total Dissolved Solids (mg/L)} = \frac{\text{weight of residue and crucible (g)} - \text{weight of crucible (g)}}{\text{volume of the sample (L)}} X\ 1000$$

Equation 4

3.3.5 Frost Heave Test

A one-dimensional frost heave test setup was developed to measure the heaving value of the base material. The primary focus of this test set-up is to replicate the field frost heaving condition of the pavement base layer. Frost heave test was performed in two different conditions.

3.3.5.1 Condition 1- Varying temperature gradient

The first condition involves simulating the varying temperature gradient across the depth of the base layer (a cold-warm temperature gradient). In this configuration, the bottom 1/3rd of the sample was kept warm using insulation and a heating arrangement, and the top 2/3rd was kept frozen. This setup was designed to simulate the cryosuction phenomenon, in which water from unfrozen wet soil or aggregate fines migrate upward toward frozen part of the base layer.

In this test, blended base materials meeting the gradation requirements for Minnesota Class 5 granular aggregates, were compacted into polyvinyl chloride (PVC) molds with internal dimensions of 150 mm in diameter and 300 mm in height. Following compaction, the specimens were subjected to controlled freezing within a freezer. Figure 3.8 shows the complete testing processes and the setup.

To facilitate cryosuction phenomenon during freeze conditions, each mold was perforated with 1.6 mm diameter apertures. Circumferential perforations were spaced at 12.5 mm intervals and positioned approximately 6 mm above the mold base. Additionally, four bottom perforations were introduced per quadrant, maintaining a uniform radial distance of 50 mm from the mold center. This configuration

enabled water ingress during freezing events. A similar methodology was adopted by Guthrie and Hermansson (2003) in their study.

Aggregate placement was performed in four discrete lifts, with each layer compacted via 41 blows from a 4.5 kg rammer dropped from a vertical height of 18 inches. The blow count was selected to ensure energy equivalency with the compaction effort in standard Proctor test.

In trials assessing salt-induced heave response, a saline solution of 19.2 g/L was utilized as pore fluid. This dosage was selected based on the study conducted by Johnson and Olson (2008). The salinity level of the base materials collected from the potholes under the current study was much lower than the 19.2 g/L reported in above mentioned study. Following compaction, each test specimen was submerged in deionized water for a duration of 24 hours to ensure complete saturation—simulating the worst-case moisture condition prior to freezing. The saturated specimens were then transferred to the frost-heave test setup and positioned such that the lower one-third of each sample was enclosed within a Styrofoam-insulated box, while the remaining upper two-thirds were left exposed to the ambient subzero environment.

A steel tray filled with water and equipped with heat tape was placed within an insulated enclosure to maintain a bath temperature of 4–6 °C. This configuration established a controlled vertical thermal gradient across the specimen, allowing the uninsulated upper portion to freeze while the lower section remained unfrozen and in contact with the liquid water.

To monitor thermal conditions, two calibrated thermocouples (temperature measuring sensor) were installed in each specimen at designated depths. A hard circular plastic plate was placed over the test sample, and a digital indicator was placed on top of that plate to measure the heaving. All specimens were subjected to a continuous 96-hour freezing period, with heave measurements recorded at 24-hour intervals. The duration was selected to allow sufficient time for capillary-driven water migration, which is essential for frost heave manifestation. A similar freeze exposure period was employed in the frost heave investigation conducted by Ćwiąkała et al. (2016).

a) Predrilled mold (Upside down)

b) Thermocouple attached inside the PVC mold

c) Sample compaction

d) Compacted sample

e) Sample saturation inside the water filled bucket

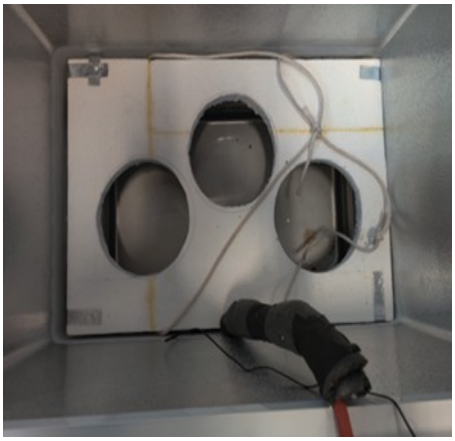

f) Styrofoam insulated chamber inside the freezer

g) Samples inside the freezer

Figure 3.8 Complete frost heave testing process and the setup

3.3.5.2 Condition 2- Uniform temperature gradient

The second testing condition subjected compacted aggregate samples to a uniform temperature of -40 °C (-40 °F) within a freezing chamber, thereby eliminating thermal gradients. This temperature was selected to replicate the typical minimums experienced by Minnesota pavements. This isothermal condition simulates the effects of prolonged exposure to extreme cold, promoting the formation of uniform ice lenses throughout the depth of the specimen. Sample preparation procedure was the same in both conditions 1 and 2.

3.3.6 Permeability/ Hydraulic Conductivity Test

A hydraulic conductivity (also known as permeability) test was conducted to measure the drainage properties of the base material. The test followed ASTM D2434-68, a standard for permeability testing of coarse-grained soils. The objective was to compute the coefficient of permeability/hydraulic conductivity for different aggregate base gradations. This coefficient is defined as the rate of water discharge through a unit cross-sectional area of soil at 20°C under laminar flow conditions. The unit of measurement is cm/sec or ft/day, which is the same as velocity. Its computation is based on Darcy's law, which states that the amount of water flowing through the soil is directly proportional to the soil cross-sectional area and the difference in water head levels and inversely proportional to the length of the soil specimen.

The equation for the coefficient of permeability is derived from the Darcy's law and is given below.

$$K = \frac{QL}{\Delta hAt} \qquad \text{Equation 4}$$

Where,

Q= Quantity of the flow
t= time of the flow
Δh= Difference in water levels/ head difference
A= Area of the soil specimen
L = Length of the soil specimen

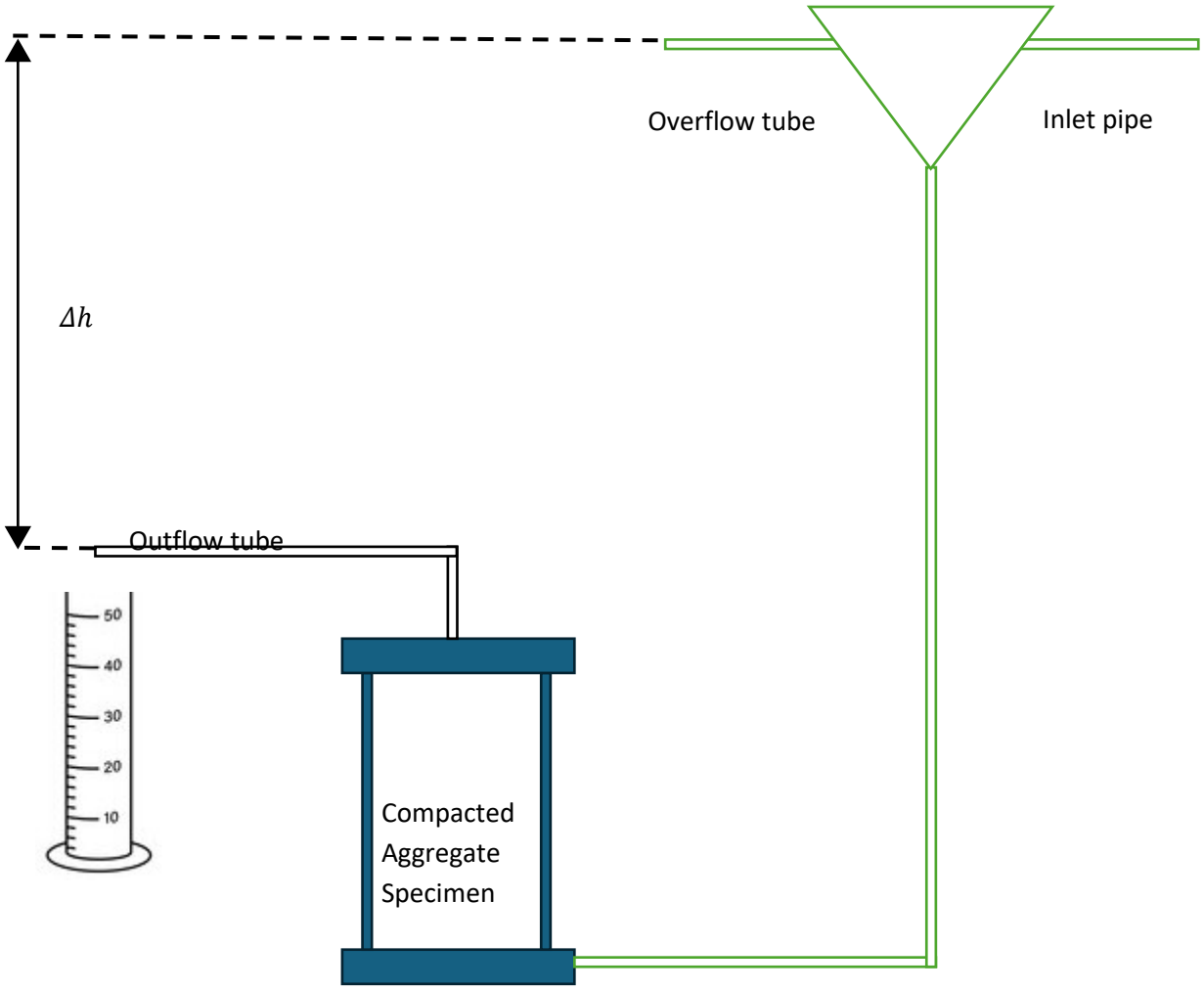

Figure 3.9 Diagram of the constant head permeability test setup

A schematic diagram of the permeability test setup is shown in Figure 3.9. The aggregate base materials collected from the field were dried first in the oven at 60°C to remove excess moisture. The dried materials were mixed thoroughly to ensure that there were no lumps in the mix. The dried aggregate was then mixed with its respective optimum moisture content to achieve the highest degree of compaction. The specimens were prepared to achieve the maximum density, replicating actual field conditions. After mixing the aggregate blend with water, it was compacted in the mold using the tamping weight, as shown in Figure 3.10. Before placing the aggregate sample inside the mold, a porous stone and filter paper were placed at the bottom of the mold. Then, the aggregate mix was placed in three layers in the mold and compacted. The specimen weight was measured after compaction to determine the achieved compaction relative to the maximum dry density (MDD) of the mix.

Figure 3.10 Aggregate mixed with water at OMC and Compacted sample in the permeability test mold.

After compaction, another porous stone and filter paper were placed on top of the sample. Then, the top lid was placed on top of the mold. Vacuum grease was applied to the sides of the mold before closing the lid to ensure an airtight seal. The specimen was attached to the inlet water pipe to allow water to run through the sample. The flow of water was adjusted slowly until a constant water head level was achieved. The specimens were kept under this water flow until they were completely saturated. Water was collected in a graduated cylinder from the outflow tube, and the collection time was recorded. This process was repeated multiple times until readings were consistent, indicating steady flow. The closest three readings were used to compute the coefficient of permeability. Water temperature was also recorded to determine the viscosity correction factor. The head difference in the water level, or the height difference between the inflow and outflow, was also recorded. Figure 3.11 shows two images of the constant head test setup.

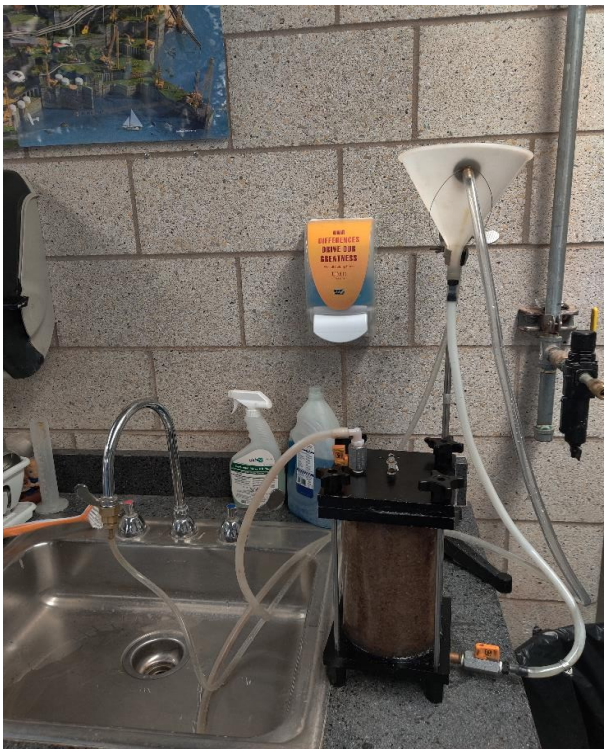

Figure 3.11 Permeability test setup images

3.3.7 Specific Gravity Test

The specific gravity of the blend was determined by calculating the weighted proportion of coarse and fine aggregates in each blend. The following formula was used to calculate the specific gravity of the blend.

$$G_{sb} = \frac{P_{CA}+P_{FA}}{\frac{P_{CA}}{G_{CA}}+\frac{P_{FA}}{G_{FA}}} \qquad \text{Equation 5}$$

Where,

G_{sb} = Specific Gravity of the blend
P_{CA} = % of coarse aggregate in the blend
P_{FA} = % of fine aggregate in the blend
G_{CA} = Specific gravity of coarse aggregate
G_{FA} = Specific gravity of fine aggregate

The procedures for specific gravity test are described below.

3.3.7.1 Specific Gravity Test of Coarse Aggregate

The test was performed in accordance with ASTM C127. The aggregates were dried in the oven for 24 hours at 110°C. Approximately 2,500g of coarse aggregate was taken and submerged in water for 24 hours. Then, the water was drained, and the aggregates were placed on a non-pervious surface. The aggregates were dried using a cloth towel until all surface water film was removed to bring the aggregates into a saturated surface dry (SSD) condition. After removing all the surface water, the SSD test sample was weighed and immediately submerged in water by placing the aggregates in a wire mesh basket, and the submerged weight was recorded, which is shown in Figure 3.12. The specific gravity was then calculated using the following equation.

$$\text{Bulk specific gravity} = \frac{\text{Weight of SSD test sample in air}}{\text{Weight of SSD test sample in air} - \text{Weight of saturated test sample in water}}$$

Equation 6

Figure 3.12 Coarse aggregate submerged in the water

3.3.7.2 Specific Gravity Test of Fine Aggregate

The testing procedure for fine aggregate parallels that of coarse aggregate and was conducted in accordance with ASTM C128. First, the aggregates were dried in the oven. Then, the aggregates were placed in a bowl and submerged in water for 24 hours. The excess water was then drained very slowly from the bowl to ensure no fines were lost. The wet aggregate was spread on a non-absorbent surface (steel tray) and dried using a heat gun and the drying process continued until achieving saturated surface dry (SSD) particles as per ASTM C128 (Figure 3.13). During the drying process, the aggregates were mixed frequently to ensure homogeneous drying.

Figure 3.13 Fine aggregate drying using heat gun (left) and checking for SSD condition (right)

Upon achieving the SSD condition, approximately 500g of aggregate was placed in a pycnometer. The pycnometer was filled to approximately 80% of its total volume. It was then agitated for about 3-4 minutes to remove air bubbles from the aggregate-water mix. The water level in the pycnometer was brought to its calibrated capacity, and the total weight of the pycnometer, plus the sample and water, was determined. After recording the weight, the water-aggregate mix was placed in a bowl and kept in the oven for drying. The pycnometer was refilled with water up to the calibration mark, and the weight was recorded. Finally, the dry aggregate weight was taken once aggregates was completely dried.

The specific gravity of the fine aggregate was then determined using Equation 7.

$$Bulk\ Specific\ Gravity\ =\ A/(B+S-C) \qquad \text{Equation 7}$$

Where,

A = weight of oven dry test sample in air
B = Weight of pycnometer filled with water in air
S = Weight of saturated surface dry sample in air
C = Weight of pycnometer filled with SSD sample and water

3.3.8 Test for Studying Moisture Affinity of Salt-mixed Aggregate Samples

While salt-mixed aggregates typically attract moisture via osmosis, this effect may be negligible in laboratory settings due to the reduced scale compared to field conditions. To investigate this, a comparative experiment measured moisture uptake in salt-mixed versus un-salted aggregates. Samples were compacted at Optimum Moisture Content (OMC) in 100 mm × 200 mm PVC molds. The mold bases were perforated with 1.57 mm holes spaced at 12.7 mm to permit water ingress and facilitate potential osmotic flow. Figure 3.14 shows the diagram and image of the test setup. The samples were prepared with a constant salt dosage of 19.2 g/l. The compacted test samples were kept for saturation for 24 hours. After saturation, the test samples were placed on a steel tray filled with water. The weight of the samples before and after saturation was compared to determine the moisture uptake by salt-mixed aggregate samples from the tray.

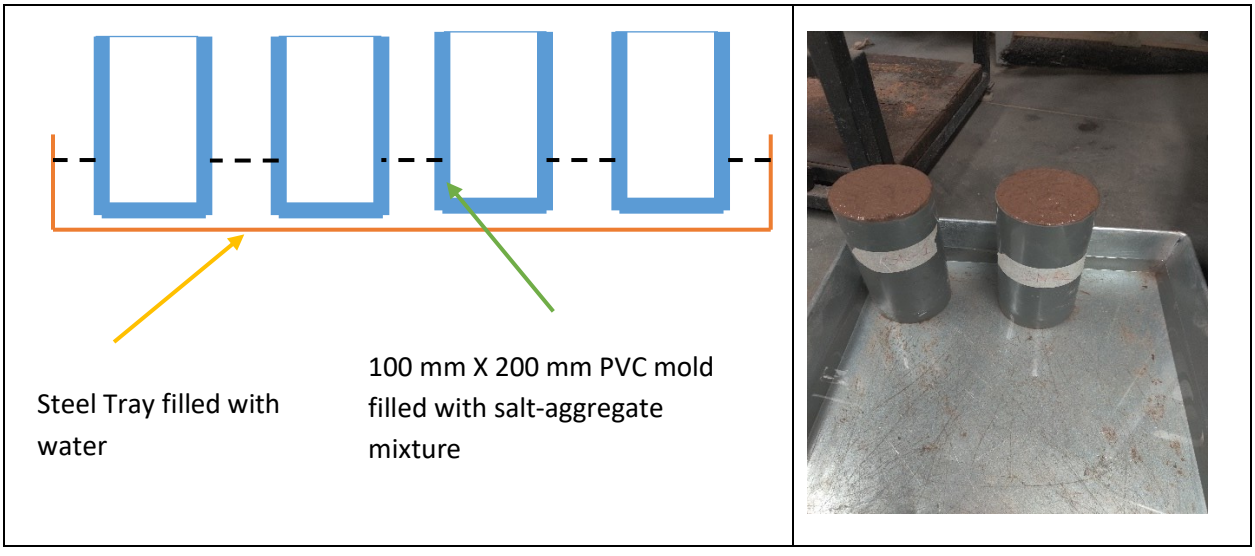

Figure 3.14 Moisture affinity study.

Chapter 4: Results and Discussions

This chapter synthesizes the results obtained from field measurements, pavement performance analysis, and laboratory testing. Data are presented through comprehensive tables and figures to illustrate key trends. The chapter provides with a detailed discussion of the results.

4.1 Quantitative Assessment of Tenting in Field Conditions

4.1.1 Tenting Measurement in this Study

Figure 4.1 presents the average peak tenting height (or simply tenting) measured across the six road sections. The results presented in this figure are the average results of the four to six cracks measured in each road section. In each crack, at least three measurements were taken. The readings of the six cracks in Wallace Avenue, where tenting was quite high, are presented in Figure 4.2 for showing the variation in the tenting at different cracks at one location; these measurements were taken in winter.

Two sections exhibited significant tenting, with average tenting heights reaching 14 mm. Notably, four of the six sites retained measurable tenting even during the summer. Conversely, two sections displayed negative tenting (cupping); this phenomenon was associated with wide, deteriorated cracks in one section, and sawed-and-sealed transverse cracks in the other.

Figure 4.3a, b and c show the correlation of the tenting with the base layer thickness, asphalt surface layer thickness, and AADT. The correlation between tenting and base thickness was weak. It shall be noted that each data point is the average of the tenting measured at three different locations along the crack length. The correlation between tenting and the HMA thickness is also weak, as shown in Figure 4.3b. The data points are scattered throughout the graphs, indicating no relation between these two. Figure 4.3c shows the correlation between tenting and AADT. The R^2 value is 0.5, indicating a moderately positive correlation, suggesting that higher traffic volumes accelerate tenting by promoting moisture and fines infiltration. The weak to moderate correlations of the tenting with the factors mentioned was expected, as a full factorial analysis could not be performed due to the limited data size. For example, when assessing the influence of base and asphalt layer thickness, roads with identical AADT values could not be directly compared due to the absence of sites with matching traffic volumes.

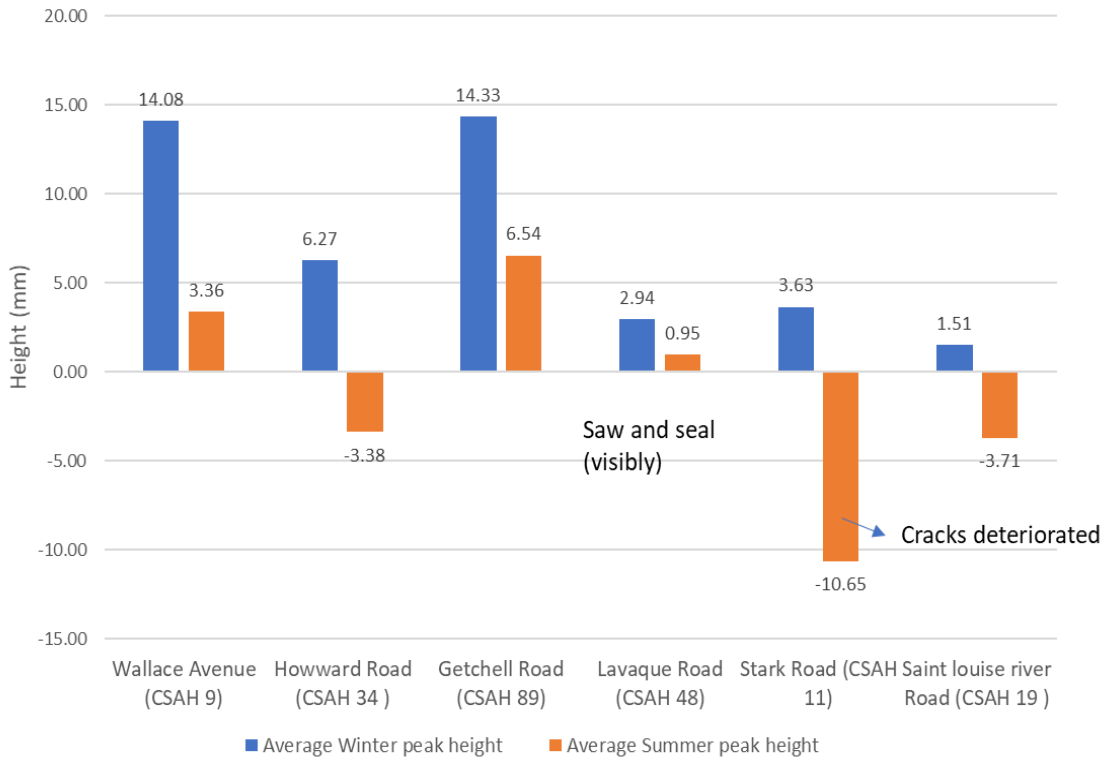

Figure 4.1: Average winter and summer tenting peak height of different roads.

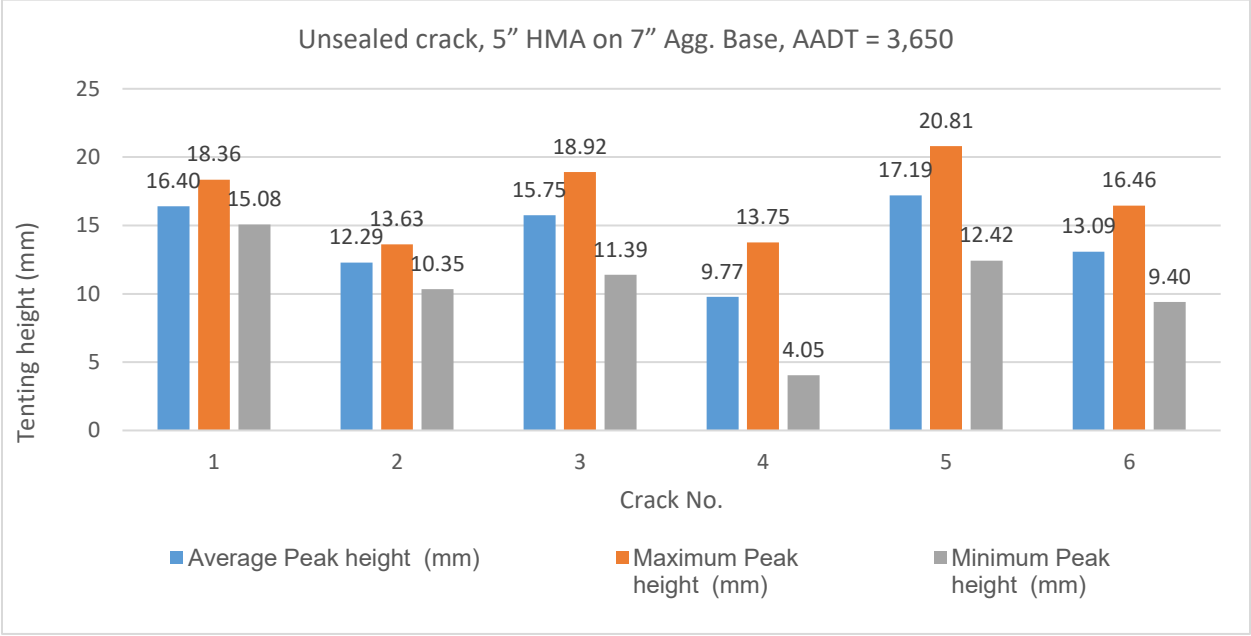

Figure 4.2: Average winter tenting peak height data of Wallace Avenue (CSAH 9).

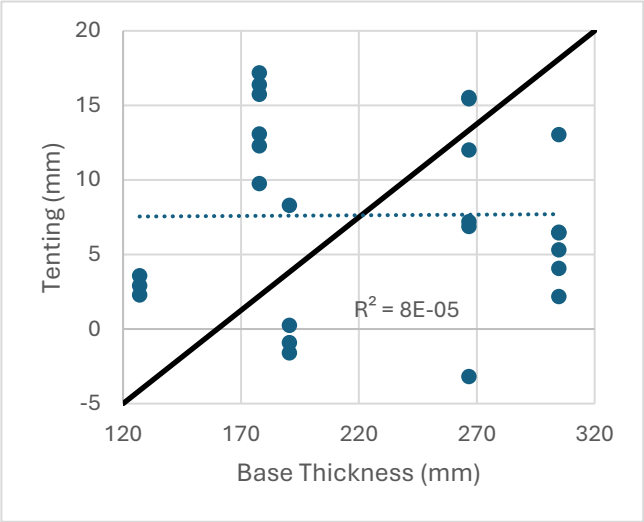

a) Tenting vs base thickness

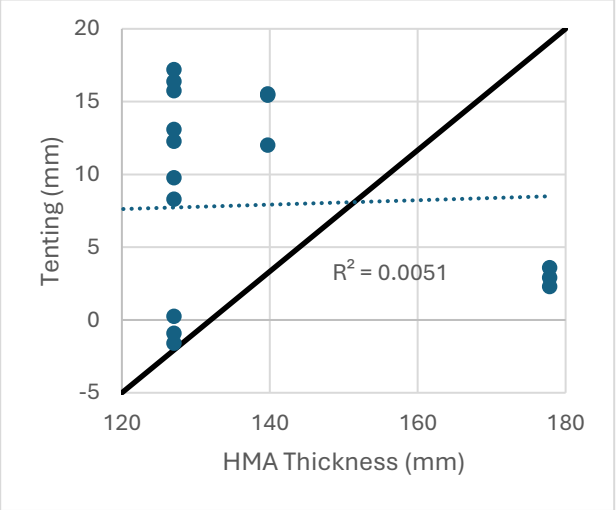

b) Tenting vs HMA thickness

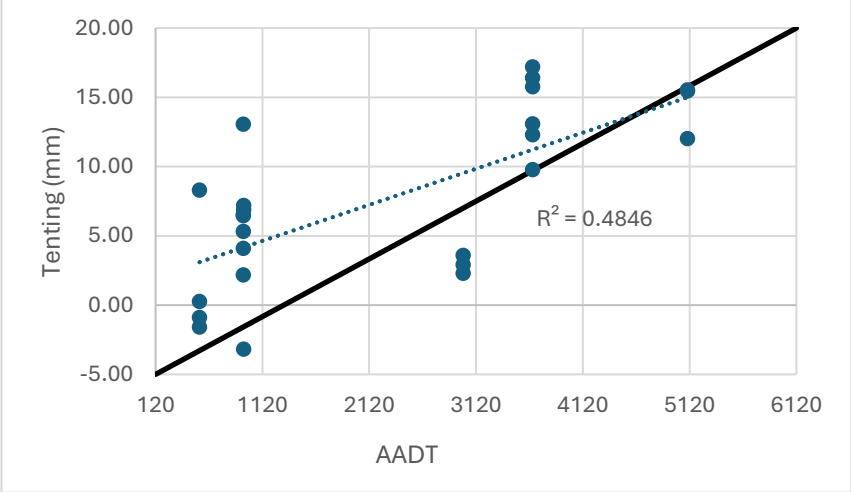

c) Tenting vs traffic volume

Figure 4.3: Tenting comparison with the base thickness, HMA thickness, and traffic volume (AADT)

4.1.2 Tenting Measurement in Zegeye-Teshale et al. (2021) Study

Zegeye-Teshale et al. (2021) measured tenting in three highways in MnDOT District 1, namely, MN-37D, US-169D, and US-169I in 2020 (winter, February) and 2021 (summer, June) using the MnDOT's multi-

sensor survey van; the data was analyzed by commercially available ROAD DOCTOR software. Table 4.1 provides the details (surface and base layers information) of the three highways mentioned above. Figure 4.4, Figure 4.5, and Figure 4.6 show the locations of the three highway sections.

Table 4.1: Details of the three highways where tenting was measured in Zegeye-Teshale et al. (2021) study.

Highway	Direction	Surface layer	Base layer	Last rehabilitation year	Length, km	Comments
MN 37	WB	AC (20 cm)	Aggregate base (42 cm)	2018	23	No comment
US 169	WB	AC (17 cm)	RCA + aggregate base (20 cm + 25 cm)	2002	20	Most complained
US 169	EB	AC (17 cm)	RCA + aggregate base (20 cm + 25 cm)	2002	20	Most complained
MN 73	Urban	AC (25 cm)	Aggregate base (28 cm)	2005	11.2	More tenting than previous year

Note: This table also includes details of MN 73, which is not considered in this report; 20 cm = 7.9 in; 17 cm = 6.9 in. AC = asphalt concrete, RCA = rubblized concrete aggregate, WB= westbound, EB = eastound

Figure 4.4: MN-37D Test Section.

Figure 4.5: US-169D Test Section (red line - 2021, and magenta line -2020).

Figure 4.6: US-169I Test Section (red line - 2021, and magenta line -2020).

The winter tenting results, presented in Figure 4.7, Figure 4.8, and Figure 4.9 showed that tenting peak height was as much as 7 mm, 9 mm and 8 mm at some locations in the MN-37D, US169D, and US-169I, respectively. These ranges of tenting were also observed in the two of the six roads measured in the present study (Figure 4.1).

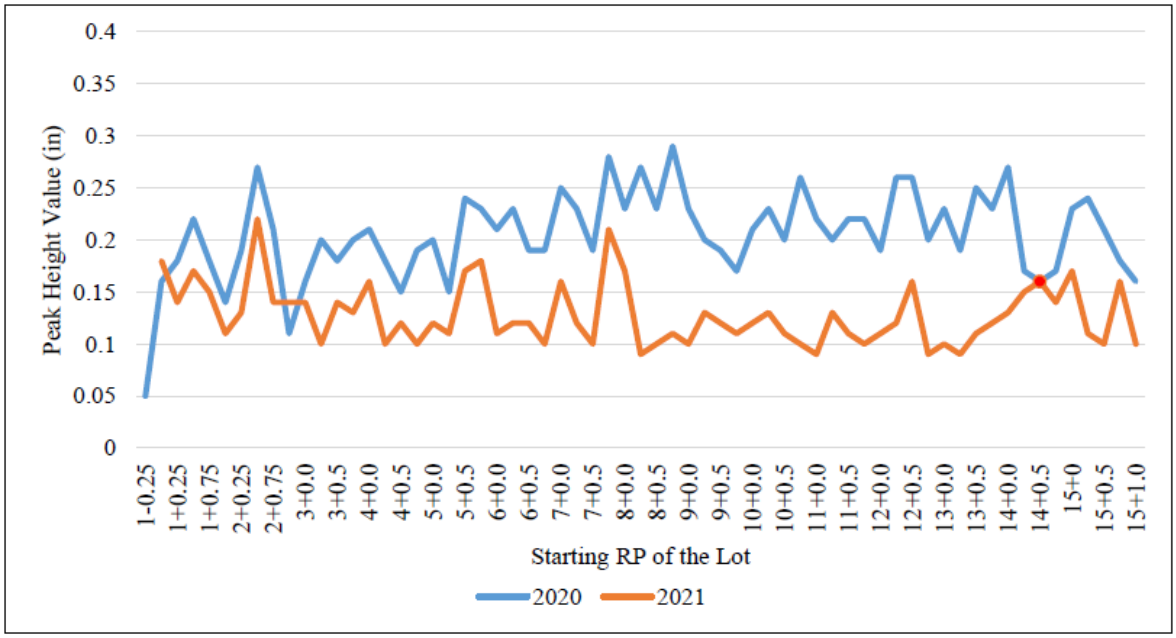

Figure 4.7: Tenting Results for MN-37D.

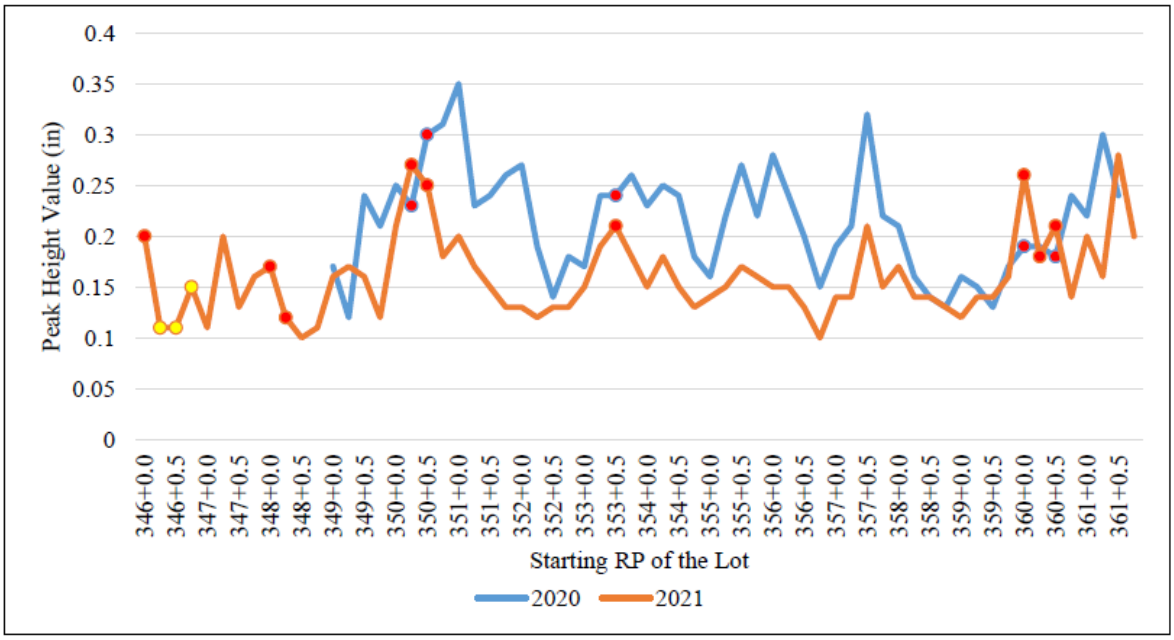

Figure 4.8: Tenting Results for US-169.

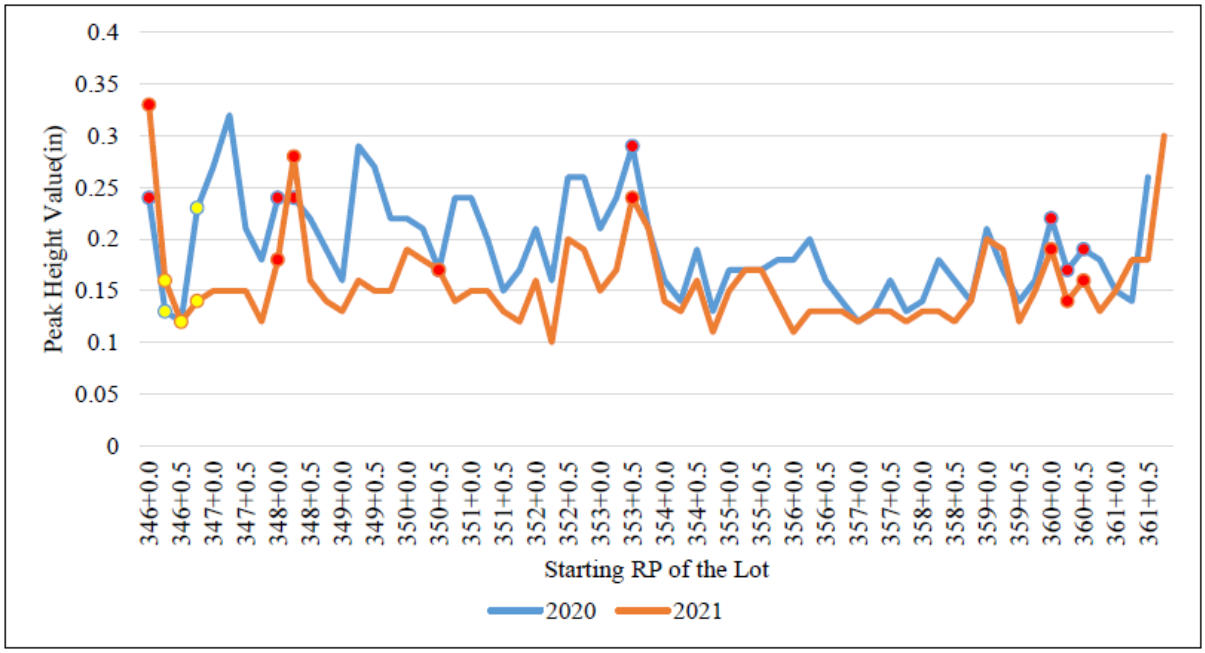

Figure 4.9: Tenting Results for US-169I.

4.1.3 MnDOT District 1 Roads with Tenting Distress

Several road sections in MnDOT District 1 experienced tenting distress. Table 4.2 lists some roads in District 1 that experienced tenting. Note that only roads (13 total) with documented comments regarding tenting are included in this table. This table does not include quantitative tenting measurements; however, the documented comments on severity and qualitative assessments indicate that all listed roads experienced moderate to severe tenting. The information covers three pavement types: bituminous over aggregate base (BAB), bituminous over bituminous (BOB), and bituminous over concrete (BOC).

The important observation from Table 4.1 and Table 4.2 is that all three types of roads experience tenting, irrespective of the surface and base layer thicknesses and AADT. The above mentioned two tables included roads with AADT from 44 to 24,626 which experienced tenting. The range of surface layer thickness is from 5 to 10 inches. The base layer thickness varies from 6 to 18 inches.

Table 4.2: List of some Roads in MnDOT District 1 that experienced tenting distress.

Hwy.	Begin Ref Point	End Ref. Point	Pvmt. Type	Last Rehab Yr.	AADT	Subarea	Comment on Tenting	Current Road Structure Info
169	346+00.900	362+00.110	BAB	2002	8,780	Range	One of the most complained	6.5" Bit over 8" rubbilized conc.,

Hwy.	Begin Ref Point	End Ref. Point	Pvmt. Type	Last Rehab Yr.	AADT	Subarea	Comment on Tenting	Current Road Structure Info
							about areas by public	over 10" Agg. Base
169	349+00.512	362+00.154	BAB	2002	8,845	Range	One of the most complained about areas by public	6.5" Bit over 8" rubbilized conc., over 10" Agg. Base
194	14+00.190	14+00.661	BOC	2009	24,626	Duluth	Very Bad Tenting	6.5" Bit over 7" Conc. Over 5.5" Agg. Base
2	245+00.258	246+00.786	BOC	2007	4,808	Duluth	Very Bad Tenting	8.6" Bit over 18" Agg. Base
1	190+00.000	198+00.000	BOB	2002	282	Border	More tenting than previous years	6.1" Bit over avg. of 7.2" of Agg. Base
1	198+00.000	215+00.424	BOB	2022	282	Border	More tenting than previous years	6.8" Bit over avg. of 9" of Agg. Base
65	220+00.000	223+00.710	BOB	2022	49	Border	More tenting than previous years	6.8" Bit over avg of 13.2" Agg. Base.
65	223+00.710	225+00.058	BAB	2022	44	Border	More tenting than previous years	5" Bit over 6" Agg. Base
65	225+00.058	226+00.211	BOB	2022	55	Border	More tenting than previous years	6.2" Bit over avg of 14.8" Agg. Base.

Hwy.	Begin Ref Point	End Ref. Point	Pvmt. Type	Last Rehab Yr.	AADT	Subarea	Comment on Tenting	Current Road Structure Info
65	226+00.211	227+00.500	BOB	2022	55	Border	More tenting than previous years	4.8" Bit over avg. of 13" Agg. Base
65	227+00.500	230+00.000	BOB	2022	55	Border	More tenting than previous years	5.7" Bit over avg. of 10.9" Agg. Base
73	110+000	114+00.637	BOB	2002	808	Border	More tenting than previous years	0.6" Bit over avg. of 7.9" Agg. Base
73	114+00.637	116+00.000	BOB	2001	642	Border	More tenting than previous years	10.1" Bit over var. depth agg base of 10"-12"

4.2 Effectiveness of Pavement Treatments

Tenting of the transverse cracks affect road roughness. Zegeye-Teshale et al. (2021) concluded that IRI and tenting have a good correlation as evident by Figure 2.5. The R^2 of the correlation between the IRI and tenting is 0.62, which can be considered as reasonable given the potential influence of other distresses on IRI, such as potholes, longitudinal cracks, and surface irregularities.

As mentioned previously, this study included the review and analysis of pavement performance data. The mean improvement in pavement riding quality followed by a pavement treatment was studied. Figure 4.10 shows the comparison of the IRI improvement (i.e., reduction in the pavement IRI, which is also referred to as the effectiveness of treatment (ET) in this study) of different treatment methods on three different pavement types. It may be noted that the data from all eight MnDOT districts have been used in this analysis. Figure 4.10a shows the mean ET value for chip seal on different pavement types. In all three pavement types (BAB, BOB, BOC), the mean ET value is negative. This indicates that the chip seal was not able to reduce the IRI followed by its implementation. The mean improvement is the lowest on BOC and highest on the BAB pavement.

Figure 4.10b shows the distribution of improvement percentages for chip seals applied to the three different pavement types. The distribution of IRI improvement percentages is very close to being centered around 0 for all three pavement types (BAB, BOB, BOC). This raincloud plot suggests that some chip seal treatments resulted in positive improvement, but there is a wider range of negative

improvement percentages than positive ones. That is why the mean improvement was calculated as negative.

The variability in the improvement percentages for BOC pavement is more compared to BAB and BOB. As shown in Figure 4.10b, the cloud for BOC is wider, especially on the negative side, indicating a larger spread of improvement percentages. Overall, the raincloud plot suggests that chip seal treatments in this data set resulted in mostly small positive improvements for all pavement types with a significant amount of data points are on the negative side, which led to a negative mean improvement. Moreover, chip seal is applied as preventive maintenance, which means it is used when the pavement is in relatively good condition, so the pavement IRI is not expected to drop significantly. Consequently, the IRI difference before and after may not be large, resulting in a lower mean improvement ET value for chip seal.

Figure 4.10c shows the mean IRI improvement percentage followed by crack fill. On BAB and BOC pavements, the mean improvement is positive, and on BOB pavement, it is negative. Figure 4.10d shows the distribution of the data points of improvement percentages for crack fill applied on the three pavement types. The distribution of the improvement percentage is centered above zero. This indicates that most of the crack fill resulted in some positive improvement but there is a significant number of negative improvements too. The BAB cloud is more speared on the positive side. A similar trend is observed in the BOC cloud plot. That is why the mean improvement percentage is positive in these two pavement types. In the case of BOB pavement type, the wide range of data sets are on the negative side, which resulted in a negative mean improvement for crack fill.

The data distribution and the mean improvement trend for crack repair, which is shown in Figure 4.10e and Figure 4.10f, is similar to the ones observed in crack fill. However, their improvement percentage is much more than the crack fill.

Figure 4.10g and Figure 4.10h show the mean improvement and the cloud distribution plot of the crack seal. The improvement trends for the crack seal and chip seal are found to be similar. The mean improvement percentage is negative in all three pavement types. The distribution for the improvement is close to being centered around zero for BAB type. However, the density is more towards the negative side. For BOB and BOC, the distribution curve is skewed towards the negative side, indicating the majority of crack seals showed negative improvement on BOB and BOC pavement type.

Figure 4.10i and Figure 4.10j show the mean improvement percentage and the improvement percentage distribution on different pavement types for micro surfacing treatment. In all three pavement types, micro-surfacing showed the highest mean improvement compared to the others. The data distribution centered above zero with a skew towards the positive side in all three pavements. It can be seen that the majority of the micro surfacing treatment has resulted in positive improvement. However, there are some data points that are on the negative side, too, but they are significantly less than the other treatments.

Figure 4.10k and Figure 4.10l show plots for patching. The mean improvement percentage is positive in all three pavement types, like the micro-surfacing treatment. The cloud distribution of the improvement percentage peaked above zero and skewed to the positive side, which indicates that most of the patching resulted in positive improvement, but there is a significant amount of negative improvement too. The range of negative improvements in BOB pavement is more than the other two pavement types.

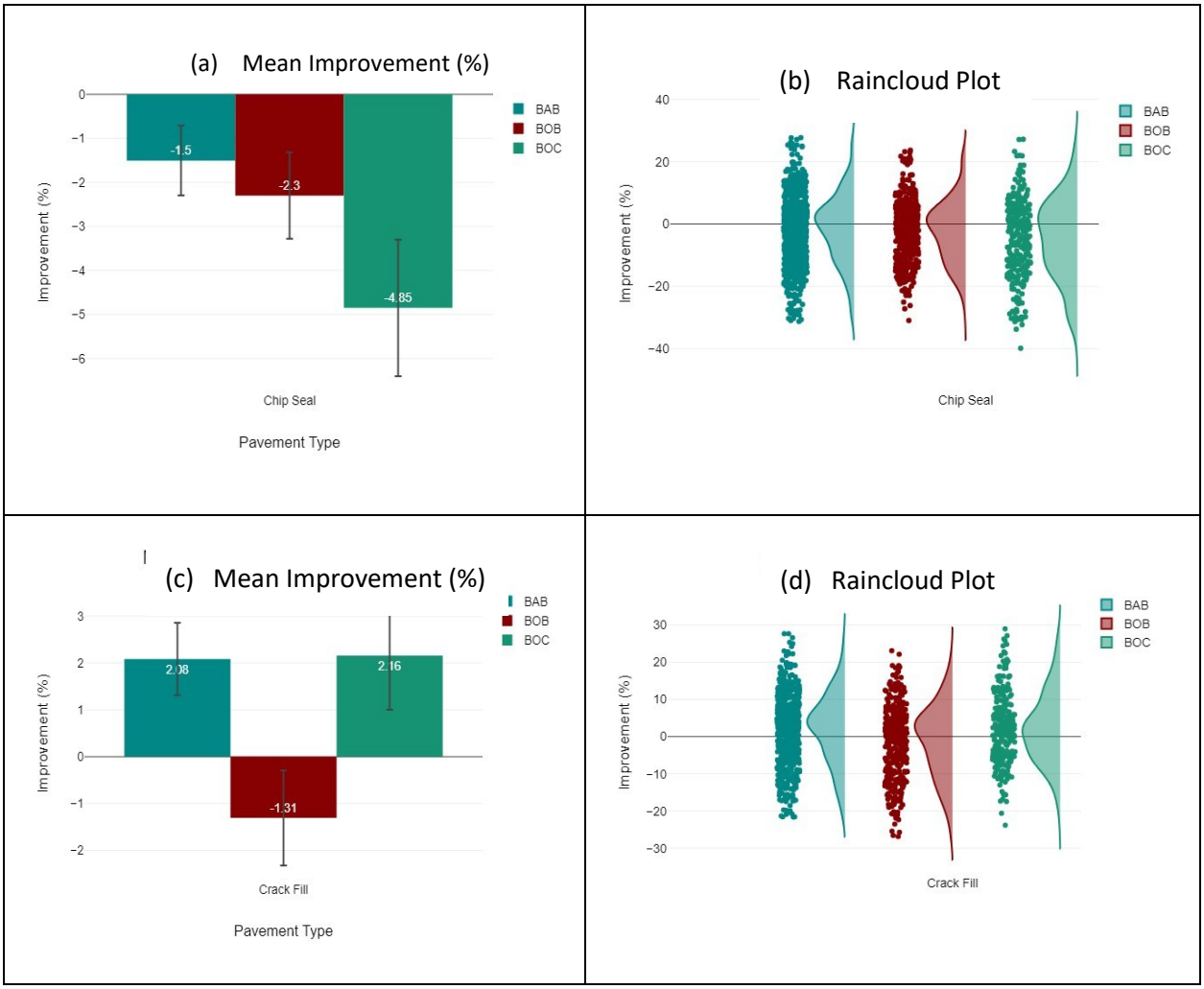

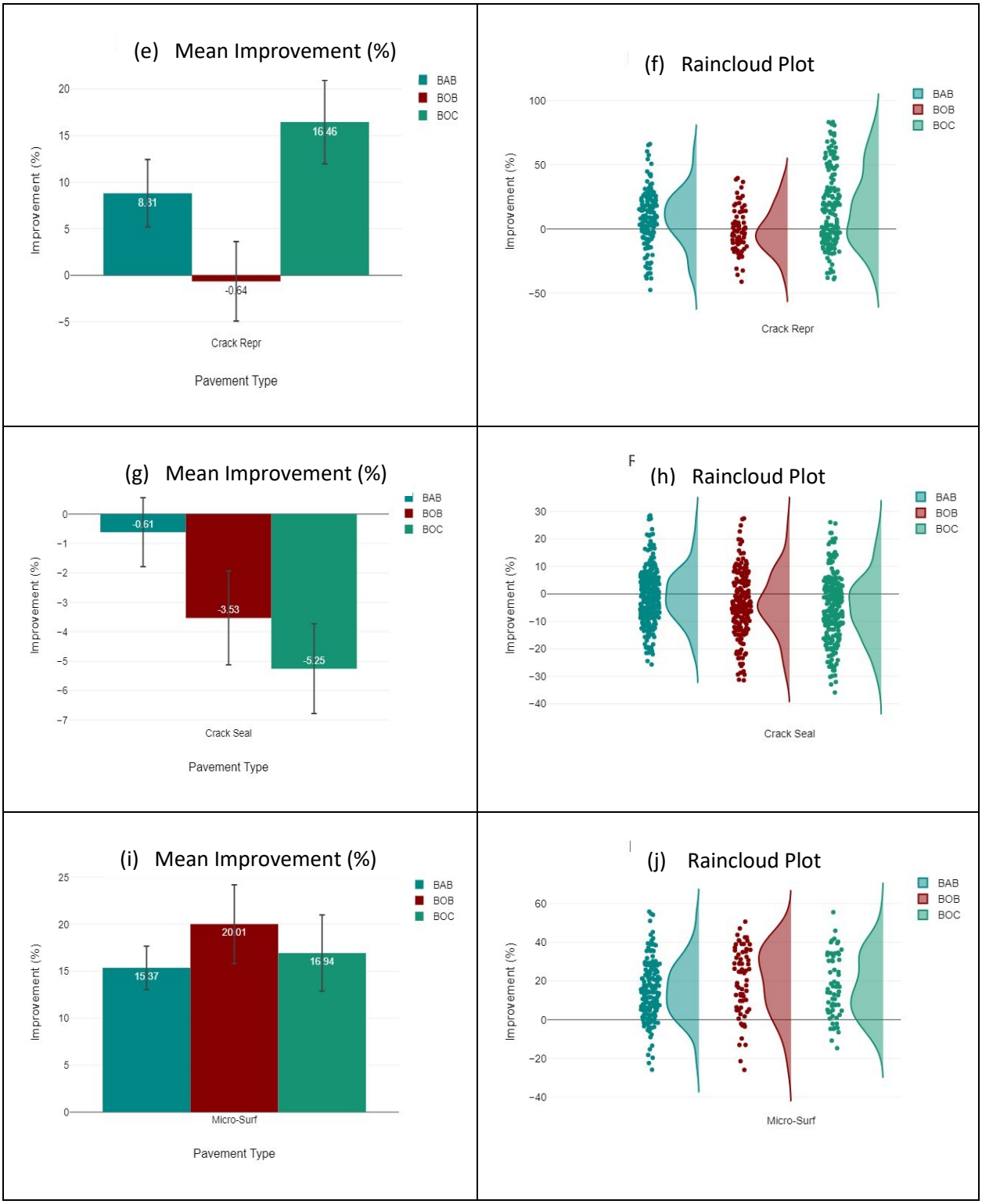
(e) Mean Improvement (%)
BAB
BOB
BOC
Improvement (%)
20
15
10
5
0
−5
8.31
-0.64
16.46
Crack Repr
Pavement Type
(f) Raincloud Plot
BAB
BOB
BOC
Improvement (%)
100
50
0
−50
Crack Repr
(g) Mean Improvement (%)
BAB
BOB
BOC
Improvement (%)
0
−1
−2
−3
−4
−5
−6
−7
-0.61
-3.53
-5.25
Crack Seal
Pavement Type
(h) Raincloud Plot
BAB
BOB
BOC
Improvement (%)
30
20
10
0
−10
−20
−30
−40
Crack Seal
(i) Mean Improvement (%)
BAB
BOB
BOC
Improvement (%)
25
20
15
10
5
0
15.37
20.01
16.94
Micro-Surf
Pavement Type
(j) Raincloud Plot
BAB
BOB
BOC
Improvement (%)
60
40
20
0
−20
−40
Micro-Surf

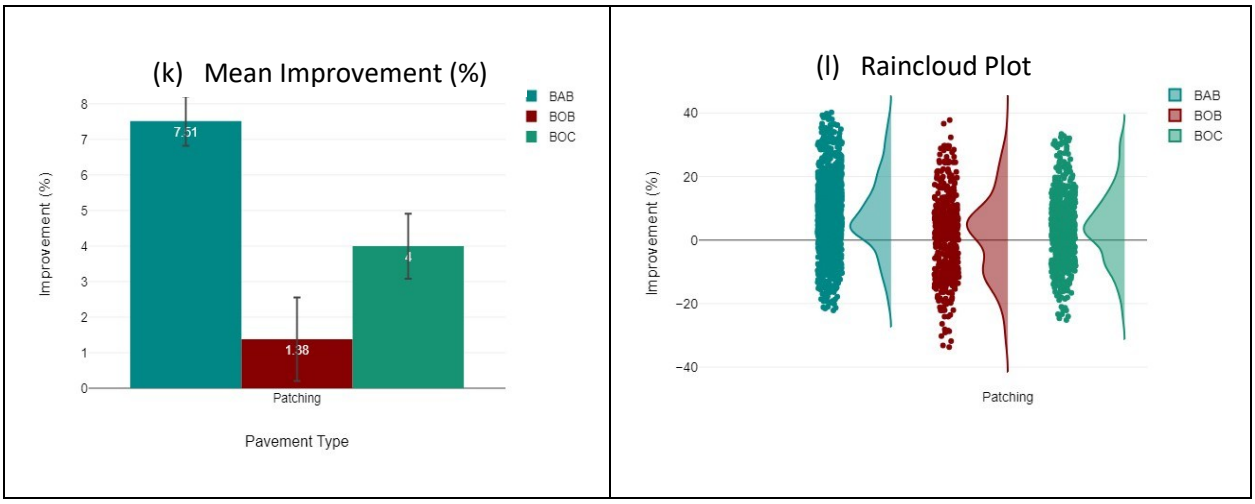

Figure 4.10: The Average IRI improvement and the distribution of the IRI improvement data of different treatment; (a) &(b): cheap seal, (c) &(d): crack fill, (e) &(f): crack repair, (g) &(h): crack seal, (i) &(j): micro surfacing, (k) &(l): patching.

4.2.1 Correlation between ET and different variables through Machine Learning Models

A statistical study was performed to investigate the correlation between the improvement of IRI (or ET) and different variables such as AADT, treatment type, pavement type, and AADT was split into four categories as shown in Table 4.3. Additionally, IRI improvement data was also split with respect to treatment type, pavement type.

Table 4.3: Assumed traffic categories.

Category	AADT
Category 1	>10,000
Category 2	9,000-10,000
Category 3	4,000-9,000
Category 4	<4,000

The analysis was conducted using three different machine learning predictive models such as Decision Tree, Random Forest Model, and Boosted Trees (Gradient Boosting). Summary of the results are presented below. This analysis helped identify the significant variables.

4.2.2 Results of the Machine Learning Models

Table 4.4, Table 4.5, and Table 4.6 show the statistics of the three machine learning models mentioned above. A higher number of splits for a variable suggests it is more important to the model. Similarly, a higher sum of squares (SS) indicates the variable is more effective at reducing prediction error.

Table 4.4: Summary of the Decision Tree model statistics

Term	Number of Splits	SS	Portion
Treatment type	11	128,021.7	0.66
Pavement Type	17	29,749.8	0.15
Traffic category	14	19,528.4	0.10
AADT	10	16,129.4	0.08
Total	52		1.00

Note: R^2 for Training = 0.21; R^2 for validation = 0.24

Table 4.5: Summary of the Random Forest model statistics

Term	Number of Splits	SS	Portion
Treatment type	1503	83,867.1	0.68
Pavement Type	1331	17,046.9	0.14
Traffic category	1351	11,677.2	0.09
AADT	1395	11,205.2	0.09

R^2 for Training = 0.21; R^2 for validation = 0.23

Table 4.6: Summary of the Boosted Tress (gradient boosting) model statistics

Term	Number of Splits	SS	Portion
Treatment type	453	51,1979.9	0.68
Pavement Type	368	95,131.40	0.13
Traffic category	307	81,442.89	0.11
AADT	454	67,176.01	0.09

Note: R^2 for Training = 0.22; R^2 for validation = 0.23

All three models showed very close performance in both training and validation dataset. While the R^2 is not high, all the models suggested that the most significant variable is the treatment type followed by the pavement type. AADT is the least significant variable. The finding indicates that the pavement treatment type and pavement type will affect the IRI improvement, irrespective of the AADT.

Figure 4.11 and Figure 4.12 show the comparison of the actual IRI and predicted IRI improvements for the three models for both training and validation datasets.

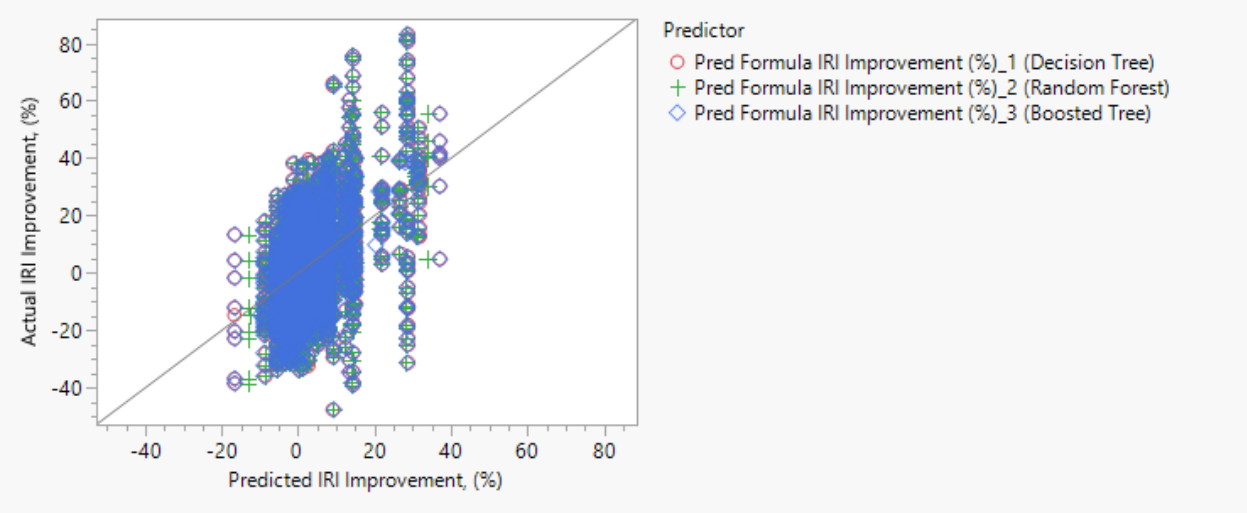

Figure 4.11: Actual vs. predicted IRI improvement comparison (training data)

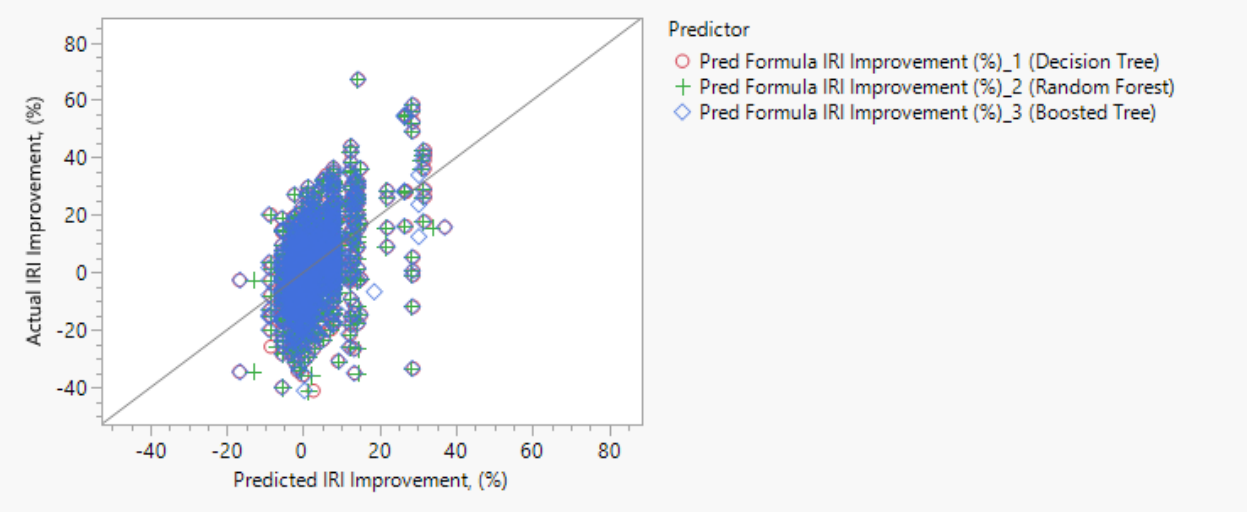

Figure 4.12: Actual vs. predicted IRI improvement comparison (validation data)

4.2.3 Ranking of Treatments

As the IRI improvement was found to correlate with the treatment type and pavement type, the ranking of the treatments is determined for the three types of the pavement. The analysis of variance (ANOVA) statistical test was performed to determine the ranking. Table 4.7 below shows the list of hypotheses that were considered for the testing.

Table 4.7: Hypotheses of the ANOVA test

Null hypotheses	Alternative hypotheses
There is no difference between the groups of the treatment type/ maintenance method in relation to improvement (%).	There is a difference between these groups.
There is no difference between the groups of the pavement type in relation to the improvement (%).	There is a difference between these groups
There is no interaction between the two variables, treatment type and pavement type in relation to the improvement (%).	There is an interaction between the two variables, treatment type and pavement type in relation to the improvement (%).

Table 4.8 shows the ANOVA test results. It was observed that the p-value for all the cases was found to be less than 0.05, which indicates the null hypothesis is wrong, and the alternate hypothesis is true. So, it was evident from the test results that there are significant differences between the treatment types and pavement types in relation to improvement (%). Moreover, there is a significant interaction between the treatment type and pavement type, indicating that the IRI improvement (%) on different types of pavements depends on the type of treatment. This means that the IRI improvement level of different types of pavements is not independent; it depends on the type of treatment that will be applied, which is expected. However, the residual sum of squares value was found to be quite high compared to the other sources of variance, which indicates that a large portion of the total variance in the improvement (%) is not fully explained by the treatment type, pavement type, or their interaction.

The Bonferroni post hoc statistical test was conducted after the ANOVA test to make a multiple comparison of the groups' means (improvement % of different treatments and pavement types) that are different from each other. From the test results, as shown in Appendix Table A1, a composite score was calculated to rank treatments from most to least effective within each pavement type. The composite score was calculated by computing the average mean difference for each treatment across all comparisons within the same pavement type.

Table 4.8: ANOVA test results

Variables	Sum of Squares	Df	Mean Square	F	p	η2p
Treatment Name	155855.2	5	31171.04	195.8	<.001	0.14
Pavement Type	16689.76	2	8344.88	52.42	<.001	0.02
Treatment Name x Pavement Type	20178.16	10	2017.82	12.68	<.001	0.02
Error (Residual)	959315.91	6026	159.2			

Table 4.9 shows the composite score and the ranking of the treatments in each pavement type. A higher composite score indicates higher relative improvement. Thus, a higher rank was assigned for the treatment on a particular pavement type. For example, on the BAB pavement type Micro-Surfacing has the highest composite score, so micro surfacing rank is 1 on this pavement type.

Table 4.9: Ranking of the different treatments on different pavement types based on the composite score

Pavement type	Treatment Name	Composite Score	Rank
BAB	Chip Seal	-11.18	5
	Crack Fill	-8.62	4
	Crack Repair	1.04	3
	Crack Seal	-11.55	6
	Micro-Surfacing	10.19	1
	Patching	4.66	2
BOB	Chip Seal	-10.28	5
	Crack Fill	-12.74	6
	Crack Repair	-9.51	3
	Crack Seal	-10.00	4
	Micro-Surfacing	11.94	1
	Patching	-2.81	2
BOC	Chip Seal	-11.59	5
	Crack Fill	-5.17	4
	Crack Repair	14.25	1
	Crack Seal	-11.62	6
	Micro-Surfacing	10.10	2
	Patching	-1.54	3

It was found that micro-surfacing was highly effective on BAB pavements compared to the other treatments. This is because of its ability to level the road surface by providing a new wearing surface, which removes any depression and undulation of the existing surface. On the other hand, crack sealing on BAB has the lowest effectiveness, possibly because it does not improve surface evenness, even though it prevents water infiltration. Micro-surfacing outperformed other treatments on BOB

pavements, too. Crack fill was found to be the least effective treatment on BOB pavement. Although it does improve roughness a little on an already bituminous surface, it addresses only small surface imperfections. Crack repair was found to be the most effective treatment on BOC pavement compared to the others. This is because concrete joints and cracks propagate through the overlay (reflective cracking), where repairing them can significantly improve the roughness of the pavement. Similar to BAB, crack sealing was found to be the least effective on BOC. The reason for this is that it does not correct the existing irregularities/ depression. In comparison between the crack repair and crack seal, crack repair outperformed crack seal in all three pavement types. Moreover, the crack repair is done when the riding quality drops significantly which generally involves more extensive corrective measures, which can significantly improve the pavement's surface roughness. Moderate ranking was observed for patching across types of pavements. Since patching repairs localized areas of distress, its effectiveness varies by the extent of underlying damage. If done correctly, pavement roughness can be significantly improved.

It may be noted that the crack seal and fill also performed before micro surfacing; from that perspective, it contributes to the overall effectiveness of the final product, micro-surfacing; therefore, crack seal and fill shall not be abandoned. While crack sealing or filling directly does not affect IRI improvement, research showed that it is effective in preventing water infiltration. The ride quality on the finished product relies greatly on workmanship.

4.3 Laboratory Test Results

A significant portion of this research focused on the laboratory study of aggregate base materials, as detailed in Chapter 3. This section presents and discusses the results of various laboratory tests conducted on the collected aggregate base materials. Aggregate gradation and results of proctor, salinity, frost heave, and permeability tests, which were performed to assess the properties and behavior of the materials under different conditions, are included in this chapter. The results provide insights into how different aggregate compositions influence compaction and frost heave, helping to identify the aggregate gradation control factors for minimizing tenting and enhancing pavement performance.

4.3.1 Aggregate Gradation

Figure 4.13 shows the 0.45-power gradation curve of the four different aggregate samples, namely SO, SN, SNN, and SON, as introduced in section 3.3.1. The 0.45-power gradation curve is used to compare and evaluate void content and the overall particle size distribution of each aggregate sample.

Table 4.10 presents the composition of the four aggregate base samples. It was found that the SNN sample is composed of 36.11% gravel, 55.65% sand, and 8.25% fines on the other hand, SN is composed of 49.69% gravel, 40.41% sand, and 9.90% fines. The SNN sample has the least amount of fine content, and the SO blend has the highest amount of fine content, which is 14.94%. SN blend has the highest

amount of gravel/ coarse aggregate content, and the SON blend has the least amount of gravel content, which is 23.72%. It was evident from the aggregate gradation curve and the composition that all the samples are unique in terms of particle size distribution. All these four samples meet the gradation limits of MnDOT's Class 5 aggregate blend.

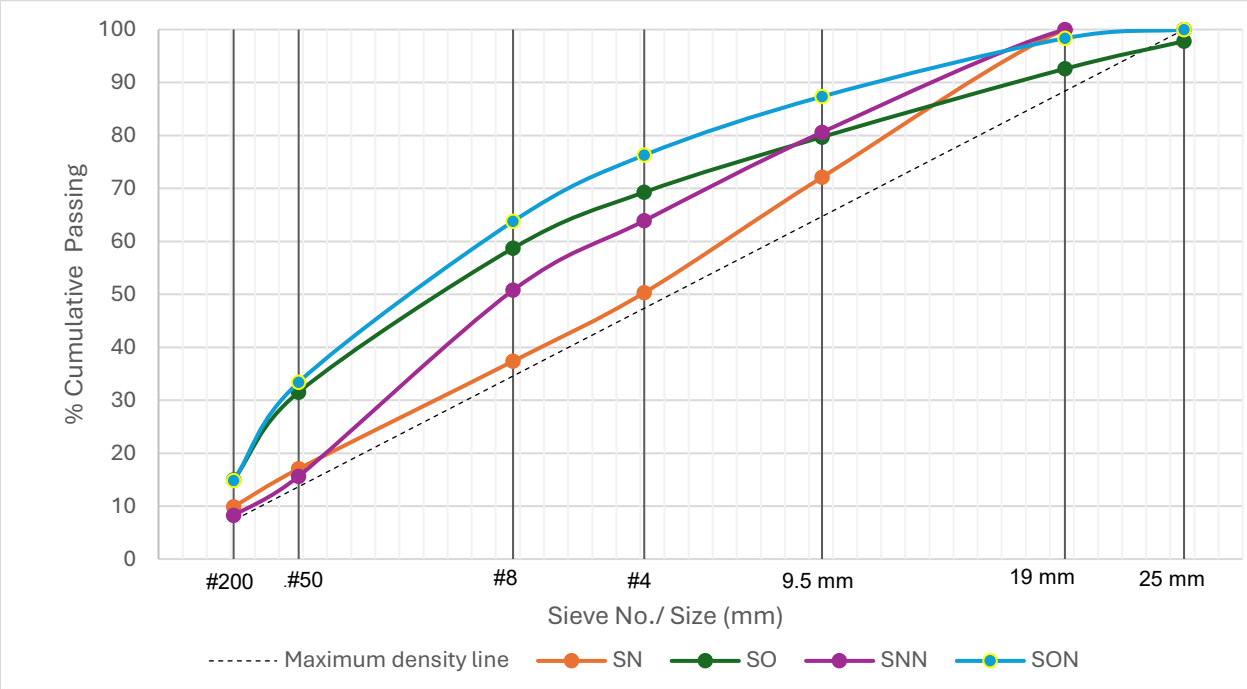

Figure 4.13 Gradation curves of the four different aggregate samples

Table 4.10 : Composition of Aggregate Blends

Blend Name	% of Gravel	% of sand	% of fines
SNN	36.11	55.65	8.25
SN	49.69	40.41	9.90
SO	30.72	54.34	14.94
SON	23.72	61.46	14.82

As shown in Figure 4.13, the SN blend gradation curve fitted closely with the maximum density line (MDL) in the fine aggregate distribution region (#200 (0.075mm) to # 4 (2.36 mm) sieve) compared to the other blends. However, in the coarse aggregate distribution region (4 (2.36 mm) to 1-inch (25 mm) sieve), gradation curve deviated away from the MDL, indicating a higher amount of uncompacted void in the coarser region. The highest amount of deviation from the MDL was observed in the SON blend. The SO blend gradation curve deviated less than the SON blend in the finer region. Moreover, its deviation was found to be lowest in the coarser region. Theoretically, more deviation from the MDL indicates more void in the aggregate distribution.

In this study, the amount of deviation of the blend curve from MDL was quantified by calculating the area between the aggregate gradation curve and MDL. The total void area was divided into two parts: one is the fine void area, which is the area between #200 sieve and #4 sieve; another one is the coarse void area, between #4 sieve and 1-inch (25 mm) sieve. The results are presented in Figure 4.14 below.

It is evident from Figure 4.14, despite having a higher fine content, the SON and SO blends have a relatively higher amount of uncompacted void area (41 mm^2 and 35 mm^2) compared to the SN and SNN blends (5.82 mm^2 and 17.53 mm^2). This is because of the lack of intermediate size aggregate fractions. SN blend has a considerably low void area on the finer side. In the coarser region, a similar trend was found for the SON and SO blend. However, a lower amount of coarser void area was found than the finer void area for these two blends. Conversely, the void area on the coarser side is more than the finer side for SN and SNN blend, which indicates a higher amount of large individual void (coarse void) is present there than the small individual void (fine void). In terms of total void area comparison, the SON and SO blend void areas are considerably higher than the SN and SNN blend.

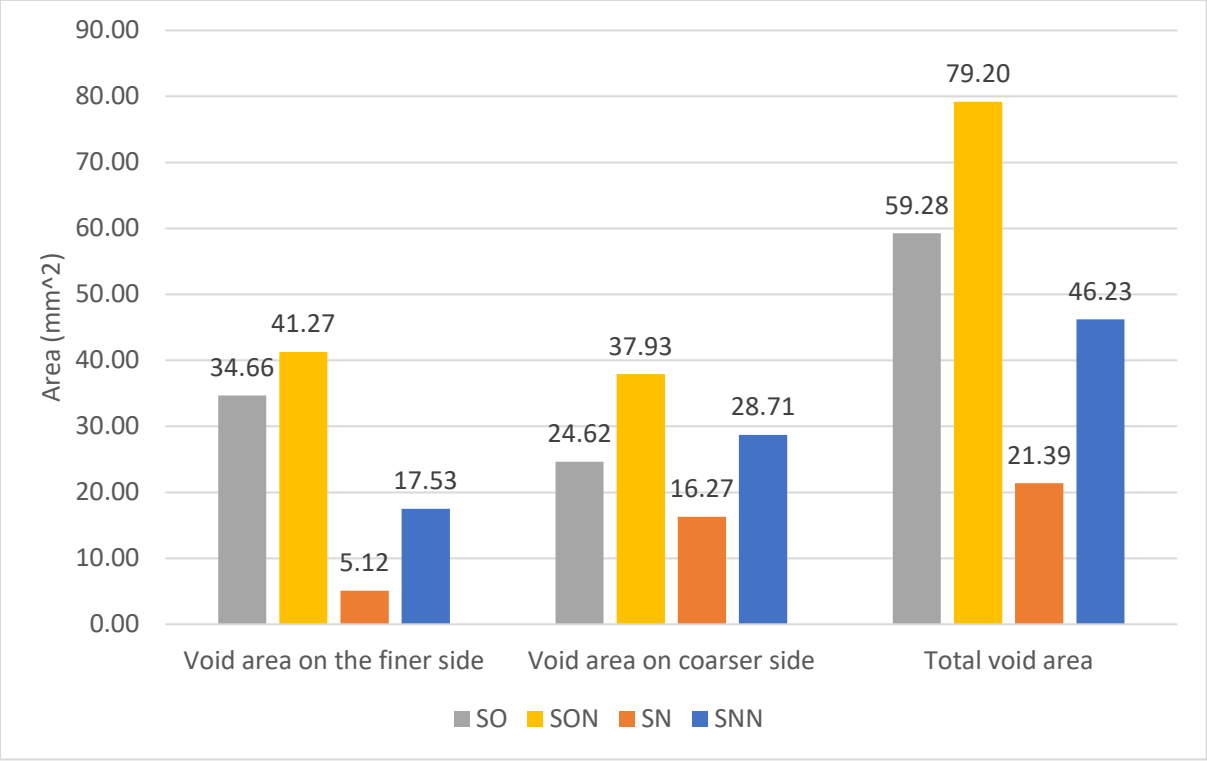

Figure 4.14: Comparison of the theoretical uncompacted void area of the four different aggregate samples

4.3.1.1 CV/FV index

To understand how the coarse (retained on sieve No. 4) and fine (passing sieve No. 4) voids affect the overall performance of the aggregate base layer with respect to frost susceptibility and hydraulic conductivity etc., a new factor, named as CV/FV index parameter is introduced. It is calculated by dividing the coarse void area by the fine void area. As demonstrated in Figure 4.15, course void (CV) is the area between the gradation curve and maximum density line (0.45 power scale) for the coarser portion of the aggregates and the fine void (FV) is the area for the finer portion of the curve. CV/FV values were computed for each of the four different blends and used as a parameter to evaluate the blend performance. Higher CV/FV values indicate a coarser void compared to a fine void and vice versa. CV/FV value was categorized into three cases which are:

- CV/FV >1 indicates coarse void is more than the fine void
- CV/FV=1 indicates coarse void and fine void is equal
- CV/FV<1 indicates coarse void is less than the fine void

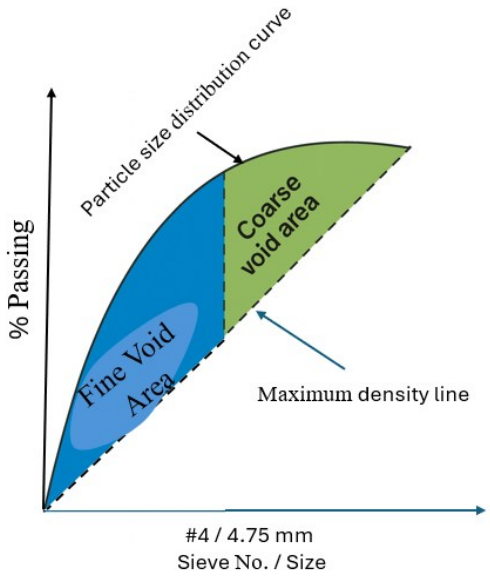

Figure 4.15: Fine void area and course void area.

The CV/FV values of different blends are presented in Figure 4.16. It was observed that the SN blend has the highest CV/FV value (3.18) compared to all other blends, indicating the highest amount of coarse void among these four different blends. The CV/FV value for the SN and SNN blend was found to be more than 1, whereas the SO and SON blends remained below 1.0. This dichotomy indicates that the SN and SNN have considerably higher amounts of coarse void and less amounts of fine void compared to the SO and SON blend. The correlation of this CV/FV value with different blend properties is discussed in the following sections.

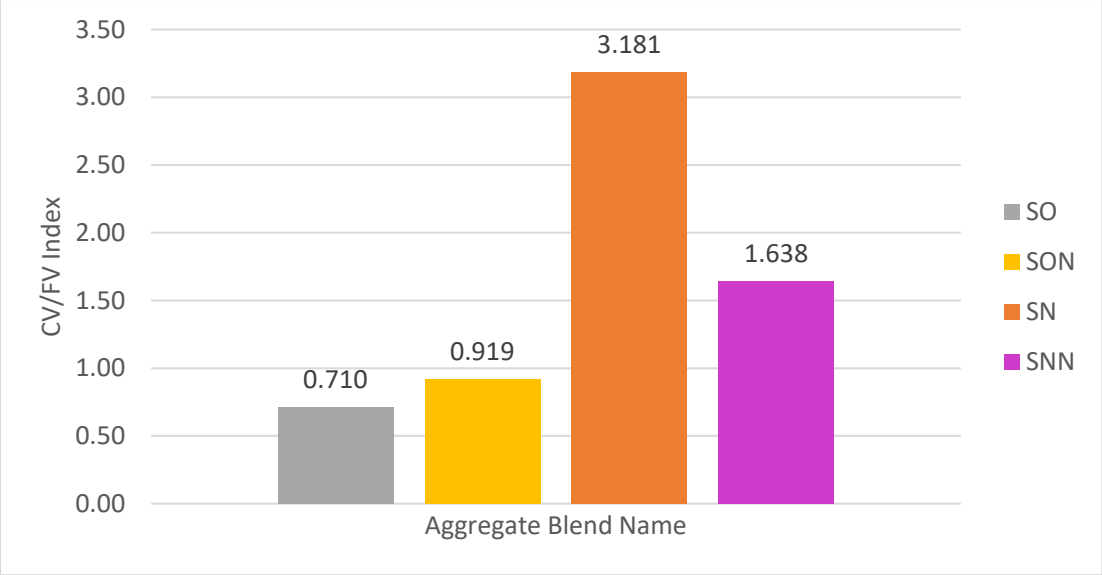

Figure 4.16: Comparison of the CV/FV value of the four different blend

4.3.2 Moisture- Density Relationships

Figure 4.17 shows the comparison of the moisture-density relation of the four different blends. It was observed that the maximum dry density (MDD) of all the blends was close to each other, but their optimum moisture content (OMC) varied. Table 4.11 below shows the MDD and OMC values of these four different blends. The MDD and OMC of SO and SON blends are very close to each other, like their CV/FV values. The SO and SON blends have a higher MDD value (144.8 and 144.2 lb./ft^3) and a lower OMC value (6.2 and 6.15%) compared to SN and SNN blends. On the other hand, the SN and SNN blends have higher OMC (8.10% and 7.25 %) and lower MDD (143.4 and 144 lb./ft^3). Despite having higher fine content in the SON and SO blends (14.94 and 14.82 %), it exhibited a lower OMC value, which may be counter intuitive. The conventional understanding of the effect of fines indicates that it should require more water for lubrication because of its high surface area to get completely compacted. However, the MnDOT Class 5 type aggregate blend compaction level may not entirely depend on the fine content. The amount of total void present in the aggregate blend can play a crucial role. Since the fines are very small size particles, they can fill the void created by the larger particle without requiring any extra water for lubrication, when the intermediate aggregate fraction is less.

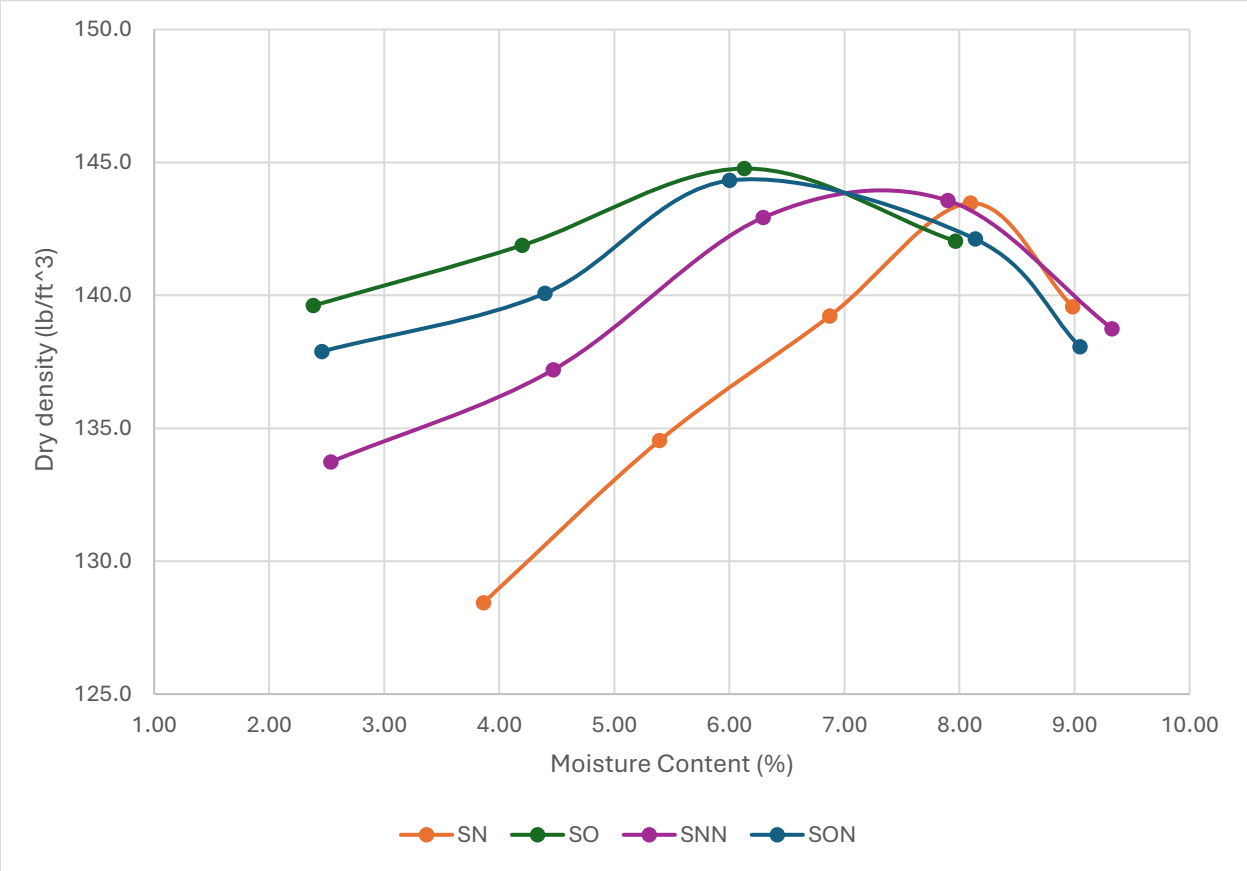

Figure 4.17: Moisture density relation of the four different aggregate blends

Table 4.11: Maximum dry density and optimum moisture content of four blends

Blend name	Maximum dry density (lb./ft^3)	Optimum moisture content (%)
SNN	144	7.25
SN	143.4	8.10
SO	144.8	6.2
SON	144.2	6.15

It was observed that there is a moderate positive correlation between the MDD and the amount of fine content, which implies that an increase in fine content leads to higher density as shown in *Figure 4.18*. This happens because adding fines in the coarse-grained soil/ or aggregate base blend fills the voids between the coarser aggregate (with less water), which eventually increases the density. However, this moderate correlation suggests that other factors, such as compaction effort, particle shape factor, distribution of effective void space and size, etc., also play influential roles here.

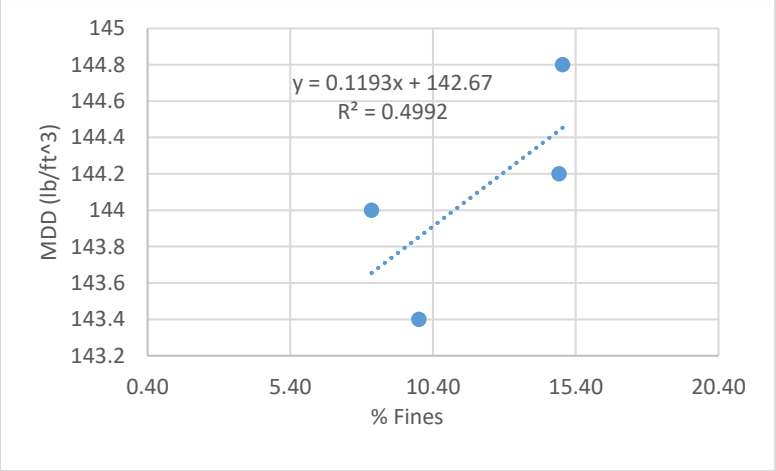

Figure 4.18: Relationship between MDD and percentage of fine

To evaluate how the CV/FV index affects the MDD of the aggregate blend, a regression plot was drawn between the MDD and the CV/FV value. As shown in Figure 4.19, the R^2 is high, suggesting a good correlation. It was observed that there is an inverse relationship between the MDD and the CV/FV value. The higher CV/FV value indicates a coarser void, which makes the aggregate base more porous. As a result, the density of the aggregate base reduces. It is evident from Figure 4.19 that the lower CV/FV index can lead to higher MDD and vice versa. That is why the SO and SON blends showed higher MDD than the SN and SNN. The SN blend has the lowest MDD and highest CV/FV value, which indicates that this would be the most porous aggregate base after compaction.

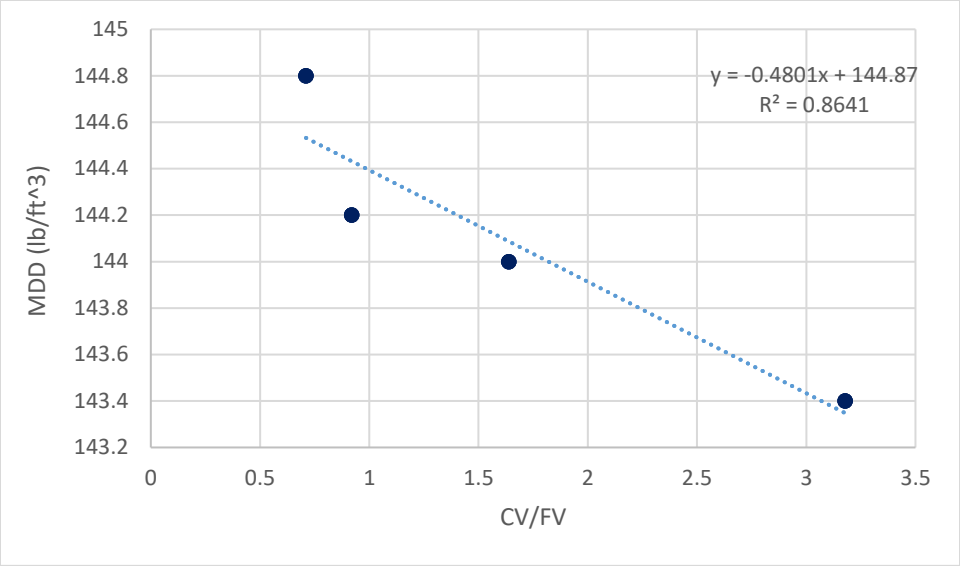

Figure 4.19: Relationship between maximum dry density and the CV/FV different aggregate blends

4.3.3 Frost Heave Test Results

The frost heave evaluation, also referred to as the tenting test, was performed under two distinct thermal conditions: (i) a temperature gradient was applied in the test sample; only two aggregate base samples were used in this exercise; different fine contents were considered; and (ii) the other utilizing a uniform temperature profile; four different types of samples were used with their original fine content. The subsequent sections detail and compare the test outcomes corresponding to each thermal condition.

4.3.3.1 Frost- Heave Test Results by Using Cold-Warm Temp. Gradient

The results given in Figure 4.20 shows the heaving/tenting value of four different samples of the SO blend. Samples were kept in the test chamber for 96 hours. It shows that SO blends with a higher percentage of fines (SO_14.94% fine) have a higher heaving compared to the one with a lower percentage of fines (SO_3% fines). This matches with the conventional frost heave theory. As the fine content increases, the specific surface area of the material also increases, which allows more water to adhere to the soil, and when this water freezes, it expands and creates more heave.

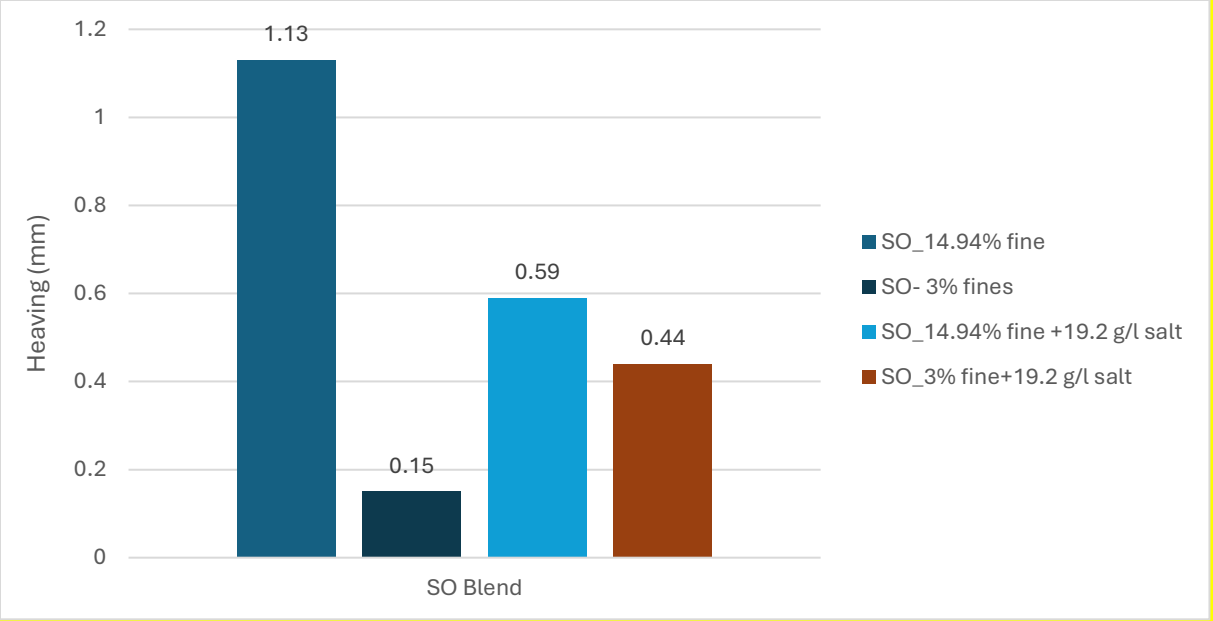

Figure 4.20: Frost heave test results of samples prepared from SO blend

Samples containing salt and having the same fine content showed less heaving than the samples without salt. The presence of salt appears to reduce the amount of frost heave compared to the samples without salt. This is because salt lowers the freezing point of water. However, there is a variation in the results for the samples having 3% fines. Here, the samples with salt resulted in more heaving than the samples without salt.

Figure 4.21 shows the frost heaving results of SN blend. A similar trend of increasing frost heave with increasing fines content is observed, which is consistent with the observations for the SO blend. As the percentage of fines increases (SN_6% fine to SN_9.9% fine), the heave also seems to increase from 2.96 mm to 3.69mm. Similar to the SO blend, the presence of salt (SN_9.9% fine+19.2 g/l salt, and SN_6% fine+19.2 g/l salt) reduces frost heave compared to the sample without salt (SN_9.9% fine). This suggests that salt lowered the freezing point of water in the SN blend as well, reducing ice formation and heave. Overall, the SN blend exhibited higher frost heave compared to the SO blend, even though SN blend has less fines than the SO blend. The reason behind this is the higher amount of coarse void in the SN blend compared to the SO blend, which contributed to more tenting, or heaving, development.

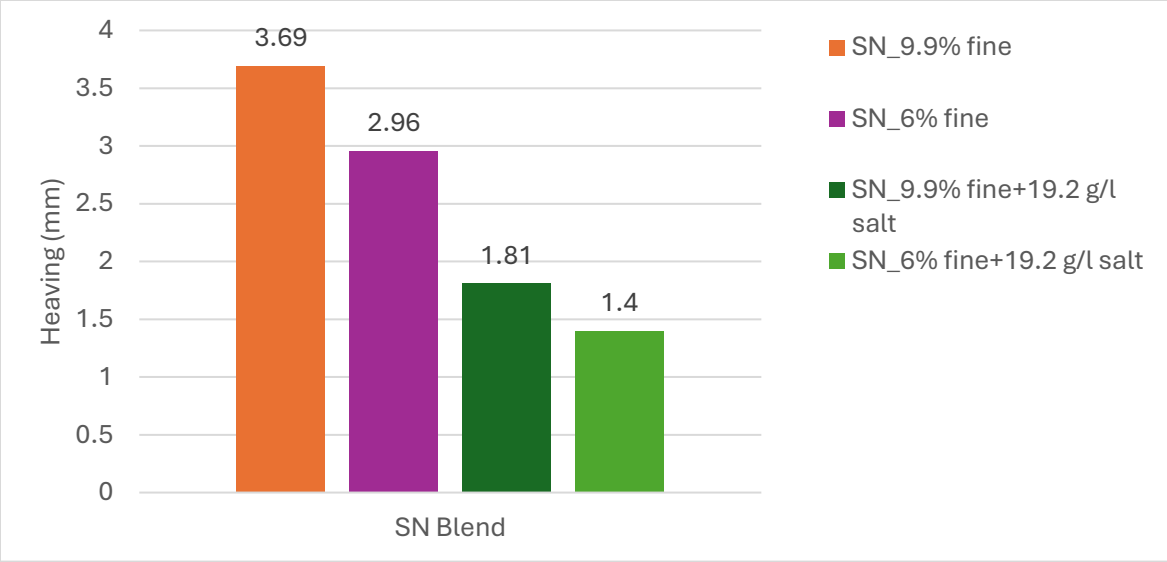

Figure 4.21: Frost heave test results of samples prepared from SN blend

Effect of Deicing Salt Type

Figure 4.22 shows the frost heave test results of SO blend samples prepared with different deicing salts but with the same salt dosage of 19.2 g/l. In total, eight different samples were prepared for this test. It was found that samples prepared with brine (salt water) exhibited the highest heaving compared to the others. Samples containing rock salt showed the lowest heaving. The heaving of samples with potassium acetate (KAC) and amp brine mixture was found to be within the range of the other two samples. Although rock salt and brine are both NaCl, brine has less concentration of NaCl since it is diluted with water. That is why brine has comparatively less effect in reducing the freezing point compared to rock salt.

The general conclusion from the comparison of the salt-mixed and unsalted test samples is that the heaving of the salt-mixed samples was less than unsalted samples because of the salt's influence in decreasing the freezing point.

As discussed previously, a separate test program was conducted to investigate the influence of salt in attracting moisture. Table *4.12* below shows the salt-moisture relation test results of the aggregate blends. It was observed that there was no significant weight change in samples subjected to the frost-heave test for all the blends, indicating that the changes in moisture content due to osmosis are minimal, at least in the laboratory tests conducted in this study. The overall impact of salt on the sample weight increment was relatively minor over the four-day period of frost-heave testing.

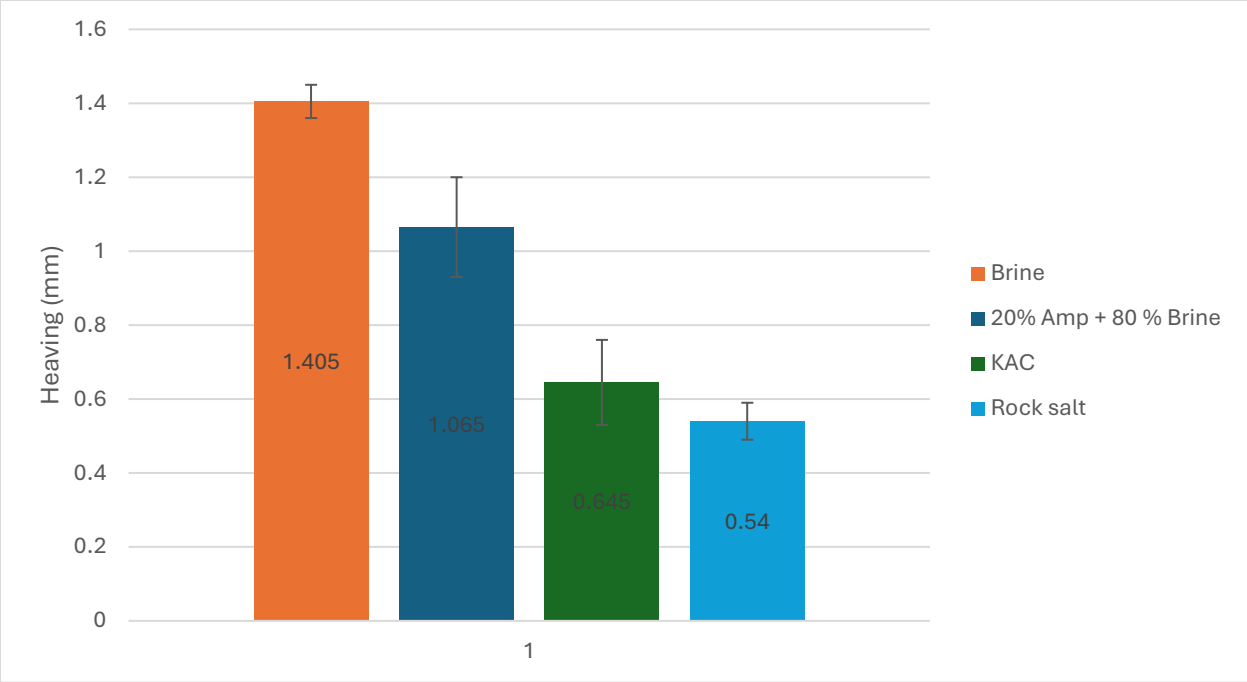

Figure 4.22: Frost heave test results of samples prepared with different deicers having the same salt dosage.

Table 4.12: Sample weight increments due to salt concentration of different blends

	SN		SO		SNN		SON	
Days	Sample weight	% weight increment	Sample weight	% weight increment	Sample weight	% weight increment	Sample weight	% weight increment
1	3905.81		3924.28		3907.66		3899.77	
2	3907.13	0.03	3925.87	0.04	3909.21	0.04	3900.56	0.02
3	3907.95	0.02	3925.75	0.00	3908.78	-0.01	3901.23	0.02
4	3906.11	-0.05	3924.83	-0.02	3908.12	-0.02	3900.86	-0.01

* all weights are grams.

4.3.3.2 Frost Heave of Samples Without Temperature Gradient

Figure 4.23 shows the frost heave test results for four different aggregate blends (SO, SON, SN, and SNN) under a uniform temperature gradient with a sample temperature of -40 degrees Celsius. Such low temperature was selected to simulate the freezing condition at a very low temperature. In this testing, samples were tested only with their original fine content. It was found that the SN blend showed the highest amount of heaving (1.301mm) than the other blends. The SNN blend exhibited the 2nd highest heaving (0.787 mm) among the four blends. The heaving of SO and SON blend was found to be very close to each other (0.677mm and 0.678mm). Even here, there is an inverse relationship between the fine content and the frost heave. Despite having higher fine content, SO and SON blends exhibited lower heaving compared to the blends having lower fine content (SN and SNN).

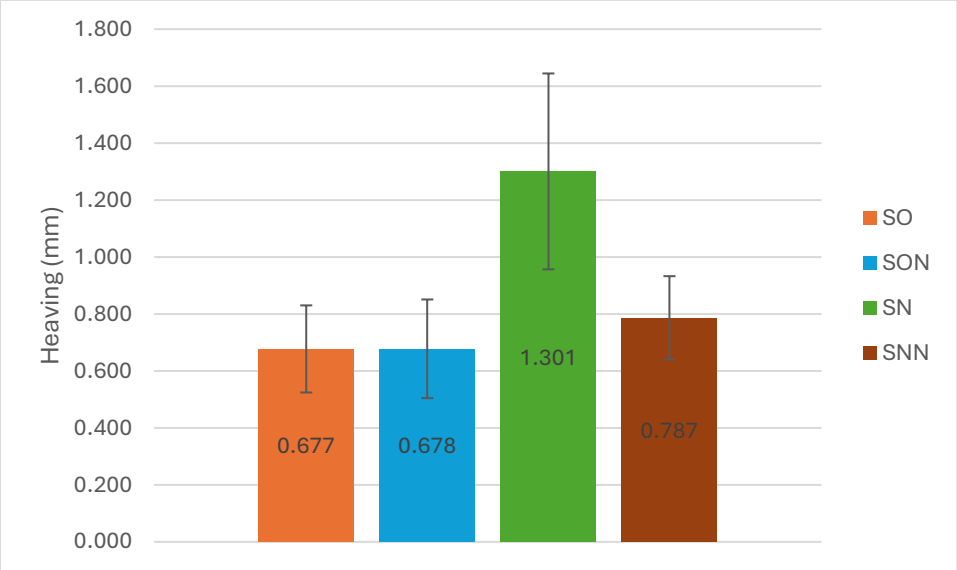

Figure 4.23: Frost heave test results of the aggregate blends using uniform temperature gradient

Figure 4.24 shows the correlation between frost heave and the CV/FV index. It was found that there is an excellent correlation between the frost heave and the CV/FV index, with an R^2 of 0.96. This finding indicates that greater CV/FV value or a higher amount of coarse void compared to the fine void will lead to higher heaving in general. Larger voids within the material allow more water for saturation. During freezing, the water undergoes volumetric expansion, which exerts pressure on the surrounding material to create heaving. Conversely, very small voids can restrict water movement due to higher flow resistance and provide extra space for water as it turns to ice, similar to how entrained air bubbles in cement concrete mitigate freeze-thaw durability issues. A similar concept is also used to determine the freeze-thaw related durability of bricks for masonry works; the maximum saturation coefficient (which is similar to the ratio of course voids and fine voids determined from cold and hot water absorption tests) is controlled to achieve the desired durability (ASTM C62, 2017).

In summary, the tenting test results demonstrate that the overall void structure of the aggregate blend plays a more critical role in frost heaving than the fine content alone. Specifically, the strong correlation between the CV/FV ratio and heaving magnitude suggests that this index is a superior predictor of performance. Consequently, prioritizing the CV/FV ratio during material selection offers a more effective strategy for mitigating frost action in base layers.

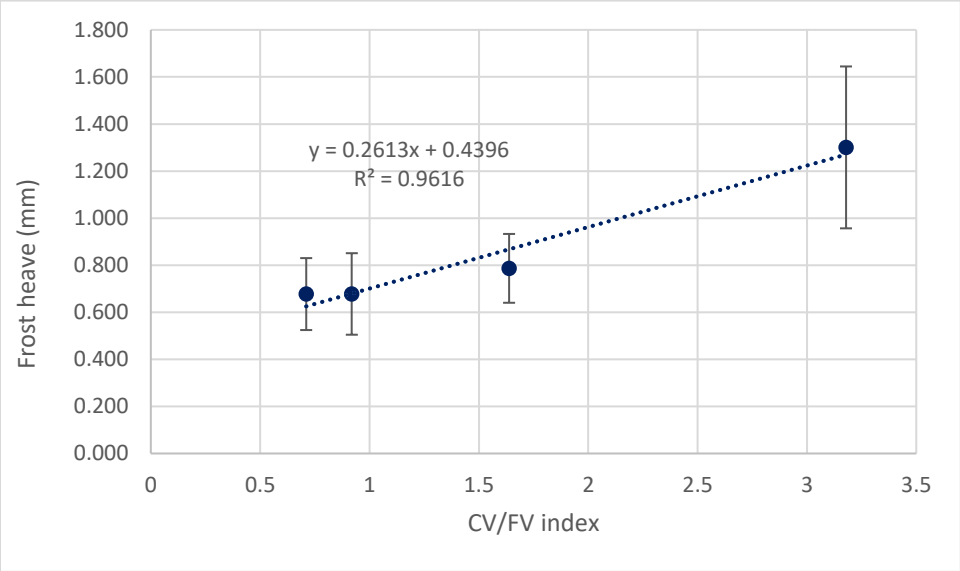

Figure 4.24: Correlation between frost heave and the CV/FV index

4.3.4 Permeability / Hydraulic Conductivity Test Result

Figure 4.25 shows the permeability or hydraulic conductivity test results. It should be noted that even though the target compaction level for preparing the samples was 100 % of the MDD, the degree of compaction (DOC) varied between the samples, because of the limitation of the manual tamping process involved. The SN blend exhibited a higher permeability, which had higher CV/FV index, compared to all other blends. The lowest hydraulic conductivity was found in the SO blend.

The hydraulic conductivity of the SNN and SON blend are very close to each other which was unexpected. There is a positive relation found with the CV/FV index and the hydraulic conductivity, as shown in Figure 4.26. It was observed that hydraulic conductivity tends to increase with the increase in CV/FV index. A higher CV/FV index indicates there will be coarser void in the blend, which will allow more water to enter and pass through aggregate layer, thus higher hydraulic conductivity.

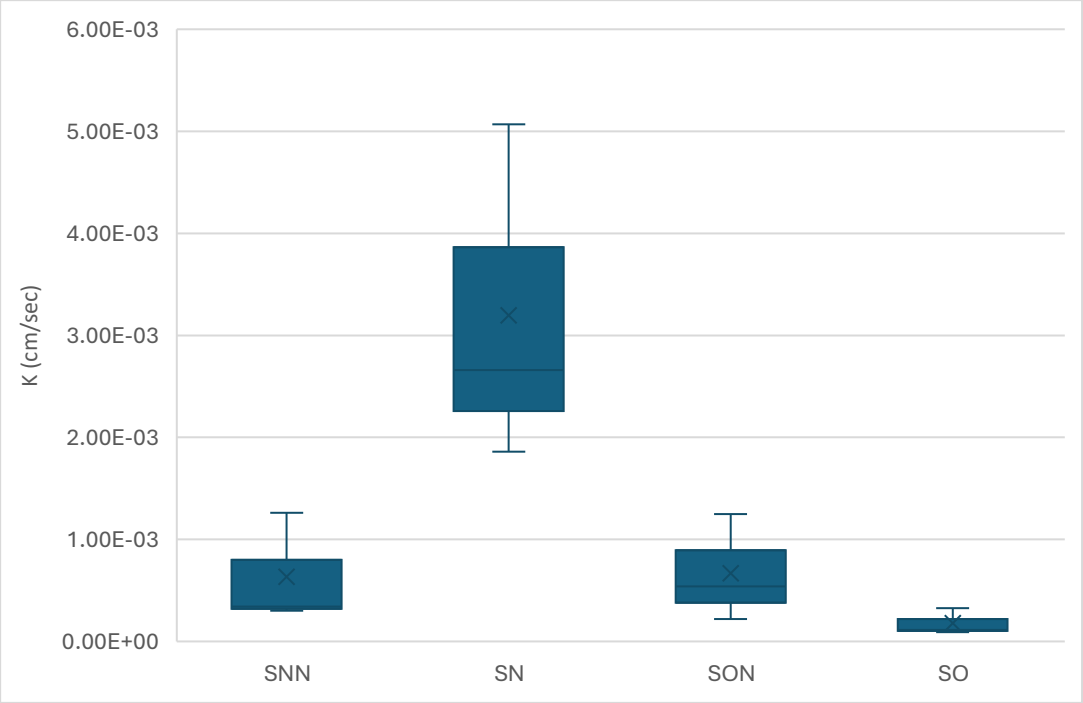

Figure 4.25: Permeability/ Hydraulic conductivity test results of the aggregate blends

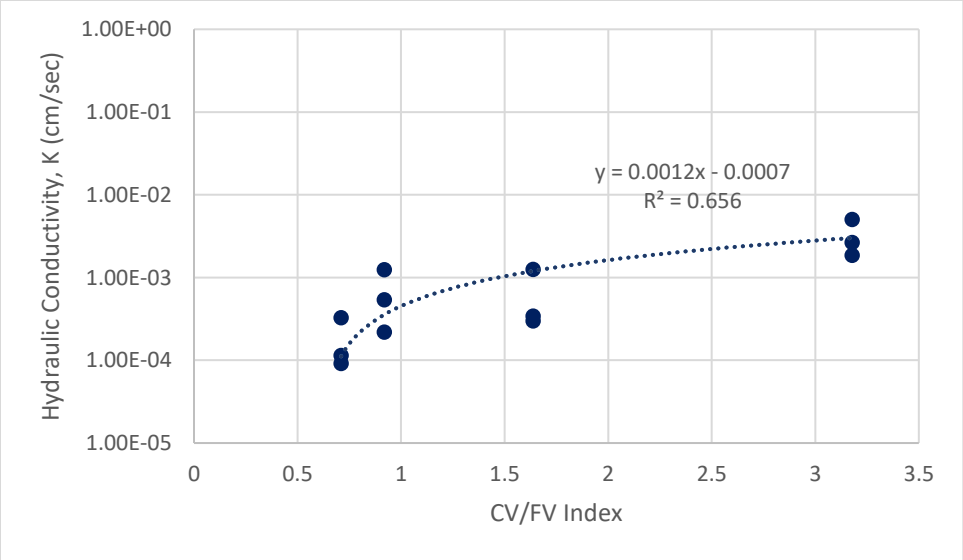

Figure 4.26: Relation between hydraulic conductivity and CV/FV index

A positive correlation was observed between permeability and frost heave, as shown in *Figure 4.27*. Higher permeability facilitates greater water movement through the voids. As the heaving or tenting depends on the volume of water entrapped in the base layer, higher permeability of the base layer can

create mixed results. If the water entered the system does not drain away before the temperature drops to freezing, then base layer may be vulnerable to heaving. However, if the pavement slope and higher permeability of the base materials help drain out water, then high permeability may be helpful in reducing heaving.

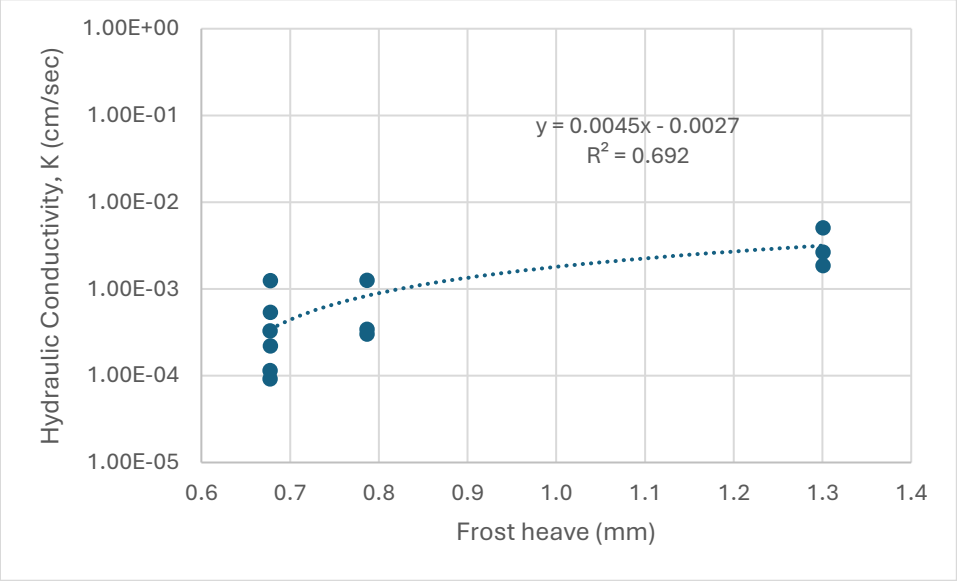

Figure 4.27: Permeability/ Hydraulic conductivity vs Frost heave relation

One critical factor in the development of tenting is the freezing of moisture at the interface between the asphalt surface and the base layer. In such cases, lower permeability of the base materials may not reduce tenting, as water can stagnate at the top of the base layer and lead to tenting. A moderate CV/FV index may help mitigate tenting by providing reasonable permeability and sufficient void space to accommodate the volumetric expansion of water when it freezes.

4.3.4.1 Effect of Percentage of Fine on Hydraulic Conductivity

Figure 4.28 shows the relationship between hydraulic conductivity and frost heave with the fine percentage present in the blend. It was observed that there was a weak negative linear relation observed between the hydraulic conductivity and the percentage of fines, as shown in Figure 4.28a. It was also observed that the percentage of fine and the frost heave has a weak relationship as well, as shown in Figure 4.28b above. In general, as the fine content increases, the void space becomes smaller and less connected, and thus, the permeability / hydraulic conductivity decreases. The weak correlation suggests that the other factors, such as aggregates' overall distribution, compacted aggregate structure, and degree of compaction, influence the hydraulic conductivity.

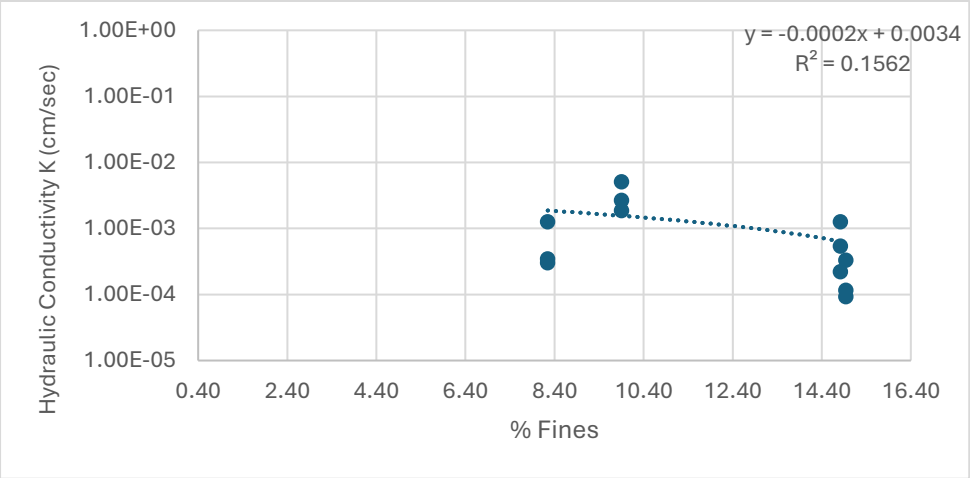

a) Hydraulic conductivity Vs % Fine

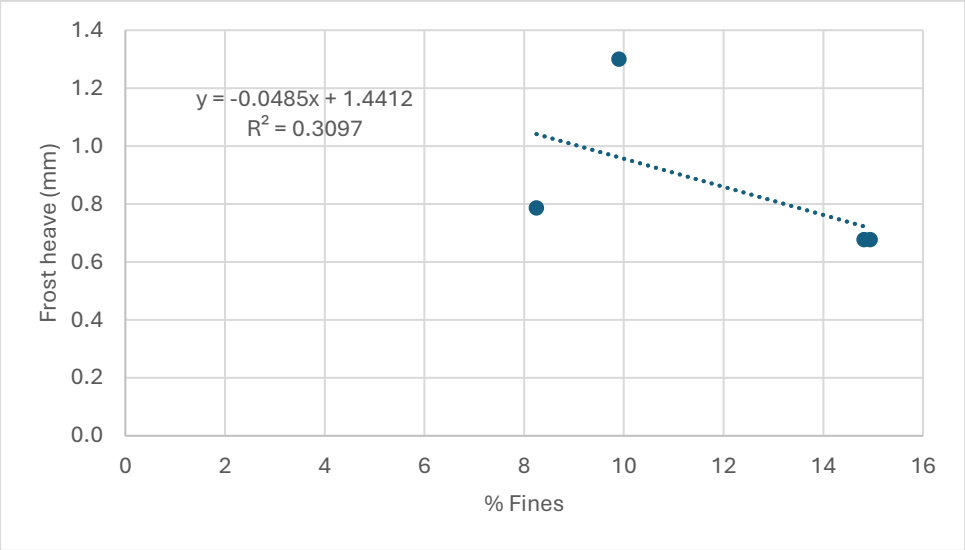

b) Frost heave Vs % Fine

Figure 4.28: Aggregate blends performance parameters comparison with the percentage of fine content

4.4 Comparison of Field and Plant Samples

Under the scope of this study, some base material samples were also collected from three field sections (referred to as field samples), where tenting was measured in winter and summer as discussed in Section 3.1. Figure 4.29 show the location of the project sites from where the base material samples were collected. Figure 4.30 shows two photographs of material collection process.

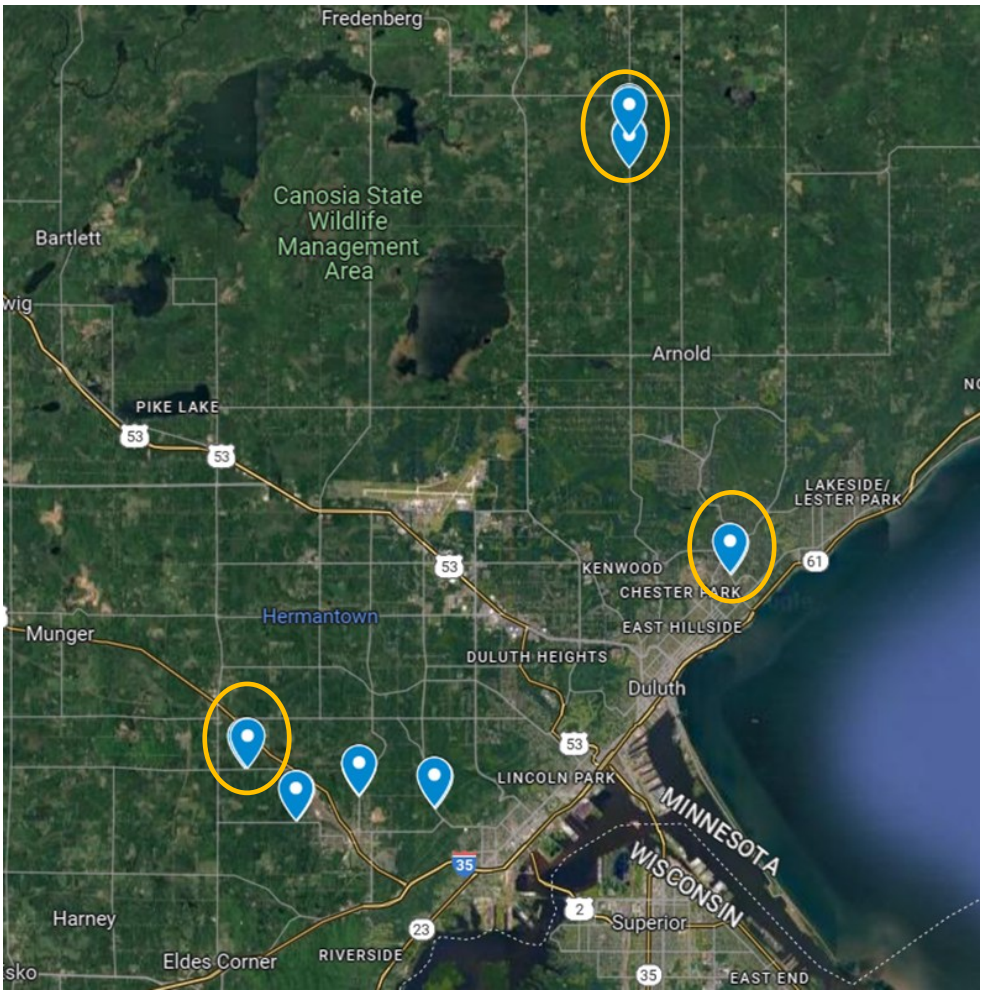

Figure 4.29: Locations (yellow circled) of the project sites from where base material samples were collected

Figure 4.30: Base materials collection from the project site

Figure 4.31 compares the gradations of field samples collected from three road sections, namely, Wallace Avenue, St. Louis Avenue, and Howard Gnesen Road.

As shown in Table 4.13, the Wallace Avenue sample is composed of 63.9% gravel, 27.8% sand, and 9.3% fines. The St. Louis Avenue sample consists of 72.35% gravel, 24.37% sand, and 3.28% fines, while the Howard Gnesen Road sample contains 74.4% gravel, 22.48% sand, and the lowest fine content at 3.12%. Notably, the St. Louis Avenue and Howard Gnesen Road samples exhibited similar gradations, suggesting comparable aggregate structure.

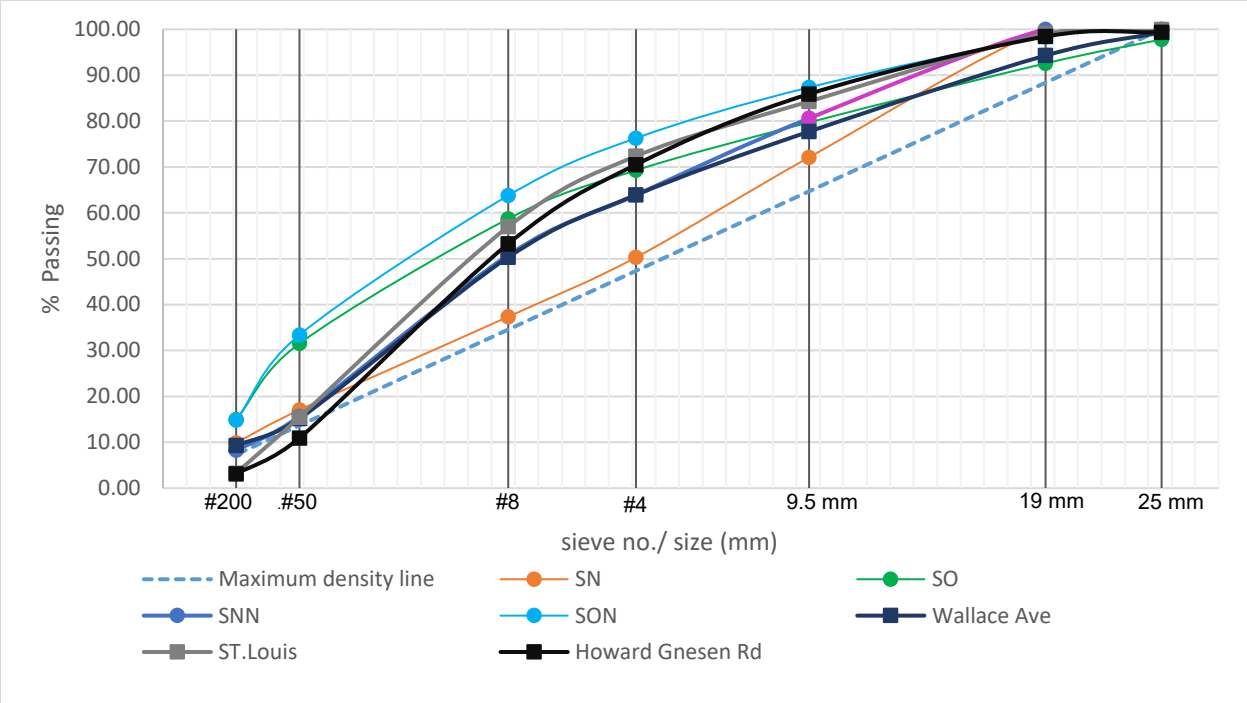

Figure 4.31: Gradation curves of the plant samples and the field samples together

Table 4.13: Composition of plant blends and field samples

Blend Name	% of Gravel	% of Sand	% of Fines
SNN	36.11	55.65	8.25
SN	49.69	40.41	9.90
SO	30.72	54.34	14.94
SON	23.72	61.46	14.82
Wallace Ave	63.90	27.80	9.30
ST. Louis	72.35	24.37	3.28
Howard Gnesen Rd	74.40	22.48	3.12

The void area analysis is presented in Figure 4.32. Overall, the three field samples have higher coarser void areas than their corresponding finer void areas. This suggests a greater prevalence of large individual voids (coarse voids) compared to small individual voids (fine voids). Among the three field samples, Wallace Avenue sample displayed the lowest total void area, while St. Louis Avenue and Howard Gnesen Road samples had total void areas exceeding those of the SN and SNN blends but lower than the SO and SON blends.

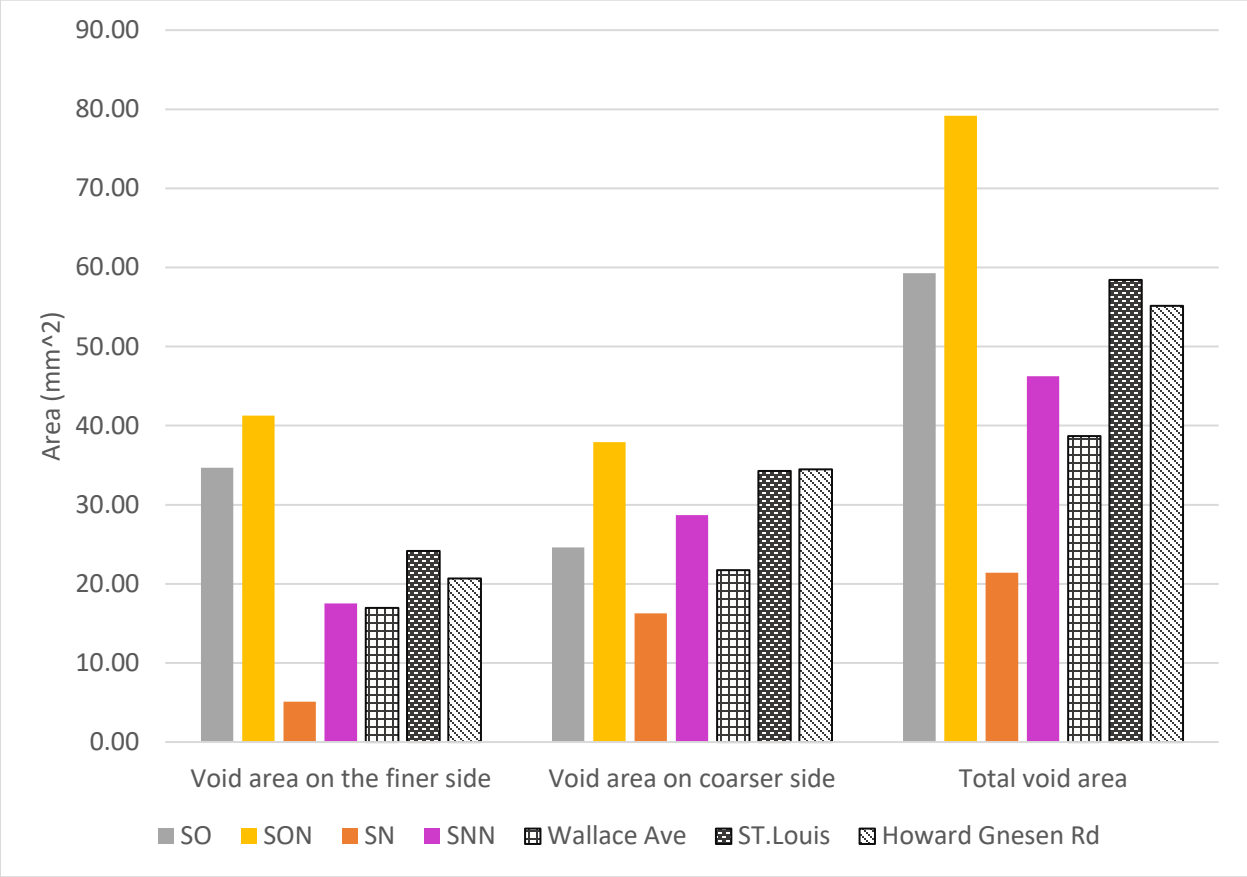

Figure 4.32: Quantitative comparison of the theoretical uncompacted void of the four different plant samples and the three different field samples

The CV/FV index for the field samples and the aggregate blends are shown in Figure 4.33. Howard Gnesen Road exhibited the highest CV/FV ratio among the field samples, followed by St. Louis Avenue. When compared to the plant blends, all field samples demonstrated higher CV/FV ratios than the SO and SON blends but lower ratios than the SN and SNN blends, with the exception of Howard Gnesen Road, which had a CV/FV ratio exceeding that of the SNN blend.

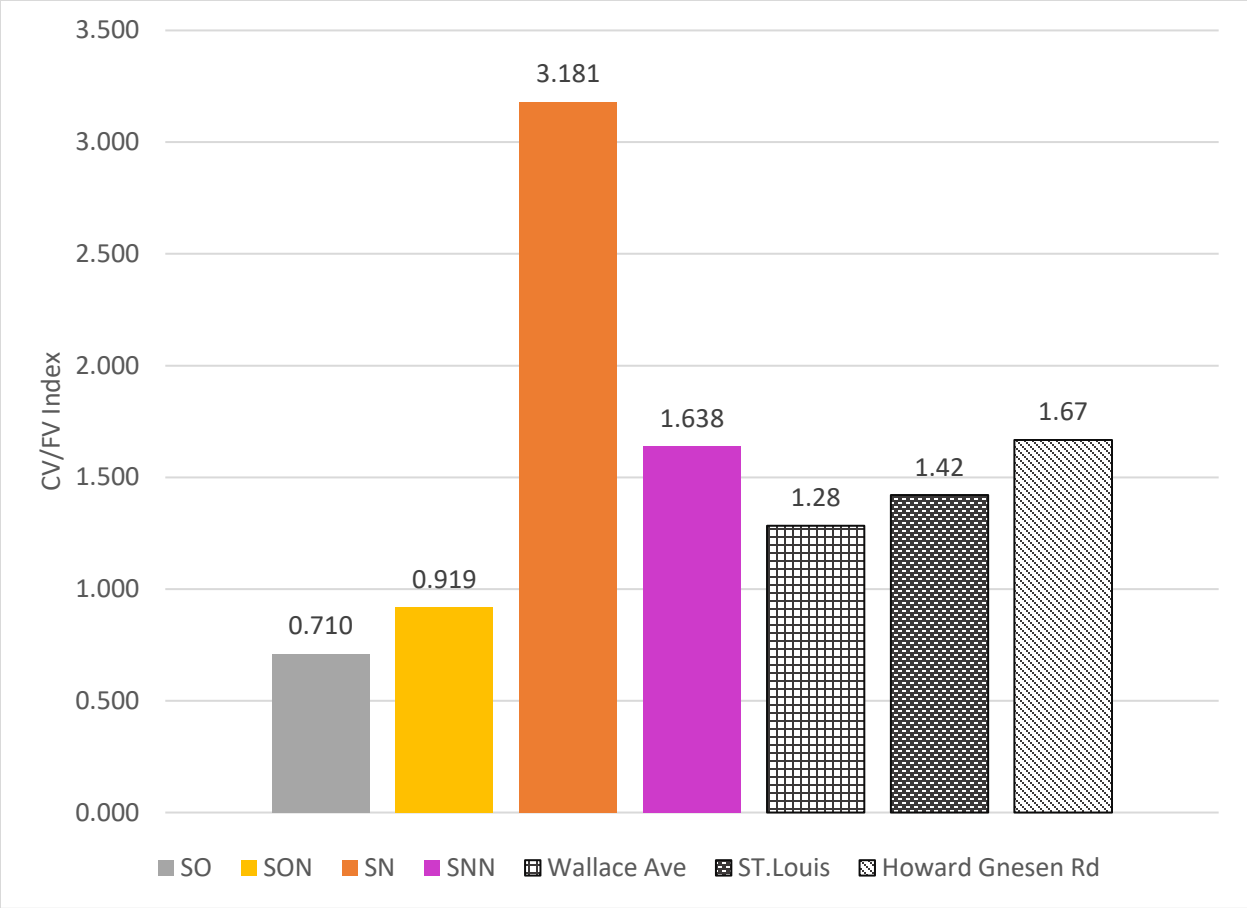

Figure 4.33: Comparison of CV/FV value of the plant samples and the field samples

Figure 4.34 compares the moisture-density relationships of the three field samples with those of the four aggregate blends (SO, SON, SN, and SNN). The results indicate that the maximum dry density (MDD) values for the field samples are relatively similar but lower than those of the field blends. Among the field samples, Wallace Avenue exhibited the highest MDD at 135.1 lb./ft^3, while the lowest MDD among the plant blends was observed for the SN blend at 143.4 lb./ft^3. These findings are summarized in Table 4.14, which presents the MDD and optimum moisture content (OMC) values for the field samples. Interestingly, all field samples exhibited similar OMC values.

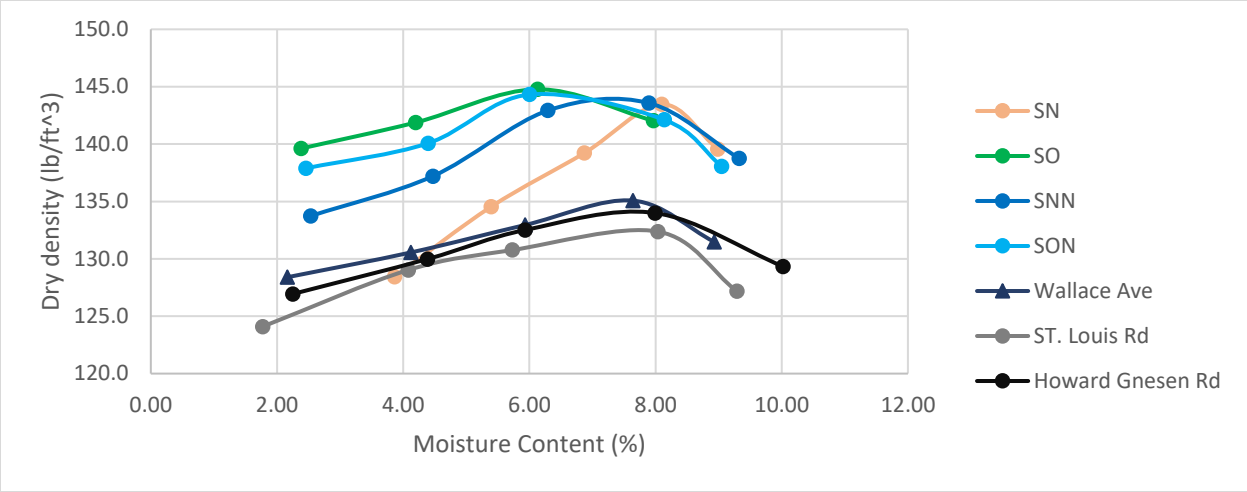

Figure 4.34: Moisture density relation of the four plant samples and the three field samples

Table 4.14: Comparison of plant and field sample with respect to their MDD and OMC

Blend name	Maximum dry Density (lb./ft^3)	Optimum Moisture Content (%)
SNN	144	7.25
SN	143.4	8.10
SO	144.8	6.2
SON	144.2	6.15
Wallace Ave	135.1	7.6
ST. Louis	132.4	7.8
Howard Gnesen Rd	134.1	7.62

Figure 4.35 illustrates the frost heave test results for four plant-produced aggregate blends and three field samples subjected to a uniform temperature gradient at -40°C. Among the field samples, the Wallace Avenue sample exhibited the highest frost heave value at 1.168 mm, followed by the Howard Gnesen Road sample at 0.991 mm. The St. Louis Avenue sample showed the lowest frost heave among the field samples, measuring 0.576 mm.

When compared to the plant-produced blends, both the Wallace Avenue and Howard Gnesen Road samples displayed higher frost heave values than all the blends except for the SN blend, which recorded a heave of 1.30 mm.

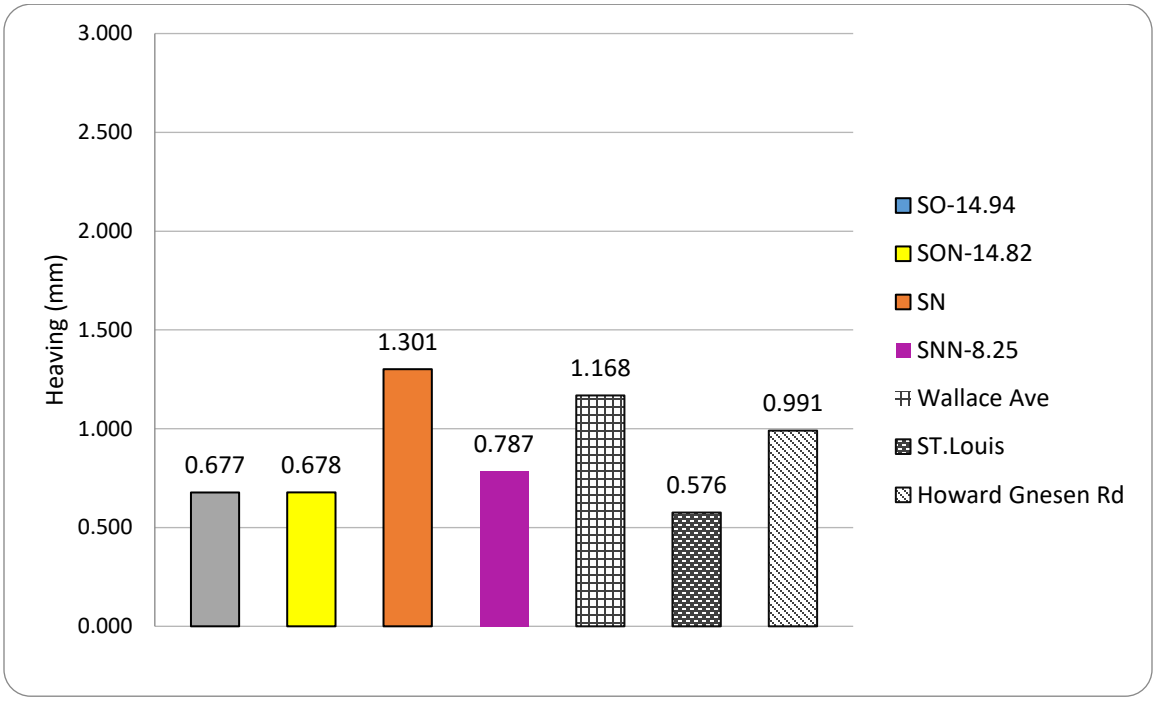

Figure 4.35: Frost heave test results of the aggregate blends using uniform temperature gradient

It is noteworthy that the St. Louis Avenue and Howard Gnesen Road samples, despite having similar fine contents (3.28% and 3.12%, respectively), exhibited different frost heave values. The Howard Gnesen Road sample demonstrated a substantially higher frost heave compared to the St. Louis Avenue sample. This finding reaffirm that fine content does not strongly correlate with frost heaving behavior.

Figure 4.36 presents a comparison of field measured tenting values during winter for samples from Wallace Avenue, Howard Gnesen Road, and St. Louis Avenue with frost heave values obtained from laboratory tests on aggregate base samples from the same locations. The results indicate that Wallace Avenue, which recorded the highest tenting value in the field, also exhibited the highest frost heave value during laboratory testing. Similarly, Howard Gnesen Road ranked second, followed by St. Louis Avenue, with the same order observed in both field and laboratory measurements.

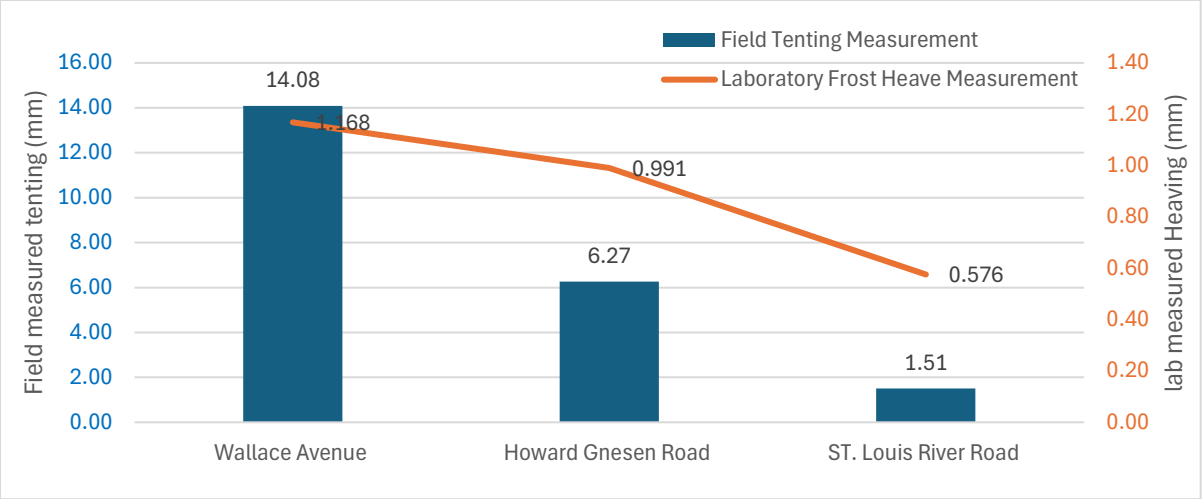

Figure 4.36: Comparison of measured tenting values between laboratory tests and field observations

Figure 4.37 presents frost heave results with respect to the CV/FV index for both sets of samples (3 aggregate samples collected from fields and 4 from plants). While the field results are a bit scattered, the heaving result of one project site is in proximity of the trendline drawn for all the data points. Overall, the heaving value is found to be increasing the CV/FV index.

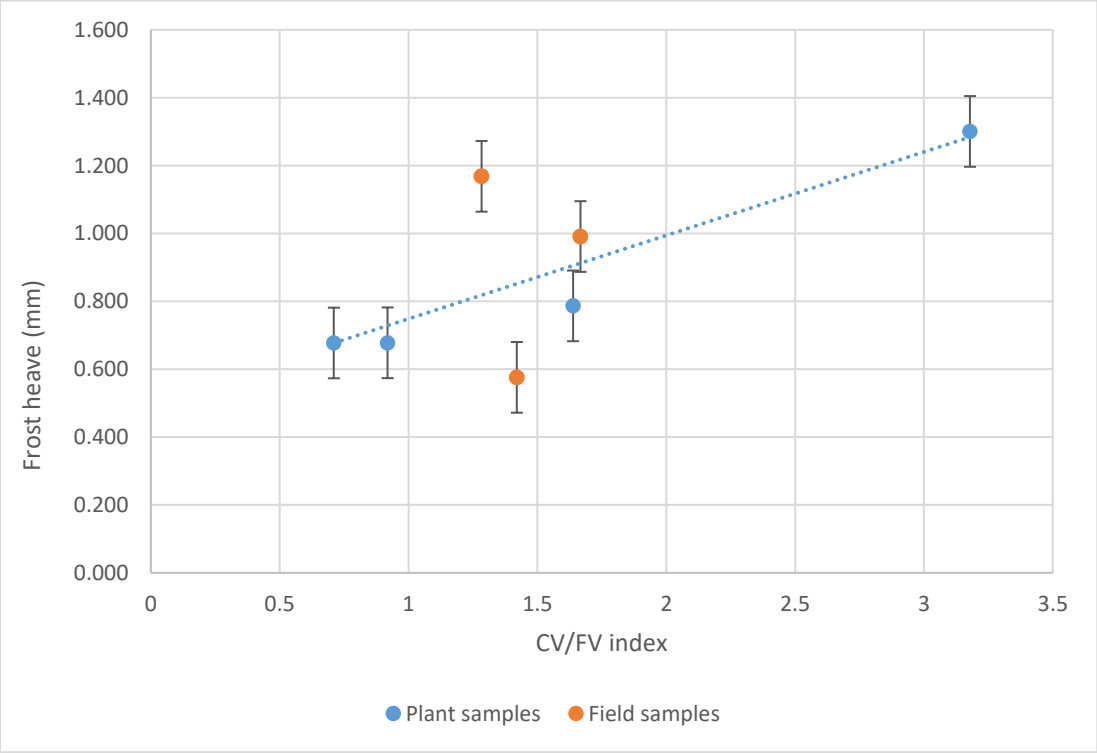

Figure 4.37: Updated frost heave vs. CV/FV index.

Figure 4.38 shows the correlation between lab-measured frost heave and field-measured tenting for the three samples. Although the small dataset is a limitation, the correlation observed in Figure 4.38 suggests a relationship between frost heave test results and field tenting is possible.

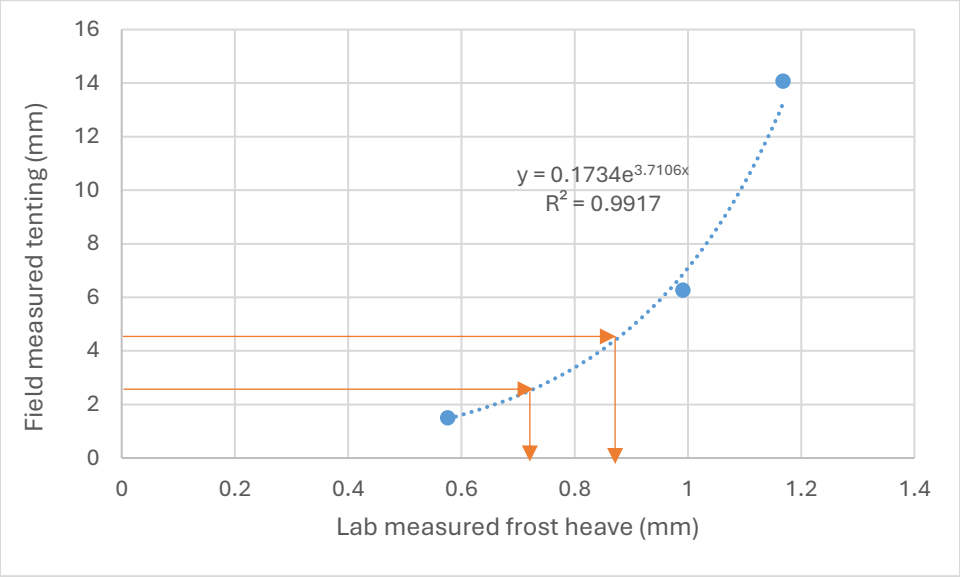

Figure 4.38: Correlation between field-measured tenting values and laboratory-measured frost values.

4.5 Road Condition vs. Tenting vs. CV/FV index

The MnDOT study conducted by Zegeye-Teshale et al. (2021) developed a method to classify road conditions into three categories based on tenting peak height value (PHV), as shown in Figure 4.39. Roads in good condition have PHV less than 2.5 mm, moderate condition roads have PHV between 2.5 mm and 4.4 mm, and poor condition roads have PHV greater than 4.4 mm. Using correlations presented in Figure 4.39, this study determined the corresponding lab-measured frost heave results and CV/FV index for these three categories as shown in Table 4.15. It should be noted that overall tenting may result from frosting within the base material, as well as from the freezing of accumulated water at the interface between the surface and base layers. Consequently, both tenting and frost heave within the base material are possible. The CV/FV ranges provided in Table 4.15 for the three road conditions shall be further verified with more data.

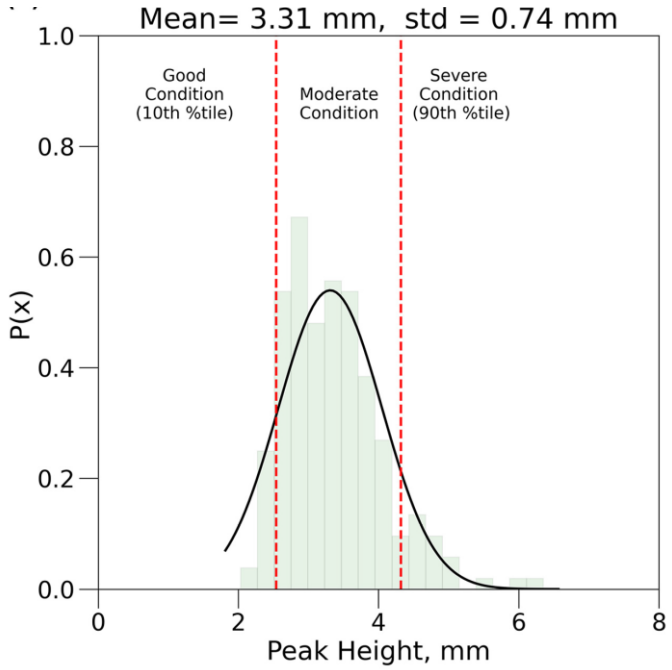

Figure 4.39: Road condition vs tenting peak height value (PHV) in Zegeye-Teshale et al. (2021) study.

Table 4.15: Road Condition vs. Tenting height and CV/FV index.

Road Condition	Tenting PHV (mm)	Lab-measured Frost heave (mm)	CV/FV Index
Good	< 2.5	< 0.72	0.88
Moderate	2.5 to 4.4	0.72 to 0.87	0.88 to 1.42
Poor	> 4	> 0.87	> 1.42

Chapter 5: Development of Decision Trees

This chapter presents the decisions tress developed in this study. The key findings from the study have been used to develop three decision trees.

The first decision tree is provided in Figure 5.1. The first one is to facilitate the selection of the most appropriate treatment to decrease the road roughness and mitigate the tenting of the existing roads. In this decision tree, the optimal, intermediate, and least effective pavement treatments (specific to road roughness and tenting) are recommended for three different types of pavements. The pavement treatment ranking presented in Section 4.3.2 (Table 4.9) is used for developing this decision tree. While Table 4.9 ranked six treatment methods, only the first three are included in the decision tree (Figure 5.1). It is worth noting that the three treatments excluded from the decision tree—crack seal, crack fill, and chip seal, were not shown to improve road roughness. However, this does not imply they lack value. For instance, crack sealing and filling are effective in preventing water infiltration, which can significantly reduce moisture accumulation in transverse cracks, a key factor contributing to tenting.

As illustrated in Figure 5.1, micro surfacing emerges as the most effective treatment for both BAB and BOB pavements. Patching serves as the intermediate option for these pavement types, typically applied as a maintenance measure on moderately deteriorated roads nearing the end of their design life. While crack repair is the least effective among the three treatments, combining it with patching where necessary could provide a practical strategy prior to undertaking major rehabilitation efforts.

Crack repair was found to be the most effective treatment on BOC pavement compared to the others. This is because concrete joints and cracks propagate through the overlay (reflective cracking), where repairing them can significantly improve the roughness of the pavement. Micro surfacing is the second-best option followed by patching.

The next decision tree, shown in Figure 5.2, distinguishes between localized treatments and pavement surface treatments. Based on the pavement type, either patching or crack repair can be selected as localized treatments. Micro-surfacing is identified as the most effective surface treatment.

This research has dedicated substantial effort to developing a frost-heaving test procedure, including the test setup and a practical method for evaluating the vulnerability of base materials to frost heave. Currently, frost mitigation strategies focus primarily on controlling the percentage of fines in the base materials. While excessive fines are known to contribute to frost heaving, this study reveals that the overall void structure, beyond just fine content, offers a more comprehensive characterization of base materials and may be more effective in mitigating tenting.

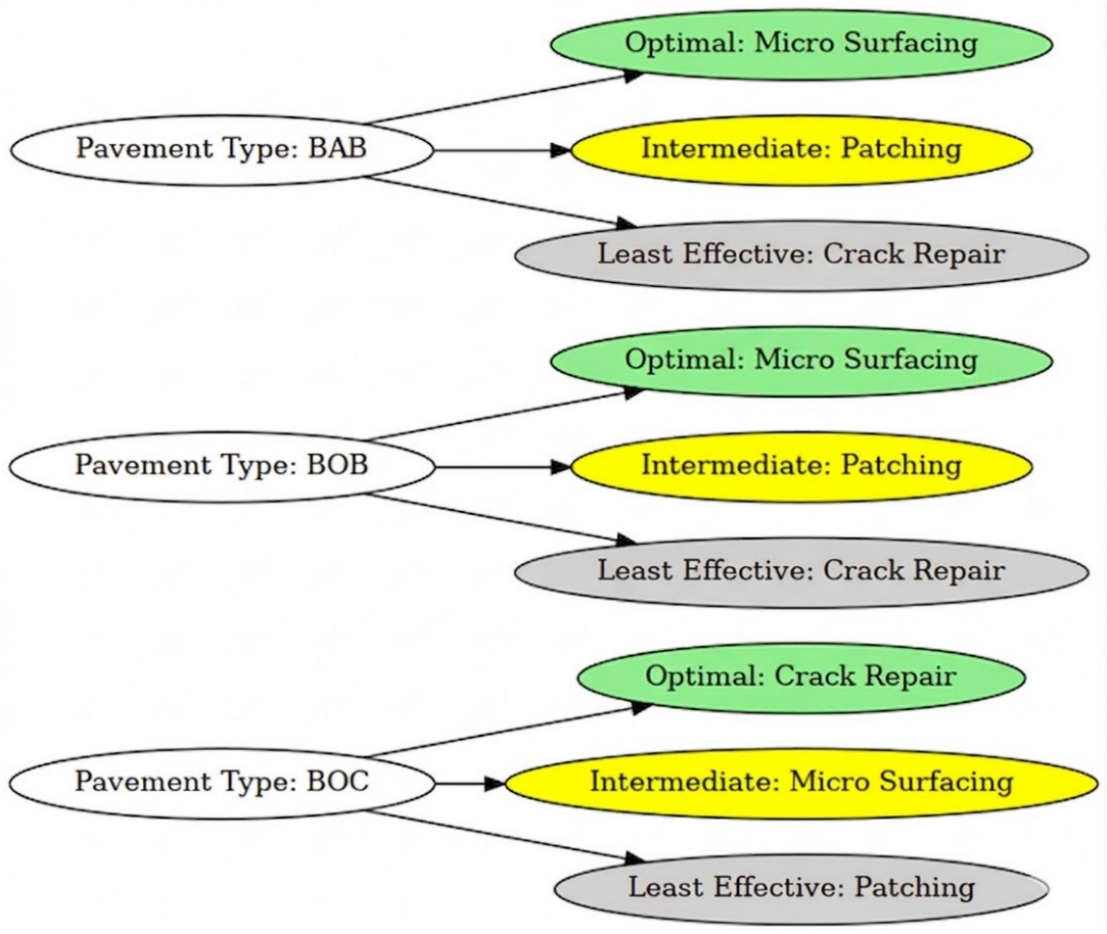

Figure 5.1: Decision tree for selecting pavement treatment to decrease tenting on the existing pavement.

The third decision tree provides guidance for the base material gradation (Figure 5.3). Based on the threshold values of IRI or tenting, recommendations are made on the target CV/FV index. A CV/FV index value less than 0.88 may result in tenting less than 2.5 mm, indicating a favorable performance outcome. The fine content is limited to 10%.

In conclusion, it seems the longest lasting fixes for the most severe tenting involved identifying and mitigating any issues in underlying base/embankment. If no issues exist in base/embankment, or if the work is not practical due to other reasons (the pavement is relatively new), then the decision trees presented in Figure 5.1 and Figure 5.2 should be implemented to decrease the tenting.

MnDOT guidance on crack fill and seal (Ulring, 2022)

Crack Clean and Fill – typically performed on older pavements having cracks > 3⁄4" to 1inch in width. Crack is cleaned with compressed air and filled with sealant.

Crack Route and Seal – is performed on newer pavements having cracks ≤ 3⁄4 inch to 1inch in width. This process involves routing a reservoir typically 3⁄4 inch wide and 3⁄4 inch deep. Sealant is placed in the crack with an overband to better seal the crack and help keep the sealant in place. The overband should be less than 3 inches wide and no more than 1/8” thick (high).

Crack Repair- is addressing more significant treatments than just filling or sealing, often targeting underlying problems. It is typically performed on cracks that have deteriorated beyond the point where simple filling or sealing is effective. Preparatory repairs—such as filling cupped cracks or patching adjacent small potholes—may be carried out before the cracks are ready for filling or sealing treatments.

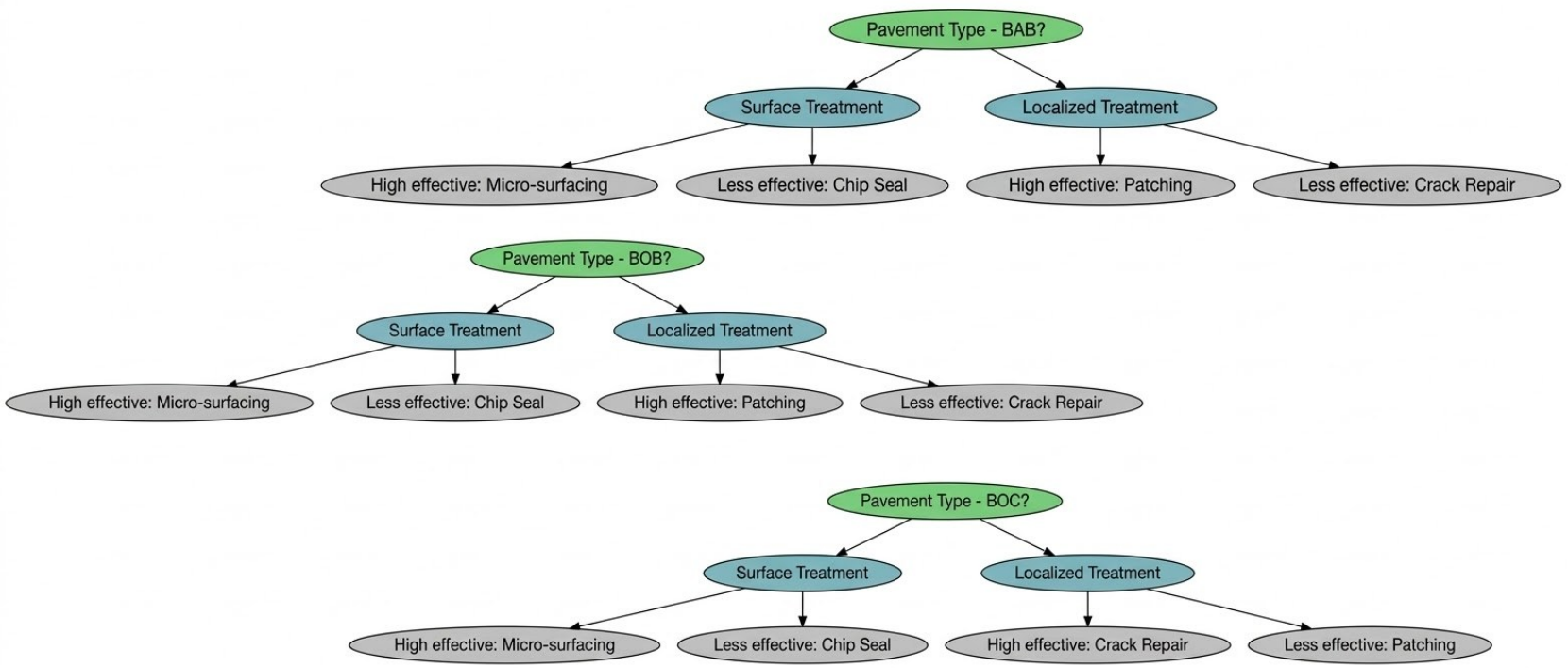

Figure 5.2: Decision tree for selecting localized and pavement surface treatment to decrease tenting on the existing pavement.

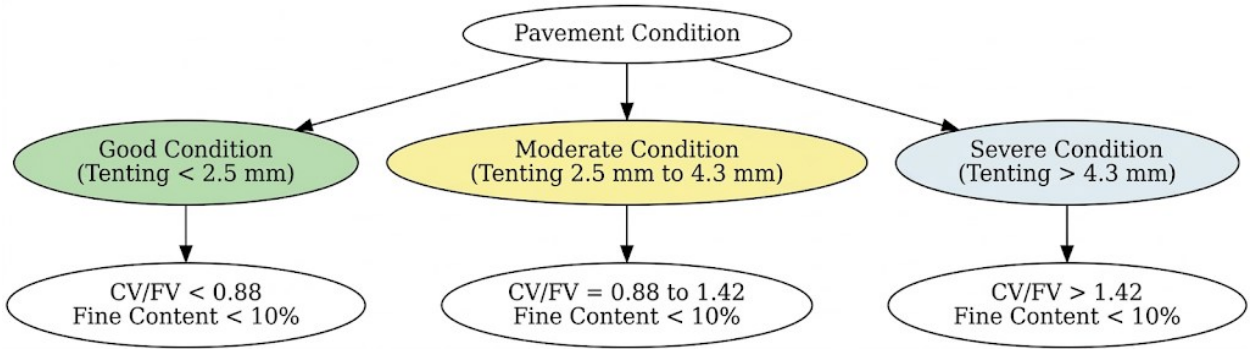

Figure 5.3: Decision tree for selecting CV/FV ratio based on the road condition.

It is important to note that the three decision trees were developed using a limited dataset. To enhance the reliability of the CV/FV index, further optimization is needed through additional laboratory testing of base materials collected from field sites with documented tenting conditions. A comprehensive study should be conducted to establish the correlation between field-measured tenting and laboratory-measured frost susceptibility and CV/ FV index. Moreover, the current study did not include strength testing of the base materials. Therefore, the optimization of the CV/FV index should account for both frost heave potential and base material strength characteristics.

Chapter 6: Conclusions and Recommendations

Tenting of the transverse crack in asphalt pavement is a concern for pavement surface smoothness and ride comfort. The integrity of the pavement surface is significantly affected by its occurrence, which deteriorates the crack. As a result, the crack widens and can turn into a pothole over time. Only a very limited number of studies have directly addressed the tenting issue in asphalt pavement.

The goal of this study was to identify the treatment methods to mitigate tenting and establish the base material characterizing factors that can be controlled to decrease the frost heaving of the base materials. Under the scope of this study, multiple tasks were performed to achieve the goal. These tasks included a literature review to understand the tenting problem, tenting measurement in the field, road-based material collection for laboratory testing, pavement roughness data analysis, and several laboratory tests such as sieve tests, permeability tests, and frost heave tests.

This report presents the findings from the literature review, fieldwork, pavement distress/performance data analysis and laboratory test results. The following are some major conclusions.

- Tenting is a localized distress primarily caused by moisture infiltration in the base layer and fine generation or intrusion at the interface of the surface and the base layer.
- Tenting severity is measured by the peak height of the heaved crack. The higher the peak height value, the more severe the tenting. Pavement surface smoothness is significantly affected by the occurrence of tenting, and the international roughness index (IRI) directly correlates with the tenting peak height value and severity.
- Some mitigation measures implemented by various transportation agencies include crack seal, chip seal, slurry seal, mill and overlay, and other preventive maintenance treatments.
- Based on the limited field data, tenting severity varies significantly from pavement to pavement. Roads having higher AADT exhibited high severity tenting due to higher moisture and fine particle infiltration.
- The field study results confirm that tenting does not disappear completely in the summer, indicating the presence of intruded fines underneath the crack. Some roads exhibit permanent tenting, which leads to higher crack deterioration even after winter. Moreover, some tented cracks can form cupping (reduction of crack elevation from pavement base level), indicating the loss of fines underneath the crack.
- Since the effect of tenting remains in the pavement year-round, pavement surface IRI is significantly affected by it throughout the year.
- The analytical study shows that analyzing pavement roughness data can help evaluate the effectiveness of various treatment methods. The roughness study results revealed that pavement surface IRI improvement is dependent on the function of pavement type and maintenance method. It also showed that micro-surfacing is a good method for improving road

roughness, particularly on Bituminous over Aggregate Base (BAB) and Bituminous over a Bituminous layer (BOB) pavement types.

- For tenting mitigation, localized repair methods such as crack fill, crack seal, and crack repair may be effective. Therefore, crack repair is helpful for all three pavement types: BAB, BOB, and Bituminous over Concrete layer (BOC), since it has a relatively higher composite score than crack fill and seal. Supposedly, crack repair involves more extensive repair of cracks, which includes cleaning the fines from the crack, routing, drying, and applying sealant, making the joint stronger and more durable against moisture and fine infiltration.
- Laboratory test results revealed that the fine content fraction does not directly correlate with the aggregate permeability and frost heave. It is the overall aggregate distribution, which creates coarse and fine voids in the aggregate mix, that affects the blend performance in terms of frost heaving.
- This study introduced the CV/FV index, defined as the ratio of coarse voids to fine voids within aggregate base materials. Laboratory testing demonstrated a strong correlation between the CV/FV index, hydraulic conductivity, and frost-heave susceptibility. A higher CV/FV index was associated with increased frost susceptibility and greater permeability. These findings suggested the CV/FV index could serve as a practical control parameter to mitigate frost heave in base layers. Analogous to how entrained air voids are managed in cement concrete to improve freeze-thaw durability, the CV/FV index may offer a mechanism for controlling frost-related damage in unbound aggregate bases. Materials exhibiting a CV/FV index less than 0.88 showed enhanced resistance to frost heaving; however, further research, including field validation, is required to establish an optimal CV/FV range for design applications.
- The laboratory-tested frost heave value was found to be significantly less than the field-measured tenting value, even less than the tenting threshold value (2.5mm). This discrepancy can be attributed to two primary factors. First, the pavement structure in field conditions differs substantially from the controlled laboratory setup. Second, frost heave induced by the base materials is not the sole factor contributing to tenting; moisture accumulation at the interface between the asphalt layer and the base layer plays a considerable role.
- Salt-contained samples showed less heaving than the unsalted sample since salt drops the freezing point.
- The laboratory frost heave test results for field samples showed a consistent trend with the measured winter tenting values observed in the field. Wallace Avenue, which exhibited the highest frost heave value in laboratory tests, also recorded the highest tenting value during field measurements among the three field samples collected. A similar pattern was observed for the Howard Gnesen Road and Saint Louis Avenue samples, where the frost heave results aligned closely with their respective tenting values recorded in the field.
- The study developed three decision trees. The first one is to facilitate the selection of the most appropriate treatment to decrease the road roughness and mitigate the tenting of the existing roads. The second decision tree separates the localized and pavement surface treatments. The third decision tree provides guidance for the base material gradation. Based on the threshold

values of IRI or tenting, recommendations are made on the target CV/FV index. A CV/FV index value less than 0.88 may result in tenting less than 2.5 mm, indicating a favorable performance outcome. The fine content is limited to 10%.

REFERENCES

1. American Association of State Highway and Transportation Officials. (2020). *Standard method of test for materials finer than 75-µm (No. 200) sieve in mineral aggregates by washing* (AASHTO Designation: T 11). AASHTO.
2. ASTM International. (2006). *Standard test method for permeability of granular soils (constant head)* (ASTM D2434-68). ASTM International.
3. ASTM International. (2015). *Standard test method for relative density (specific gravity) and absorption of coarse aggregate* (ASTM C127-15). ASTM International.
4. ASTM International. (2015). *Standard test method for relative density (specific gravity) and absorption of fine aggregate* (ASTM C128-15). ASTM International.
5. ASTM International. (2018). *Standard test methods for filterable matter (total dissolved solids) and nonfilterable matter (total suspended solids) in water* (ASTM D5907-18). ASTM International.
6. ASTM International. (2023). *Standard test methods for electrical conductivity and resistivity of water* (ASTM D1125-23). ASTM International.
7. Bush, A. J., & Brooks, E. W. (2007). *Geosynthetic materials in reflective crack prevention*. Oregon Department of Transportation, Research Unit. https://rosap.ntl.bts.gov/view/dot/21846
8. Ćwiąkała, M., Gajewska, B., Kraszewski, C., & Rafalski, L. (2016). Recapitulation of research on frost susceptibility of unbound mixtures for pavement structures. *Roads and Bridges — Drogi i Mosty*, *15*(4), 285–300. https://doi.org/10.7409/rabdim.016.018
9. Doré, G., Konrad, J. M., & Roy, M. (1997). Role of deicing salt in pavement deterioration by frost action. *Transportation Research Record*, *1596*(1), 70-75.
10. Federal Highway Administration. (2001). *1999 Status of the nation's highways, bridges, and transit: Conditions and performance* (Report No. FHWA-PL-08-017). U.S. Department of Transportation. http://www.fhwa.dot.gov/policy/1999cpr/index.htm
11. Guthrie, W. S., & Hermansson, Å. (2003). Frost heave and water uptake relations in variably saturated aggregate base materials. *Transportation Research Record*, *1821*(1), 13–19. https://doi.org/10.3141/1821-02
12. Johnson, E. N., & Olson, R. C. (2008). *Investigation of winter pavement tenting* (Report No. MN/RC 2008-03). Minnesota Department of Transportation.
13. Kestler, M. A., Krat, A. S., & Roberts, G. E. (2000). *Winter tenting of highway pavements: Test program and discussion of causes and mechanisms* (Report No. FHWA-NH-RD-12323C). Federal Highway Administration.
14. Khattak, M. J., & Alrashidi, M. (2013). Performance of preventive maintenance treatments of flexible pavements. *International Journal of Pavement Research and Technology*, *6*(3), 184.
15. Marquis, B. (2004). *Experimental use of sawed and sealed joints to minimize thermal cracking: Final report* (Report No. 96-25). Maine Department of Transportation.

16. Minnesota Department of Transportation. (2002). The moisture-density relations of soils using a 2.5kg (5.5 lb) rammer and a 305mm (12 inch) drop. *MnDOT laboratory manual*. MnDOT. https://www.dot.state.mn.us/materials/labmanual.html
17. Minnesota Department of Transportation. (2018). *Earthwork series — fill placement: Unified Soil Classification System (USCS) guide* (AT-TC3CN025-18-T1-JA03). MnDOT.
18. Minnesota Department of Transportation. (2019, July 10). *Pavement design manual*. MnDOT. https://www.dot.state.mn.us/materials/pvmtdesign/manual.html
19. Minnesota Department of Transportation. (2022). Flexible pavement crack treatments guidance. *MnDOT pavement preservation engineer*. MnDOT.
20. Sharma, A. K., & McIntyre, J. A. (1991). *Reflective cracking and tenting in asphaltic overlays* (Report No. 1300). Transportation Research Board, Washington DC.
21. Ulring, J. (2022). *Flexible pavement crack treatments guidance*. MnDOT.
22. Zegeye-Teshale, E., Calhoon, T., & Johnson, E. (2021). *Comparison of pavement tenting on MN-37D, US-169D, and US-169I in summer and winter months*. MnDOT Office of Materials and Research.
23. Zegeye-Teshale, E., Calhoon, T., Johnson, E. N., & Dai, S. (2021). Application of advanced multi-sensor non-destructive testing system for the evaluation of pavements affected by transverse crack-heaving. *Transportation Research Record*, *2675*(9), 1149–1162. https://doi.org/10.1177/03611981211006430

APPENDIX A:
BonfrroPost-Tests results for Ranking Pavement Treatments

Table A-1 Bonferroni Post-Tests results

Pavement Type + Treatment Name	Pavement Type + Treatment Name	Mean Difference	SE	t	p	Comments
BAB - Chip Seal	BOB - Chip Seal	0.8	0.793	1	1	Statistically No Difference
BAB - Chip Seal	BOC - Chip Seal	3.35	0.907	3.69	0.034	Statistically Different
BAB - Chip Seal	BAB - Crack Fill	-3.59	0.705	-5.09	0.001	Statistically Different
BAB - Chip Seal	BOB - Crack Fill	-0.2	0.823	-0.24	1	Statistically No Difference
BAB - Chip Seal	BOC - Crack Fill	-3.66	0.915	-4	0.009	Statistically Different
BAB - Chip Seal	BAB - Crack Rear	-10.31	1.161	-8.88	0.001	Statistically Different
BAB - Chip Seal	BOB - Crack Rear	-0.86	1.611	-0.53	1	Statistically No Difference
BAB - Chip Seal	BOC - Crack Repr	-17.97	1.085	-16.55	0.001	Statistically Different
BAB - Chip Seal	BAB - Crack Seal	-0.89	0.89	-1	1	Statistically No Difference
BAB - Chip Seal	BOB - Crack Seal	2.02	1.012	2	1	Statistically No Difference
BAB - Chip Seal	BOC - Crack Seal	3.75	0.947	3.96	0.012	Statistically Different
BAB - Chip Seal	BAB - Micro-Surf	-16.87	1.088	-15.51	0.001	Statistically Different
BAB - Chip Seal	BOB - Micro-Surf	-21.52	1.6	-13.45	0.001	Statistically Different
BAB - Chip Seal	BOC - Micro-Surf	-18.44	1.682	-10.96	0.001	Statistically Different
BAB - Chip Seal	BAB - Patching	-9.02	0.604	-14.92	0.001	Statistically Different
BAB - Chip Seal	BOB - Patching	-2.88	0.752	-3.83	0.021	Statistically Different
BAB - Chip Seal	BOC - Patching	-5.5	0.71	-7.75	0.001	Statistically Different
BOB - Chip Seal	BOC - Chip Seal	2.55	1.006	2.54	1	Statistically No Difference
BOB - Chip Seal	BAB - Crack Fill	-4.38	0.829	-5.29	0.001	Statistically Different
BOB - Chip Seal	BOB - Crack Fill	-0.99	0.932	-1.07	1	Statistically No Difference

Pavement Type + Treatment Name	Pavement Type + Treatment Name	Mean Difference	SE	t	p	Comments
BOB - Chip Seal	BOC - Crack Fill	-4.46	1.013	-4.4	0.003	Statistically Different
BOB - Chip Seal	BAB - Crack Repr	-11.11	1.24	-8.96	0.001	Statitically Different
BOB - Chip Seal	BOB - Crack Repr	-1.66	1.669	-0.99	1	Statistically No Difference
BOB - Chip Seal	BOC - Crack Repr	-18.76	1.17	-16.04	0.001	Statitically Different
BOB - Chip Seal	BAB - Crack Seal	-1.69	0.991	-1.7	1	Statistically No Difference
BOB - Chip Seal	BOB - Crack Seal	1.23	1.101	1.12	1	Statistically No Difference
BOB - Chip Seal	BOC - Crack Seal	2.95	1.042	2.83	0.71	Statistically No Difference
BOB - Chip Seal	BAB - Micro-Surf	-17.67	1.172	-15.08	0.001	Statitically Different
BOB - Chip Seal	BOB - Micro-Surf	-22.31	1.658	-13.45	0.001	Statitically Different
BOB - Chip Seal	BOC - Micro-Surf	-19.24	1.738	-11.07	0.001	Statitically Different
BOB - Chip Seal	BAB - Patching	-9.81	0.745	-13.17	0.001	Statitically Different
BOB - Chip Seal	BOB - Patching	-3.68	0.87	-4.23	0.003	Statitically Different
BOB - Chip Seal	BOC - Patching	-6.3	0.833	-7.56	0.001	Statitically Different
BOC - Chip Seal	BAB - Crack Fill	-6.94	0.939	-7.39	0.001	Statitically Different
BOC - Chip Seal	BOB - Crack Fill	-3.54	1.03	-3.44	0.089	Statistically No Difference
BOC - Chip Seal	BOC - Crack Fill	-7.01	1.105	-6.34	0.001	Statitically Different
BOC - Chip Seal	BAB - Crack Repr	-13.66	1.316	-10.38	0.001	Statitically Different
BOC - Chip Seal	BOB - Crack Repr	-4.21	1.726	-2.44	1	Statistically No Difference
BOC - Chip Seal	BOC - Crack Repr	-21.31	1.25	-17.05	0.001	Statitically Different
BOC - Chip Seal	BAB - Crack Seal	-4.24	1.084	-3.91	0.015	Statitically Different
BOC - Chip Seal	BOB - Crack Seal	-1.32	1.186	-1.11	1	Statistically No Difference

Pavement Type + Treatment Name	Pavement Type + Treatment Name	Mean Difference	SE	t	p	Comments
BOC - Chip Seal	BOC - Crack Seal	0.4	1.132	0.36	1	Statistically No Difference
BOC - Chip Seal	BAB - Micro-Surf	-20.22	1.252	-16.15	0.001	Statitically Different
BOC - Chip Seal	BOB - Micro-Surf	-24.86	1.716	-14.49	0.001	Statitically Different
BOC - Chip Seal	BOC - Micro-Surf	-21.79	1.792	-12.16	0.001	Statitically Different
BOC - Chip Seal	BAB - Patching	-12.37	0.865	-14.29	0.001	Statitically Different
BOC - Chip Seal	BOB - Patching	-6.23	0.975	-6.39	0.001	Statitically Different
BOC - Chip Seal	BOC - Patching	-8.85	0.942	-9.39	0.001	Statitically Different
BAB - Crack Fill	BOB - Crack Fill	3.39	0.859	3.95	0.012	Statitically Different
BAB - Crack Fill	BOC - Crack Fill	-0.07	0.946	-0.08	1	Statistically No Difference
BAB - Crack Fill	BAB - Crack Repr	-6.72	1.186	-5.67	0.001	Statitically Different
BAB - Crack Fill	BOB - Crack Repr	2.73	1.629	1.67	1	Statistically No Difference
BAB - Crack Fill	BOC - Crack Repr	-14.38	1.112	-12.93	0.001	Statitically Different
BAB - Crack Fill	BAB - Crack Seal	2.7	0.922	2.93	0.526	Statistically No Difference
BAB - Crack Fill	BOB - Crack Seal	5.61	1.04	5.4	0.001	Statitically Different
BAB - Crack Fill	BOC - Crack Seal	7.34	0.978	7.51	0.001	Statitically Different
BAB - Crack Fill	BAB - Micro-Surf	-13.29	1.115	-11.92	0.001	Statitically Different
BAB - Crack Fill	BOB - Micro-Surf	-17.93	1.618	-11.08	0.001	Statitically Different
BAB - Crack Fill	BOC - Micro-Surf	-14.85	1.699	-8.74	0.001	Statitically Different
BAB - Crack Fill	BAB - Patching	-5.43	0.651	-8.34	0.001	Statitically Different
BAB - Crack Fill	BOB - Patching	0.71	0.791	0.89	1	Statistically No Difference
BAB - Crack Fill	BOC - Patching	-1.91	0.75	-2.55	1	Statistically No Difference

Pavement Type + Treatment Name	Pavement Type + Treatment Name	Mean Difference	SE	t	p	Comments
BOB - Crack Fill	BOC - Crack Fill	-3.46	1.037	-3.34	0.129	Statistically No Difference
BOB - Crack Fill	BAB - Crack Repr	-10.11	1.26	-8.03	0.001	Statitically Different
BOB - Crack Fill	BOB - Crack Repr	-0.66	1.684	-0.39	1	Statistically No Difference
BOB - Crack Fill	BOC - Crack Repr	-17.77	1.191	-14.92	0.001	Statitically Different
BOB - Crack Fill	BAB - Crack Seal	-0.69	1.016	-0.68	1	Statistically No Difference
BOB - Crack Fill	BOB - Crack Seal	2.22	1.124	1.98	1	Statistically No Difference
BOB - Crack Fill	BOC - Crack Seal	3.95	1.066	3.7	0.034	Statitically Different
BOB - Crack Fill	BAB - Micro-Surf	-16.68	1.193	-13.98	0.001	Statitically Different
BOB - Crack Fill	BOB - Micro-Surf	-21.32	1.673	-12.74	0.001	Statitically Different
BOB - Crack Fill	BOC - Micro-Surf	-18.24	1.752	-10.41	0.001	Statitically Different
BOB - Crack Fill	BAB - Patching	-8.82	0.778	-11.34	0.001	Statitically Different
BOB - Crack Fill	BOB - Patching	-2.68	0.898	-2.99	0.428	Statistically No Difference
BOB - Crack Fill	BOC - Patching	-5.3	0.862	-6.15	0.001	Statitically Different
BOC - Crack Fill	BAB - Crack Repr	-6.65	1.321	-5.03	0.001	Statitically Different
BOC - Crack Fill	BOB - Crack Repr	2.8	1.73	1.62	1	Statistically No Difference
BOC - Crack Fill	BOC - Crack Repr	-14.3	1.255	-11.39	0.001	Statitically Different
BOC - Crack Fill	BAB - Crack Seal	2.77	1.091	2.54	1	Statistically No Difference
BOC - Crack Fill	BOB - Crack Seal	5.69	1.192	4.77	0.001	Statitically Different
BOC - Crack Fill	BOC - Crack Seal	7.41	1.138	6.51	0.001	Statitically Different
BOC - Crack Fill	BAB - Micro-Surf	-13.21	1.258	-10.51	0.001	Statitically Different
BOC - Crack Fill	BOB - Micro-Surf	-17.86	1.72	-10.38	0.001	Statitically Different

Pavement Type + Treatment Name	Pavement Type + Treatment Name	Mean Difference	SE	t	p	Comments
BOC - Crack Fill	BOC - Micro-Surf	-14.78	1.796	-8.23	0.001	Statitically Different
BOC - Crack Fill	BAB - Patching	-5.36	0.874	-6.13	0.001	Statitically Different
BOC - Crack Fill	BOB - Patching	0.78	0.982	0.79	1	Statistically No Difference
BOC - Crack Fill	BOC - Patching	-1.84	0.949	-1.94	1	Statistically No Difference
BAB - Crack Repr	BOB - Crack Repr	9.45	1.872	5.05	0.001	Statitically Different
BAB - Crack Repr	BOC - Crack Repr	-7.65	1.445	-5.3	0.001	Statitically Different
BAB - Crack Repr	BAB - Crack Seal	9.42	1.304	7.22	0.001	Statitically Different
BAB - Crack Repr	BOB - Crack Seal	12.34	1.39	8.87	0.001	Statitically Different
BAB - Crack Repr	BOC - Crack Seal	14.06	1.344	10.46	0.001	Statitically Different
BAB - Crack Repr	BAB - Micro-Surf	-6.56	1.447	-4.54	0.001	Statitically Different
BAB - Crack Repr	BOB - Micro-Surf	-11.21	1.863	-6.02	0.001	Statitically Different
BAB - Crack Repr	BOC - Micro-Surf	-8.13	1.934	-4.21	0.003	Statitically Different
BAB - Crack Repr	BAB - Patching	1.29	1.129	1.14	1	Statistically No Difference
BAB - Crack Repr	BOB - Patching	7.43	1.215	6.12	0.001	Statitically Different
BAB - Crack Repr	BOC - Patching	4.81	1.189	4.05	0.009	Statitically Different
BOB - Crack Repr	BOC - Crack Repr	-17.1	1.826	-9.37	0.001	Statitically Different
BOB - Crack Repr	BAB - Crack Seal	-0.03	1.717	-0.02	1	Statistically No Difference
BOB - Crack Repr	BOB - Crack Seal	2.89	1.783	1.62	1	Statistically No Difference
BOB - Crack Repr	BOC - Crack Seal	4.61	1.747	2.64	1	Statistically No Difference
BOB - Crack Repr	BAB - Micro-Surf	-16.01	1.828	-8.76	0.001	Statitically Different
BOB - Crack Repr	BOB - Micro-Surf	-20.66	2.172	-9.51	0.001	Statitically Different

Pavement Type + Treatment Name	Pavement Type + Treatment Name	Mean Difference	SE	t	p	Comments
BOB - Crack Repr	BOC - Micro-Surf	-17.58	2.233	-7.87	0.001	Statitically Different
BOB - Crack Repr	BAB - Patching	-8.16	1.588	-5.14	0.001	Statitically Different
BOB - Crack Repr	BOB - Patching	-2.02	1.65	-1.22	1	Statistically No Difference
BOB - Crack Repr	BOC - Patching	-4.64	1.631	-2.84	0.685	Statistically No Difference
BOC - Crack Repr	BAB - Crack Seal	17.08	1.238	13.8	0.001	Statitically Different
BOC - Crack Repr	BOB - Crack Seal	19.99	1.328	15.06	0.001	Statitically Different
BOC - Crack Repr	BOC - Crack Seal	21.71	1.279	16.97	0.001	Statitically Different
BOC - Crack Repr	BAB - Micro-Surf	1.09	1.387	0.79	1	Statistically No Difference
BOC - Crack Repr	BOB - Micro-Surf	-3.55	1.817	-1.96	1	Statistically No Difference
BOC - Crack Repr	BOC - Micro-Surf	-0.48	1.889	-0.25	1	Statistically No Difference
BOC - Crack Repr	BAB - Patching	8.95	1.051	8.51	0.001	Statitically Different
BOC - Crack Repr	BOB - Patching	15.08	1.143	13.2	0.001	Statitically Different
BOC - Crack Repr	BOC - Patching	12.47	1.115	11.18	0.001	Statitically Different
BAB - Crack Seal	BOB - Crack Seal	2.91	1.173	2.48	1	Statistically No Difference
BAB - Crack Seal	BOC - Crack Seal	4.64	1.118	4.15	0.006	Statitically Different
BAB - Crack Seal	BAB - Micro-Surf	-15.99	1.24	-12.89	0.001	Statitically Different
BAB - Crack Seal	BOB - Micro-Surf	-20.63	1.707	-12.08	0.001	Statitically Different
BAB - Crack Seal	BOC - Micro-Surf	-17.55	1.784	-9.84	0.001	Statitically Different
BAB - Crack Seal	BAB - Patching	-8.13	0.848	-9.59	0.001	Statitically Different
BAB - Crack Seal	BOB - Patching	-1.99	0.959	-2.08	1	Statistically No Difference
BAB - Crack Seal	BOC - Patching	-4.61	0.926	-4.98	0.001	Statitically Different

Pavement Type + Treatment Name	Pavement Type + Treatment Name	Mean Difference	SE	t	p	Comments
BOB - Crack Seal	BOC - Crack Seal	1.72	1.217	1.42	1	Statistically No Difference
BOB - Crack Seal	BAB - Micro-Surf	-18.9	1.33	-14.21	0.001	Statitically Different
BOB - Crack Seal	BOB - Micro-Surf	-23.54	1.773	-13.27	0.001	Statitically Different
BOB - Crack Seal	BOC - Micro-Surf	-20.47	1.848	-11.08	0.001	Statitically Different
BOB - Crack Seal	BAB - Patching	-11.04	0.975	-11.33	0.001	Statitically Different
BOB - Crack Seal	BOB - Patching	-4.91	1.073	-4.57	0.001	Statitically Different
BOB - Crack Seal	BOC - Patching	-7.52	1.043	-7.21	0.001	Statitically Different
BOC - Crack Seal	BAB - Micro-Surf	-20.62	1.282	-16.09	0.001	Statitically Different
BOC - Crack Seal	BOB - Micro-Surf	-25.27	1.737	-14.54	0.001	Statitically Different
BOC - Crack Seal	BOC - Micro-Surf	-22.19	1.813	-12.24	0.001	Statitically Different
BOC - Crack Seal	BAB - Patching	-12.77	0.907	-14.07	0.001	Statitically Different
BOC - Crack Seal	BOB - Patching	-6.63	1.012	-6.55	0.001	Statitically Different
BOC - Crack Seal	BOC - Patching	-9.25	0.981	-9.43	0.001	Statitically Different
BAB - Micro-Surf	BOB - Micro-Surf	-4.64	1.818	-2.55	1	Statistically No Difference
BAB - Micro-Surf	BOC - Micro-Surf	-1.57	1.891	-0.83	1	Statistically No Difference
BAB - Micro-Surf	BAB - Patching	7.86	1.054	7.45	0.001	Statitically Different
BAB - Micro-Surf	BOB - Patching	13.99	1.145	12.22	0.001	Statitically Different
BAB - Micro-Surf	BOC - Patching	11.38	1.118	10.18	0.001	Statitically Different
BOB - Micro-Surf	BOC - Micro-Surf	3.08	2.225	1.38	1	Statistically No Difference
BOB - Micro-Surf	BAB - Patching	12.5	1.577	7.93	0.001	Statitically Different
BOB - Micro-Surf	BOB - Patching	18.64	1.639	11.37	0.001	Statitically Different

Pavement Type + Treatment Name	Pavement Type + Treatment Name	Mean Difference	SE	t	p	Comments
BOB - Micro-Surf	BOC - Patching	16.02	1.62	9.89	0.001	Statistically Different
BOC - Micro-Surf	BAB - Patching	9.42	1.66	5.68	0.001	Statistically Different
BOC - Micro-Surf	BOB - Patching	15.56	1.719	9.05	0.001	Statistically Different
BOC - Micro-Surf	BOC - Patching	12.94	1.701	7.61	0.001	Statitically Different
BAB - Patching	BOB - Patching	6.14	0.702	8.74	0.001	Statistically Different
BAB - Patching	BOC - Patching	3.52	0.656	5.36	0.001	Statistically Different
BOB - Patching	BOC - Patching	-2.62	0.794	-3.3	0.15	Statistically No Difference